THE EFFECTS OF ADIPOSE-DERIVED REGENERATIVE CELLS IN PRECLINICAL KIDNEY INJURY MODELS

Rachanchai Chawangwongsanukun
DVM, MSc (MedSci)

Submitted in fulfilment of the requirements for the Degree of Doctor of Philosophy (PhD)

School of Cardiovascular & Metabolic Health
College of Medicine, Veterinary & Life Sciences
University of Glasgow

August 2025

ABSTRACT

Chronic kidney disease is a common health issue affecting approximately 10% of the UK population. Advanced kidney failure necessitates kidney transplantation or dialysis in affected patients. The optimal treatment for end-stage kidney failure is kidney transplantation. Although the number of deceased donor kidney transplants has increased, the number of patients waiting for kidney transplantation continues to rise. Therefore, to make more kidneys available for transplantation, it is important to improve kidney transplantation techniques by using effective perfusate solutions, developing methods for organ storage, and applying additional treatments to the transplant kidney to optimise outcomes.

Adipose-derived regenerative cells (ADRCs) are a heterogeneous cell population derived from adipose tissue. These cells are composed of endothelial progenitor cells, pericytes, and adipose stromal cells. Previous studies have revealed the potential therapeutic effects of ADRCs. These effects might help kidney grafts recover from ischaemia-reperfusion injury in kidney transplantation. My project aims to examine the therapeutic effects of ADRCs on injured kidney models to assess their potential utility for optimising kidneys for transplantation. I used three approaches for investigation: 1) a systematic review to investigate the effect of mesenchymal stem cells (MSCs) on solid organ transplantation models; 2) testing kidney organoids as a complex structural model for examining the effects of ADRCs on cellular communication and organoid protection; and 3) proximal tubular cell culture to study the therapeutic effects of ADRCs. Since oxidative stress is a hallmark of injury in ischemia-reperfusion injury (IRI), hydrogen peroxide was used as an injury inducer to mimic kidney transplantation by increasing oxidative stress in both the kidney organoid model and the proximal tubular cell model.

A systematic review was conducted using the search engine program Rayyan. Data were collected from 1991 to 2020 using specific terms. Two researchers assessed these data for validity. The results showed that MSCs have anti-apoptotic, anti-fibrotic, tubular injury protection, and anti-oxidative stress properties. These findings reveal the effects of MSCs on organ transplantation in the preclinical and clinical literature to date.

In studies of ADRCs on injured kidney organoid models, embryonic kidneys at days 13.5–14.5 were collected and processed into cell pellets. These pellets were cultured for 14 days for organogenesis. Organoids were assigned to four groups for study: non-injury, injury, ADRC-treated non-injury, and ADRC-treated injury groups. Injured organoids were induced using 10 μM hydrogen peroxide for 60 minutes, and ADRCs at 10% of embryonic cells were used in the ADRC-treated groups. After assignment, organoids were cultured for 14 days before collection and downstream assays. The results showed organoid protection by maintenance of organoid size after injury, revealing the pro-survival properties of ADRCs.

In proximal tubular cell culture experiments, NRK-52E cells were used and assigned to four groups (similar to the previous study). These cells were incubated with 500 μM hydrogen peroxide for 4 hours, and ADRCs were added at a 10% ratio of total NRK-52E cells. Laboratory assays including trypan blue exclusion test, western blot, real-time polymerase chain reaction (RT-PCR), flow cytometry, caspase-3 activity assay, and nanoparticle tracking analysis were performed after 24 hours of ADRC treatment. The results showed that ADRCs tended to decrease cell death markers and increase live cell markers in the ADRC-treated injured group and decreased NGAL gene expression. These findings reveal tubular protection from injury by ADRCs in injured proximal tubular cells.

This thesis shows that ADRCs had positive effects in organ transplant models in systematic reviews, exhibited pro-survival effects on kidney organoids, and reduced kidney injury markers in NRK-52E cells. Therefore, ADRCs are a promising additional treatment to diminish IRI in transplant kidneys.

TABLE OF CONTENTS

LIST OF TABLES

LIST OF FIGURES

PREFACE

This thesis has been prepared as part of my project, “The Effects of Adipose-Derived Regenerative Cells (ADRCs) in Preclinical Kidney Injury Models.” It includes all the details of the project that I undertook.

My thesis contains three results chapters: one chapter presenting a systematic review of the therapeutic properties of mesenchymal stem cells in organ transplantation, and two chapters examining the therapeutic properties of ADRCs in in vitro models-a kidney organoid model in Chapter 4 and a proximal tubular NRK-52E cell model in Chapter 5. Due to the global COVID-19 pandemic, the kidney organoid part was shortened, and I had to change the model to the proximal tubular cell model.

In this project, I performed various laboratory techniques. Although the results were not perfect, I hope this thesis may serve as a guide for anyone examining anti-apoptotic, anti-fibrotic, tubular protection, and anti-oxidative stress properties, as well as for those studying kidney injury models in the future.

ACKNOWLEDGEMENTS

Professor Patrick Mark – Thank you for allowing me to undertake this higher degree and for your guidance. Your expertise and experience were crucial in ensuring this project progressed to its completion.

Dr Rashida Lathan- Thank you for your support, teaching me laboratory skills, patience, mentorship and friendship.

Dr Robert Pearson – Thank you for your assistance with the scientific aspects of this project, your knowledge, and friendship.

Mr Ryan Ghita – Thank you for setting the scene for this project with your hard work that preceded it, as well as for your advice, guidance, and friendship.

Professor Marc Clancy – Thank you for your support under your project licence.

Professor Rhian Touyz – Thank you for allowing me to join your laboratory meetings and for access to your laboratory facilities.

I would also like to thank my funder, the Government of Thailand, administered by the Office of Educational Affairs, the Royal Thai Embassy, for funding the studies contained in this thesis and my time at the University of Glasgow.

All members of Rhian Touyz lab	School of Cardiovascular & Metabolic Health University of Glasgow
Staff from the facility	Central Research Facility (CRF) University of Glasgow
Professor Jamie Davies	Centre for Discovery Brain Sciences University of Edinburgh

I dedicate my thesis work to my family-my mother, my father, and my brother-for their unconditional support and for helping me relieve stress during the Covid-19 pandemic.

DECLARATION

My research degree began in 2019 and ran until 2023. The research took place at the School of Cardiovascular & Metabolic Health, University of Glasgow

During the correction of this thesis, as a non-native English speaker, I have used Perplexity to assist me in the writing process to improve language, flow, and readability. However, all content is based on my first draft which I generated completely unaided. I have reviewed and edited the content as needed and I take full responsibility for the content of the whole thesis.

I declare the work presented in this thesis was conducted by myself unless otherwise stated below:

Dr Robert Pearson was the second reviewer of the systematic review on stem cell therapeutic delivery via perfusion technologies.

Rachanchai Chawangwongsanukun, *Glasgow, May 2025*

Covid-19 Statement

The Covid-19 pandemic has affected my PhD studies. It impacted various aspects of my work, and I needed a mitigation plan to complete my project.

Initial plan for this project

Initially, my project was planned to use two models: injured kidney organoids and a surgical rat model. I prepared by visiting Professor Jamie Davies's laboratory at the University of Edinburgh, where I was trained in rat surgery by an experienced surgeon. However, I could not complete the kidney organoid model due to limitations in maintaining the rat colony during the pandemic. In addition, I was unable to complete my surgical rat training because of the extended training time required and the lack of rats for training. A mitigation plan was created a few months after the pandemic began.

Methodological adjustments

During the initial phase of the pandemic, laboratory closures and strict lockdowns disrupted experimental activities. All in-person laboratory work was prohibited, and virtual laboratory meetings became the norm. My project shifted to data analysis and a literature review in the form of a systematic review. My cell culture model was adapted from a three-dimensional to a two-dimensional culture. The shorter culture time allowed for the production of more samples. I was able to perform some laboratory techniques such as western blot and flow cytometry because of the adequate sample quantity. The project methodology was changed from the initial plan to suit the time remaining to complete my PhD.

Laboratory work, collaboration and networking

Pandemic-related rules impacted my laboratory work, collaboration with colleagues, and communication with peers and supervisors. Social distancing policies affected daily laboratory operations. Only one person was allowed at a laboratory bench at a time. In the early phase of the pandemic, regulations allowed only one person in a biosafety cabinet room, even though there were two biosafety cabinets in the room. Frequently, I had to leave the biosafety cabinet room because a colleague needed to use the water bath to thaw culture media or chemical reagents. Academic conferences were limited to virtual meetings. I had less face-to-face communication with colleagues, supervisors, and peers, making it difficult

to network within the kidney research community. Additionally, the social distancing policy directly reduced my opportunities to practice English skills.

In conclusion, the Covid-19 pandemic caused many obstacles in my project. I adapted my approach to finish my thesis by developing a mitigation plan. Despite the challenges during the pandemic, I gained valuable experience in conducting scientific research under difficult circumstances. These skills will benefit my future scientific work.

PUBLICATIONS

Completed manuscripts ready for submission

Pearson R, Chawangwongsanukun R, Clancy M, Mark P (2023) Therapeutic Efficacy of Mesenchymal Stem Cell Population Delivered via Isolated Organ Perfusion – A Systematic Review.

International poster presentations

Anti-Fibrotic Property of Adipose Derived Regenerative Cells on Hydrogen Peroxide Induced Injury in NRK-52E Cells. American Transplant Congress, Boston USA, June 2022

Ischemic and Perfused Kidney Treated with Non-Cultured Adipose-Derived Regenerative Cells Increase the Immune and Regulatory Transcriptome. The Transplant Society, International Conference, Virtual, September 2020

ABBREVIATIONS

7-AAD	7-aminoactinomycin D
ADRC	Adipose derived regenerative cell
AKI	Acute kidney injury
AMPK	Activated protein kinase
APAF-1	Apoptotic protease activating factor-1
ATP	Adenosine triphosphate
BAK	BCL2 homologous antagonist/killer
BAX	BCL2-Associated X
BCA	Bicinchoninic acid assay
BCL2	B-cell lymphoma 2
BM-MSC	Bone marrow-derived mesenchymal stem cell
BrdU	5-bromo-2'-deoxyuridine
BSA	Bovine serum albumin
CASP	Caspase
CAT	Catalase
CD	Cluster of differentiation
cDNA	Complementary deoxyribonucleic acid
cDNA	Complementary deoxyribonucleic acid
CIT	Cold ischaemic time
c-MET	Mesenchymal-epithelial transition factor
c-Mye	Cellular myelocytomatosis
COL	Collagen
COVID-19	Coronavirus disease 2019
DAMPs	Damage-associated molecular patterns
DCD	Donation after circulatory death
DEPC	Diethyl pyrocarbonate
DEVD-pNA	DEVD (Aspartic acid-Glutamic acid-Valine-Aspartic acid) p-nitroanilide
DGF	Delayed graft function
DMEM	Dulbecco's modified eagle's medium
DMSO	Dimethyl sulfoxide
DNA	Deoxyribonucleic acid
dNTP	Deoxynucleotide triphosphate

DPBS	Dulbecco's phosphate-buffered saline
DTT	Dithiothreitol
ECACC	European Collection of Authenticated Cell Cultures
ECD	Expanded criteria donor
EDTA	Ethylenediamine tetra acetic acid
EGF	Epithelial growth factor
EGFP	Enhanced green fluorescent protein
eGFR	Estimated glomerular filtration rate
ELN	Elastin
EMT	Epithelial to mesenchymal transition
ERK	Extracellular signal-regulated kinase
ESC	Embryonic stem cell
ESKD	End-stage kidney disease
EV	Extracellular vesicle
FBS	Fetal bovine serum
FBS	Fetal bovine serum
FGF9	Fibroblast growth factor 9
FSC	Forward scatter
GAPDH	Glyceraldehyde-3-phosphate dehydrogenase
GFR	Glomerular filtration rate
H2DCFDA	Carboxy-2′,7′-dichlorodihydrofluorescein diacetate
HD	Haemodialysis
HGF	Hepatocyte growth factor
HIF	Hypoxia-inducible factor
HK-2	Human kidney 2
HLA	Human leukocyte antigen
IDO	Indoleamine 2,3-dioxygenase
IFN	Interferon
Ig	Immunoglobulin
IGF	Immediate graft function
IGF	Insulin-like growth factor
IGF-1	Insulin-like growth factor
IL	Interleukin
IM	Intermediate mesoderm
iPSC	inducible pluripotent stem cell

IRI	Ischaemic reperfusion injury
JNK	c-Jun N-terminal kinase
KIM-1	Kidney Injury Molecule-1
Klf4	Kruppe-like factor 4
Lgr5+	Leucine-rich repeat-containing G-protein coupled receptor 5
Lif	Leukaemia inhibitory factor
Lim1	LIM homeobox 1
LPS	Lipopolysaccharide
MAPC	Multipotent adult progenitor cell
MAPK	Mitogen-activated protein kinase
MCP-1	Monocyte chemoattractant protein-1
MDA	Malondialdehyde
MEM	Minimum essential medium
miR	MicroRNA
MMP	Matrix metalloproteinase
MSC	Mesenchymal stem cell
mTOR	Mammalian target of rapamycin
NFG	Nerve growth factor
NF-kappa-B	Nuclear factor-kappa B
NGAL	Neutrophil gelatinase-associated lipocalin
NHS	National Health Service
NMP	Normothermic machine perfusion
NPC	Nephron progenitor cell
NRK	Normal rat kidney
NSAIDs	Nonsteroidal anti-inflammatory drugs
Oct3/4	Octamer-binding transcription factor 3/4
OD	Ocular density
Osr1	Odd-skipped related transcription factor 1
PAI-1	Plasminogen activator inhibitor-1
Parp	Poly (ADP-ribose) polymerase
Pax2	Paired Box 2
PCNA	Proliferation cell nuclear antigen
PD	Peritoneal dialysis
PGE2	Prostaglandin E2
PKD	Polycystic kidney disease

pNA	p-nitroaniline
RNA	Ribonucleic acid
ROS	Reactive oxygen species
RT-PCR	Real time reverse polymerase chain reaction
SD	Sprague Dawley (rat)
SDF	Stromal derived factor-1
Smad7	Sma- and Mad-related protein 7
Smuf1	Smad ubiquitination regulatory factor 1
SOD	Superoxide dimutase
Sox2	Sex determining region Y-BOX 2
SRR	Scottish Renal registry
SSC	Side scatter
STAT3	Signal transducer and activator of transcription 3
TGF	Tumour growth factor
TLR4	Toll-like receptor 4
TNF	Tumour Necrosis Factor
TNFR	Tumour necrosis factor receptor
TSG	Tumour necrosis factor-stimulated gene
TUNEL	Terminal deoxynucleotidyl transferase dUTP nick end labelling
UNOS	United Network for Organ Sharing
VEGF	Vascular endothelial growth factor
WIT	Warm ischaemic time
Wt1	Wilms' tumour 1
WU	Wroblewski units

Chapter 1: Introduction

1.1 Kidney transplantation and the need for graft optimisation

1.1.1 The need for kidney transplantation

Chronic kidney failure is a common health problem, affecting approximately 10% of the population in the United Kingdom. Patients with kidney failure (end-stage kidney disease) require either kidney transplantation or dialysis, but transplantation is the optimal treatment due to lower long-term mortality and better quality of life compared to dialysis (Tonelli et al., 2011). Therefore, increasing the number of kidneys available for transplantation is a research priority.

According to the NHS Blood and Transplant report from May 2022, there was a 20% increase in deceased kidney donors and a 17% increase in deceased donor kidney transplants in 2021–2022 compared to 2020–2021 (NHSBT, 2022) (**Figure 1-1**). More patients were reactivated on the transplant list, leading to these increased numbers following the height of the COVID-19 pandemic, during which many hospitals stopped performing transplants due to shortages in intensive care beds. There were 5,023 patients waiting for a kidney transplant in 2022. The increase in the number of deceased kidney donors from 1,106 in 2020–2021 to 1,331 in 2021–2022 led to an increase in the number of transplants from 1,931 to 2,263, according to the NHSBT report. This implies that there are still many patients waiting for a kidney transplant, as the number of people on the waiting list far exceeds the number of organs available for transplant.

In Scotland, the Scottish Renal Registry (SRR) 2022 annual report stated that there were 5,488 prevalent patients receiving kidney replacement therapy (KRT) on 31 December 2021 (Scotland, 2022) (**Figure 1-2**). According to this report, 61% of these patients had a functioning kidney transplant, 35% were being treated with haemodialysis (HD), and 4% were being treated with peritoneal dialysis (PD).

These reports highlight the ongoing need for kidney transplantation and the increasing demand as more patients are activated on the national transplant waiting list. This reflects the importance of kidney transplantation and research in this field to increase the number of kidneys available for transplant. In addition, the COVID-19 pandemic has

affected healthcare systems worldwide over the past three years. Like other healthcare services, transplantation was affected by the pandemic. The effects were seen both in the number of transplanted organs and in the numbers offered and retrieved.

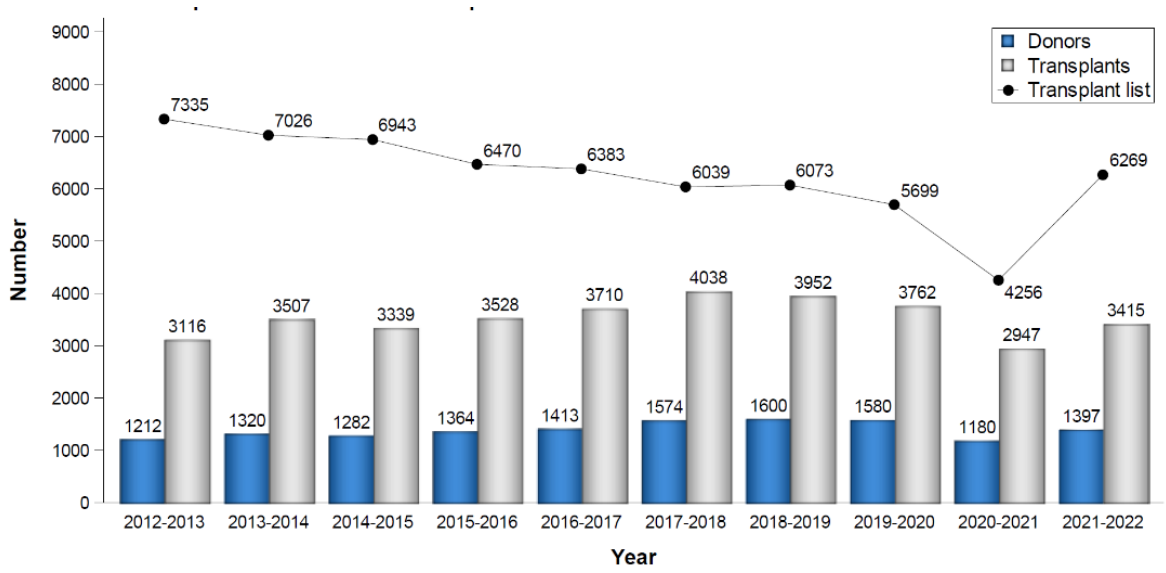

Figure 1-1 Number of deceased donors, transplants, and patients on the transplant list in the United Kingdom from 2012 to 2022 (NHSBT, 2022)

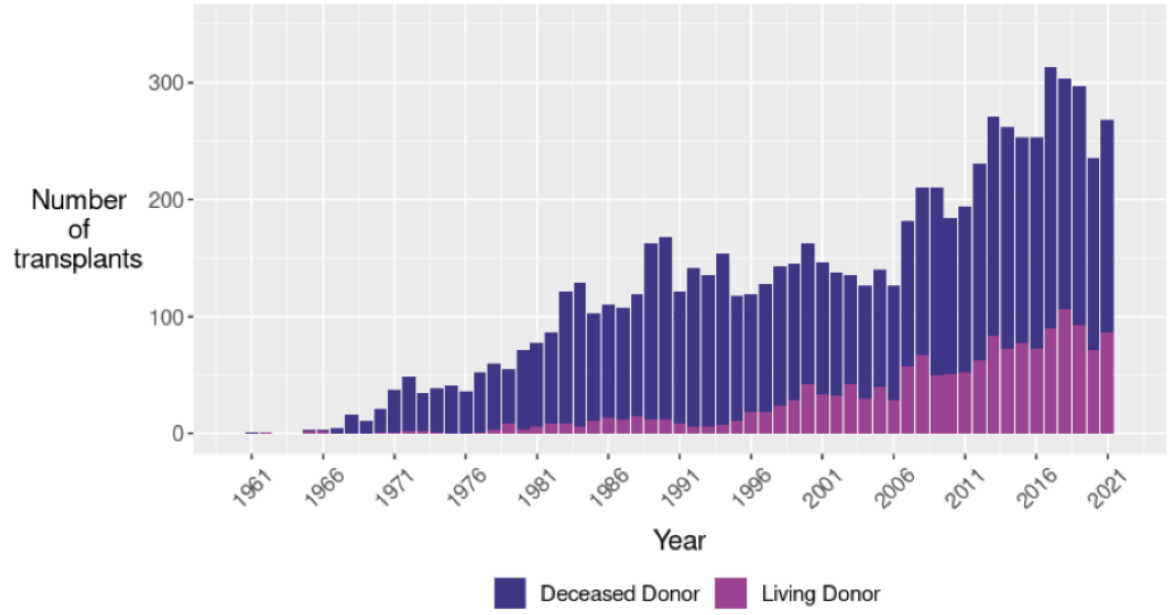

Figure 1-2 Number of deceased donors and living donor kidney transplants performed in Scotland from 1960 to 2021 (Scotland, 2022).

1.1.2 Delayed Graft function (DGF)

In kidney transplantation, a common complication is delayed graft function (DGF). DGF is typically defined as acute kidney injury that manifests as the need for dialysis within the first week after transplantation (Schroppel et al., 2014; Gill et al., 2016). This complication is associated with an increased risk of graft rejection, which decreases the number of kidneys available for transplant and represents a major clinical challenge in organ transplantation (Li et al., 2023). DGF is also linked to early infectious complications, such as urinary tract infections and human polyomavirus 1 infection, following kidney transplantation (Alshaikh et al., 2023).

Delayed graft function reduces graft survival. Wang et al. showed that 36% of DGF cases were associated with graft failure, compared to immediate graft function, which is characterized by rapid postoperative recovery of renal function (Wang et al., 2018). Another study using United Network for Organ Sharing (UNOS) data in the United States reported that DGF reduced the five-year graft survival rate by 10–15% (Ponticelli, 2014). Therefore, reducing DGF is essential to improving the success of kidney transplantation. DGF remains a major clinical challenge in kidney transplantation research.

There are several risk factors involved in delayed graft function (DGF) in kidney transplantation, including donor-related, recipient-related, preservation-related, and transplant-related factors (Mannon, 2018) (**Table 1-1**). Among these, the main factors influencing the development of DGF are cold ischemic time and warm ischemic time, which refer to the duration the organ is kept under hypothermic and normothermic conditions during preservation and transportation, respectively (Mannon, 2018).

The impact of cold and warm ischemic times has been demonstrated in several studies. A prospective study by Barba et al. (2011) investigated the relationship between cold ischemic time (CIT) and renal graft survival, showing that a CIT of less than 18 hours does not negatively affect five-year graft survival (91%), whereas a CIT of more than 18 hours results in an 84% five-year graft survival. After 18 hours, each additional hour of CIT significantly decreases graft survival (Barba et al., 2011). Another cohort study by Serrano et al. (2018), which evaluated data from 81,945 kidney transplant recipients, found that a 10-hour increase in CIT can lead to a 41% increase in delayed graft function and is associated

with a 4% increase in length of hospital stay (Serrano et al., 2018). These studies indicate a clear relationship between ischemic time and the development of DGF.

Table 1-1 Risk factors for delayed graft function (Mannon, 2018)

Donor-related	Recipient-related
• Female gender • Increasing age • Body mass index • Deceased vs. living donation • Donation after cardiac death • Increasing donor serum creatinine	• Male gender • African-American race • Body mass index • Previous transplant • Diabetes
Preservation	**Transplant-related**
• Cold ischaemic time (CIT) • Warm ischaemic time	• Sensitization • Human leukocyte antigen (HLA) mismatches

1.1.3 Ischaemic reperfusion injury (IRI) in kidney transplantation

During cold and warm ischaemia in kidney transplantation, a typical complication known as ischaemia-reperfusion injury (IRI) occurs, which is the main pathophysiological mechanism underlying delayed graft function (DGF). IRI refers to tissue injury that arises after a temporary restriction of blood flow during organ transportation, followed by restoration of blood supply and re-oxygenation. This process can also occur after organ infarction, sepsis, and transplantation. IRI leads to inflammation, leukocyte activation, production of reactive oxygen species (ROS), and tissue injury (Thompson et al., 2020). Several studies indicate that IRI is a critical factor in reducing long-term graft survival (Quiroga et al., 2006; Su et al., 2004; Roodnat et al., 2003). Therefore, ameliorating IRI is essential for improving kidney graft outcomes.

Although the pathophysiology of IRI is not completely understood, it involves two main cellular stages: ischaemia and reperfusion. Ischaemic injury begins in the donor after haemodynamic disturbance, leading to hypoxic conditions, mitochondrial dysfunction (Ma et al., 2024), inhibition of membrane proteins such as Na+-K+ ATPase (Chen et al., 2022b),

and lysosomal leakage, and cell breakdown (Sugiyama et al., 1988). This stage also decreases anti-oxidative agents. The reperfusion stage occurs when blood supply is restored to the kidney, generating large amounts of ROS, which cause oxidative damage to proteins and DNA, contributing to apoptosis and cell death (Hendriks et al., 2019; Zhao et al., 2021).

Additionally, kidney cell necrosis releases damage-associated molecular patterns (DAMPs) (Dewolf et al., 2022), ROS, and inflammatory cytokines such as tumour necrosis factor (TNF), which activate the immune system (Zhao et al., 2018, 2021). Monocytes and neutrophils are recruited to the injured tissue (Chen et al., 2022a; Wu et al., 2007), producing further ROS and inflammatory cytokines, which enhance necrosis and result in ischaemic acute tubular necrosis (ATN) in histopathology (Jain et al., 2020). Treatment of IRI should focus on reducing apoptosis, removing ROS, and decreasing inflammation (**Figure 1-3**).

1.2 Adipose derived regenerative cells (ADRC): a promising therapy for kidney graft rehabilitation

Ischaemia-reperfusion injury increases the risk of delayed graft function (DGF) and leads to graft rejection. Therapeutic strategies for kidney transplant IRI, such as improved reperfusion techniques, drugs, and cell therapy, are being actively pursued by kidney transplantation researchers. Adipose-derived regenerative cells (ADRCs) have attracted increasing attention in recent years. ADRCs are multi-lineage cells that include mesenchymal stem cells, other progenitor cells, fibroblasts, T-regulatory cells, and macrophages derived from adipose tissue (Zuk et al., 2001). ADRC therapy is a promising new option to restore graft health after IRI.

1.2.1 Source, isolation, and composition of ADRC

Adipose-derived regenerative cells (ADRCs) were first described in 2001 by Zuk and colleagues (Zuk et al., 2001). In this study, ADRCs were obtained from human adipose tissue using suction-assisted lipectomy. Their stem cell properties were demonstrated by culturing the cells in media that induced differentiation toward adipogenic, osteogenic, chondrogenic, and myogenic lineages. The cellular composition of ADRCs includes fibroblasts, mesenchymal stem cells (MSCs), smooth muscle cells, mural cells, macrophages, and blood cells (Nunes et al., 2013; Vijay et al., 2020).

Unlike bone marrow-derived mesenchymal stem cells, which are present in low abundance in bone marrow, ADRCs can be collected in large quantities from either liposuction aspirate or subcutaneous extracts. Because ADRCs can be obtained using minimally invasive methods, the ethical, political, and practical issues associated with their collection are reduced (Lindroos et al., 2011).

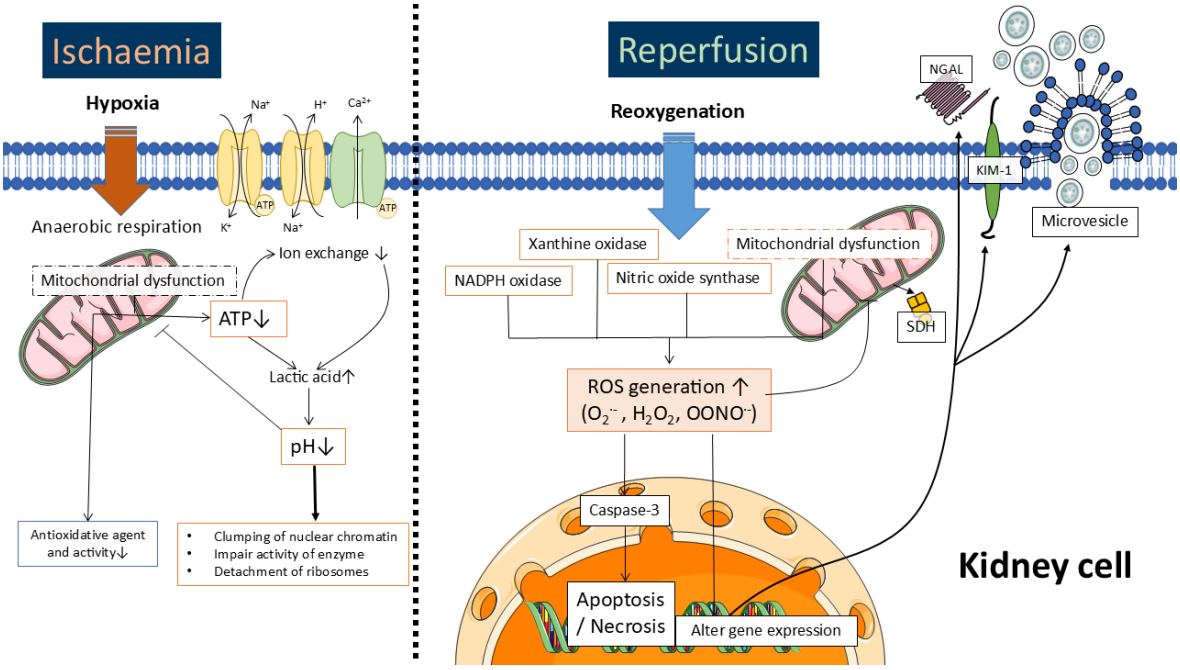

Figure 1-3 The diagram illustrates the cellular response during ischaemia-reperfusion injury (IRI) in kidney transplantation. There are two phases of IRI: the ischaemic phase and the reperfusion phase. During the ischaemic phase, reduced oxygenation to the tissue causes mitochondrial dysfunction, leading to ATP depletion and decreased antioxidative activity. The activity of ATP-dependent cell membrane receptors decreases, resulting in lactic acid accumulation and cellular acidosis. This acidosis causes nuclear chromatin clumping, impairs enzyme activity, and leads to ribosomal detachment. After re-oxygenation in the reperfusion phase, hyperoxygenation occurs due to the decreased levels of antioxidative enzymes resulting from the ischaemic phase. This leads to increased production of reactive oxygen species (ROS). The activation of apoptotic enzymes results in apoptosis or necrosis. Additionally, ROS production induces the expression of injury proteins such as NGAL and KIM-1, and triggers the release of microvesicles for intercellular communication.

1.2.2 Characteristics of ADRC

The International Society for Cellular Therapy proposed minimal criteria in 2006 to identify mesenchymal stem cells (MSCs) (Dominici et al., 2006). The criteria include: 1) adherence to plastic under standard culture conditions; 2) expression of surface markers CD105, CD73, and CD90, with a lack of expression of CD45, CD34, CD14 or CD11b, CD79α or CD19, and HLA-DR; and 3) the ability to differentiate into osteoblasts, adipocytes, and chondroblasts. These criteria are considered the accepted consensus definition and markers for MSCs.

In addition, adipose-derived regenerative cells (ADRCs) contain more than one cell type. Zimmerlin (2013) described three cell populations within ADRCs: endothelial progenitor cells (CD45−/CD31+/CD34+), pericytes (CD45−/CD31−/CD146+), and supra-adventitial adipose stromal cells (CD45−/CD31−/CD146−/CD34+) (Zimmerlin et al., 2013).

1.2.3 Therapeutic effects of ADRC

Adipose-derived regenerative cells (ADRCs) have properties similar to other mesenchymal stem cells and can secrete trophic factors such as stromal-derived factor-1 (SDF-1), hepatocyte growth factor (HGF), insulin-like growth factor-1 (IGF-1), epidermal growth factor (EGF), nerve growth factor (NGF), transforming growth factor-alpha (TGF-α), and vascular endothelial growth factor (VEGF). Although the therapeutic mechanisms of ADRCs are not fully understood, it is believed that their beneficial effects are mediated through anti-inflammatory, anti-oxidative, and anti-apoptotic actions.

In a preclinical kidney model, Donizetti-Oliveira showed that ADRCs decrease urea levels and reduce the expression of inflammatory cell chemokines, myeloperoxidase, and C-X-C motif chemokine ligand 1 (CXCL1) in immunohistochemistry after 24 hours of folic acid induction in FVB mice (Donizetti-Oliveira et al., 2012). Over a longer observation period (4 weeks), there was a reduction in interferon gamma (IFN-γ) in immunohistochemistry (Burgos-Silva et al., 2015). Another study demonstrated that ADRCs can reduce TUNEL-positive apoptotic cells and decrease superoxide production in a lucigenin chemiluminescence assay compared to a group without ADRC treatment in surgical IRI Sprague-Dawley rats (Shih et al., 2013). These studies suggest that ADRC treatment promotes repair through anti-oxidative, anti-inflammatory, and anti-apoptotic effects.

In a clinical study, ADRCs increased renal blood flow and estimated glomerular filtration rate in patients with atherosclerotic renovascular disease, with no reported adverse effects three months post-treatment (Saad et al., 2017). Other studies have shown that mesenchymal stem cells improve urine output, enhance microvascular perfusion, reduce expression of the kidney injury biomarker NGAL, downregulate the inflammatory cytokine interleukin-1β (IL-1β), and upregulate the anti-inflammatory cytokine IL-10 in kidney transplantation (Thompson et al., 2020). Additionally, a clinical study in liver cirrhosis patients demonstrated the safety of ADRCs, with no trial-related adverse events reported (Sakai et al., 2021). These studies confirm the preliminary efficacy and safety of ADRCs in reducing tissue injury in both preclinical and clinical settings.

1.3 Kidney organoids: model for the transplanted kidney

Organoids are three-dimensional tissues with structures and functions that mimic natural organs. Fatehullah et al. defined the characteristics of organoids as follows: (1) three-dimensional cellular clusters; (2) in vitro culture; (3) self-renewal; (4) self-organization; and (5) exhibition of physiological characteristics similar to primary cells (Fatehullah et al., 2016). In 1998, Thomson et al. demonstrated the undifferentiated proliferation of cell lines from human embryonic stem cells. These cells, derived from the blastocyst, survived for 4 to 5 months in culture and showed a homogeneous appearance. This research suggests that organoid cultures can fully differentiate into living tissues and allow unlimited reproduction. Takahashi and Yamanaka showed that four factors-octamer-binding transcription factor 3/4 (Oct3/4), Sex Determining Region Y-Box 2 (Sox2), cellular myelocytomatosis (c-Myc), and Kruppel-like factor 4 (Klf4)-can revert adult fibroblasts to pluripotent stem cells in mice (Takahashi and Yamanaka, 2006). This demonstrated that pluripotent stem cells can be generated from somatic cells. Their studies on somatic cell pluripotency were recognized with the Nobel Prize in 2012. Furthermore, Nature Methods selected organoid culture as the "Method of the Year" in 2017, highlighting its importance and utility in research.

Advances in organoid generation have expanded to various tissues following the discovery of iPSCs. Intestinal organoids were first generated in 2009 from Lgr5+ stem cells with microvilli (Sato et al., 2009). Since then, organoid research has continued to advance, improving methods for organoid creation and enabling the generation of a wide range of organoids in the laboratory. To date, cerebral organoids have been created from human iPSCs (Lancaster et al., 2013), liver organoids from Lgr5+ stem cells (Huch et al., 2013), and lung organoids from iPSCs (Dye et al., 2015).

Generally, kidney organoids can be produced from two original cell types: embryonic stem cells (ESCs) or induced pluripotent stem cells (iPSCs). The first studies of kidney organoids derived from PSCs used CHIR99021 and FGF9 to differentiate iPSCs into kidney tissue (Takasato et al., 2015; Takasato and Little, 2017). This research demonstrated kidney organoids with four nephron compartments: collecting duct, distal tubule, proximal tubule, and glomerulus. To model clinical conditions, one study used the CRISPR/Cas9 genome editing system to mutate polycystic kidney disease (PKD) 1 and PKD2 in human PSCs (Freedman et al., 2015), resulting in cyst formation in kidney tubular organoids by day 35 after plating.

Besides kidney organoids derived from human iPSCs, kidney organoids can also be generated from embryonic kidneys. For example, one study used mouse embryonic kidneys to generate kidney organoids and advanced the technique by implanting them into rat kidneys with local administration of VEGF (Xinaris et al., 2012), demonstrating technological progress in kidney organoid generation.

1.3.1 Injury induction in organoid models

To mimic diseases for clinical applications, various injury inducers can be used. Organoids serve as models for injury induction with drugs, reagents, toxins, or specific conditions, making them valuable preclinical tools for studying particular diseases.

Firstly, hydrogen peroxide is used to mimic oxidative injury in tissues. Barrett et al. (2015) demonstrated that 800 μM hydrogen peroxide for 2 hours induced injury in mouse intestinal organoids, altering ROS production as measured by carboxy-H2 DCFDA staining (Barrett et al., 2015). Secondly, nephrotoxins such as gentamicin and cisplatin are used to model drug toxicity. Jun et al. (2018) showed that human tubular organoids exposed to 2 mg/mL gentamicin and 5 μM cisplatin expressed higher levels of NGAL and KIM-1 (Jun et al., 2018). Similarly, Takasato et al. (2015) reported that kidney organoids derived from human iPSCs showed injury and cleaved caspase-3 expression after exposure to 20 μM cisplatin (Takasato et al., 2015). Thirdly, lipopolysaccharide (LPS) is used to mimic bacterial toxin injury. Li et al. (2019) found that 200 μg/mL LPS increased IL-6 and TNF-α levels in immunofluorescence in mouse intestinal organoids cultured under hypoxic conditions (Li et al., 2019a). These examples highlight the utility of organoids as disease models for preclinical research

1.3.2 Advantages and disadvantages of kidney organoid model in research

There are several advantages to using kidney organoids as promising models for complex structures. Firstly, kidney organoid models show potential as disease models for cystic kidney disease, glomerular disease, and kidney injury (Little and Quinlan, 2019). Secondly, kidney organoids can be used for drug and toxicity screening. For example, kidney organoids produce the kidney injury marker KIM-1 after incubation with 5 μM cisplatin for 24 hours (Morizane et al., 2015a), demonstrating their utility for drug and toxicity screening. Thirdly, kidney organoids can be used to study the mechanisms of kidney development, as they express nephrogenesis proteins during organoid development (Morizane et al., 2015a). This highlights their potential for studying kidney developmental mechanisms.

Despite these advantages, kidney organoid models also have limitations. Firstly, organoids lack vasculature structures. Although various techniques have been used to induce vascularization, mechanical factors such as fluid shear stress, interstitial flow, and the mechanical properties of the extracellular matrix still limit vessel formation (Palakkan et al., 2022). Overcoming these challenges is key to generating kidney organoids with appropriate vasculature for research. Secondly, organoids exhibit variability. One study found a strong correlation in transcription between batches of human kidney organoids, but significant differences still existed between experimental batches (Phipson et al., 2019). Thirdly, culturing kidney organoids on a large scale is expensive and time-consuming, and improved protocols are needed for large-scale culture (Sander et al., 2020, 2023). Lastly, kidney organoids lack inflammatory cells, which are critical for modelling human physiology. This absence limits the use of kidney organoids as models for immune-mediated nephropathies (Bar-Ephraim et al., 2020).

The major challenge for researchers is to generate kidney organoids that accurately replicate physiological and anatomical features of the human kidney

1.4 Kidney cell culture (2D cell culture) in IRI studies

1.4.1 Type of kidney cell line

Monolayer cell culture, or two-dimensional (2D) cell culture, is a laboratory technique commonly used to study cellular mechanisms in preclinical research. This approach is typically employed to investigate single cell types or, in the case of co-culture techniques,

two cell types. The main advantage of this method is that it limits environmental interactions, allowing researchers to focus on the cell type of interest. Additionally, this technique provides clear and direct effects between treatments and the target cells. However, monolayer cell culture has several drawbacks, including limited relevance to clinical studies, a lack of multi-cellular interactions, and an inability to replicate complex tissue structures.

In 2D cell culture, there are two main types: primary cell culture and continuous cell culture. Each type offers specific benefits and drawbacks, depending on the study's objectives. Co-culture systems can be used in studies that require investigation of cell–cell interactions between different cell populations or for creating more representative in vivo-like tissue models (Tonnus et al., 2021; Ji et al., 2019). The selection of cell culture type should be based on the study design and the markers of interest. To mimic disease conditions, appropriate injury must be induced in these cells to accurately imitate the clinical setting.

1.4.2 Injury induction in kidney cell line

There are several kidney injury inducers to injury induction at the kidney cells for imitating clinical manifestations. Firstly, hydrogen peroxide is an injury induction method to induce oxidative injury. This directly increase reactive oxygen species (ROS) in cells (Vliet and Janssen-Heininger, 2014). Secondly, hypoxic culture conditions can activate cellular apoptosis, proliferation, differentiation, and migration (Shi et al., 2018). Various techniques are used for inducing hypoxia in cell culture, for example, to culture NRK-52E cells using nitrogen gas flush in an incubator for 1% oxygen content and 5% carbon dioxide content for 24 hours and then re-oxygenation for 24 hours (Shi et al., 2018; Zhu et al., 2018). Alternatively, vacuum sealing with oxygen absorber can be used, but oxygen content in this technique is not constant (Matthiesen et al., 2021). Thirdly, high glucose is used to study an effect of diabetes mellitus. For example, using 4.5 g/L D-glucose to induce injury in NRK-52 cells (Zou et al., 2020). Fourthly, nephrotoxic drugs such as antibiotics, NSAIDs, proton pump inhibitors, thiazide diuretics, lithium, anti-epileptic drugs, and allopurinol can induce kidney injury (Kwiatkowska et al., 2021). The use of nephrotoxic drugs is to mimic adverse events in clinical medicine (Awdishu and Mehta, 2017). Lastly, lipopolysaccharide (LPS) is a bacterial endotoxin and causes sepsis. A study used 1 μg/mL of LPS to induce injury on NRK-52E cells (Li et al., 2022b). This model is to mimic acute kidney injury (AKI) caused by bacterial infection.

1.4.3 Advantages and disadvantages of kidney cell lines in research

There are several advantages of 2D cell culture, including simple technique, high reproducibility, and availability of commercial cell lines. This in vitro model is inexpensive. Simple methodology is needed for the growth and maintenance of cells. The time required for 2D culturing is as low as a few minutes to a few hours. These cells easily access nutrients and other essential compounds (Frieboes et al., 2006). Moreover, these cell lines are easier to access with simple lab techniques. The comparison of advantages and disadvantages between 2D and 3D cell culture systems is demonstrated in **Table 1-2**.

In contrast, 2D cell culture has limitations like other in vitro research models, which researchers should consider when using this cell culture technique. Similar to the 3D cell culture model, the lack of ability to produce complex structures is the main problem of cell culture. Therefore, the study of intercellular interactions is difficult. Another issue is the changing phenotype of cultured cells. A study of culturing HK-2 cells in different media showed that the cells with different media responded differently to TGF-β in the expression of fibronectin, complement 3, and interleukin-6 (Garmaa et al., 2023). This showed that the formulation of the culture medium can affect the phenotype and behaviour of 2D cell culture.

Table 1-2 Advantages and disadvantages of 2D and 3D cell culture systems

System	Advantages	Disadvantages
2D cell system	- Inexpensive - Simple methodology - Less time consuming	- Lack of ability to produce complex structures - Lack of vasculature structures and inflammatory cells - Changing phenotype of cells culture
3D cell system	- Can be a disease model - Can be used in drug and toxicity screening - Can be used for studying mechanism of kidney development	- Lack of vasculature structures and inflammatory cells - Batch variability - Expensive and time consuming

1.5 Basic potential therapeutic effects of ADRCs

1.5.1 Apoptosis and other death pathways

IRI during kidney transplantation leads to apoptosis and ischemic acute tubular necrosis (ATN) (Jain et al., 2020). Ischemic ATN is associated with DGF (Okami et al., 2025). Although various types of cell death have been linked to IRI, including necroptosis, apoptosis, pyroptosis, and ferroptosis, this chapter will focus on apoptosis as it is the aim of the study.

Apoptosis is one of the physiological and pathological processes of cell death. It plays a role in homeostasis, maintenance, and disease development. John F. Kerr, Andrew Wyllie, and Alastair Currie (1972) described the characteristics of apoptosis as "the formation of roughly spherical or ovoid cytoplasmic fragments, some of which contain pyknotic remnants of nuclei" (Kerr et al., 1972). This is the first formal description referring to apoptotic bodies, and it is important to distinguish this from other types of cell death.

Other forms of cell death are pyroptosis, ferroptosis, necroptosis, and autophagy. Pyroptosis, ferroptosis, and necroptosis share similar morphological features with cellular swelling and pore formation on the cell membrane, but autophagy is characterized by an accumulation of vacuoles. The mechanisms of these four types of cell death are different. While pyroptosis is a unique type of cell death dependent on caspase-1 and the formation of the inflammasome, IL-18, and IL-1β (Buendia et al., 1999; Brennan and Cookson, 2000), ferroptosis, necroptosis, and autophagy are caspase-independent pathways. Ferroptosis is an iron-dependent cell death resulting from an excessive amount of lipid peroxidation, which leads to rupture of the plasma membrane (Dixon et al., 2012). Necroptosis involves RIPK1 kinase activation via TNFR1 signalling and the formation of the necrosome (Chen et al., 2022c). Autophagy involves the formation of the autophagosome, which fuses with a vacuole or lysosome for cellular degradation (Mizushima et al., 1998; Tsukada and Ohsumi, 1993).

Apoptosis can be divided into caspase-dependent and caspase-independent apoptosis. Caspase-dependent apoptosis has two classic pathways: intrinsic and extrinsic (**Figure 1-4**) (Sanz et al., 2008; Havasi and Borkan, 2011). The extrinsic pathway can be triggered via cell death receptors, toll-like receptor 4 (TLR4), and tumour necrosis factor

receptor 1 (TNFR1) at the cell membrane. Pathogen-associated molecular patterns (PAMPs), including lipopolysaccharide (LPS) and lipo-oligosaccharide, stimulate TLR4 (Lee and Seong, 2009), while tumour necrosis factor-α (TNFα), a mediator of inflammation, binds to TNFR1 (Black et al., 1997; Micheau and Tschopp, 2003). This receptor activation triggers caspase-8 and caspase-10, which subsequently activate caspase-3 and caspase-7 (Brentnall et al., 2013; Tao et al., 2005). Active caspase-3/7 activates DNase, resulting in internucleosomal DNA cleavage and leading to DNA fragmentation (McIlroy et al., 1999).

The classic intrinsic pathway of apoptosis is triggered by lethal stimuli such as DNA damage, endoplasmic reticulum stress, ROS, hypoxia, and metabolic stress. These lethal stimuli mediate BCL2-Associated X (BAX) and BCL2 homologous antagonist/killer (BAK) proteins at the mitochondrial membrane, forming mitochondrial pores and leading to the release of the mitochondrial protein cytochrome c from the mitochondrial intermembrane space into the cytoplasm (Wei et al., 2001; Schweighofer et al., 2024). Thereafter, oligomers between cytochrome c and apoptotic protease activating factor-1 (APAF-1) are formed into the apoptosome (Elena-Real et al., 2018). The apoptosome assembly cleaves procaspase-9 into activated caspase-9 (Zou et al., 1999). Activated caspase-9 then cleaves and activates caspase-3, resulting in cellular apoptosis (Li et al., 1997).

Caspase-independent apoptosis involves two proteins, apoptosis-inducing factor (AIF) and endonuclease G (EndoG), which lead to DNA fragmentation and cell death (Daugas et al., 2000; Parrish et al., 2001). AIF is an oxidoreductase that is released from mitochondria and translocates into the nucleus, leading to nuclear DNA fragmentation (Daugas et al., 2000). EndoG is a nuclease that cleaves DNA and induces internucleosomal DNA fragmentation (Li et al., 2001).

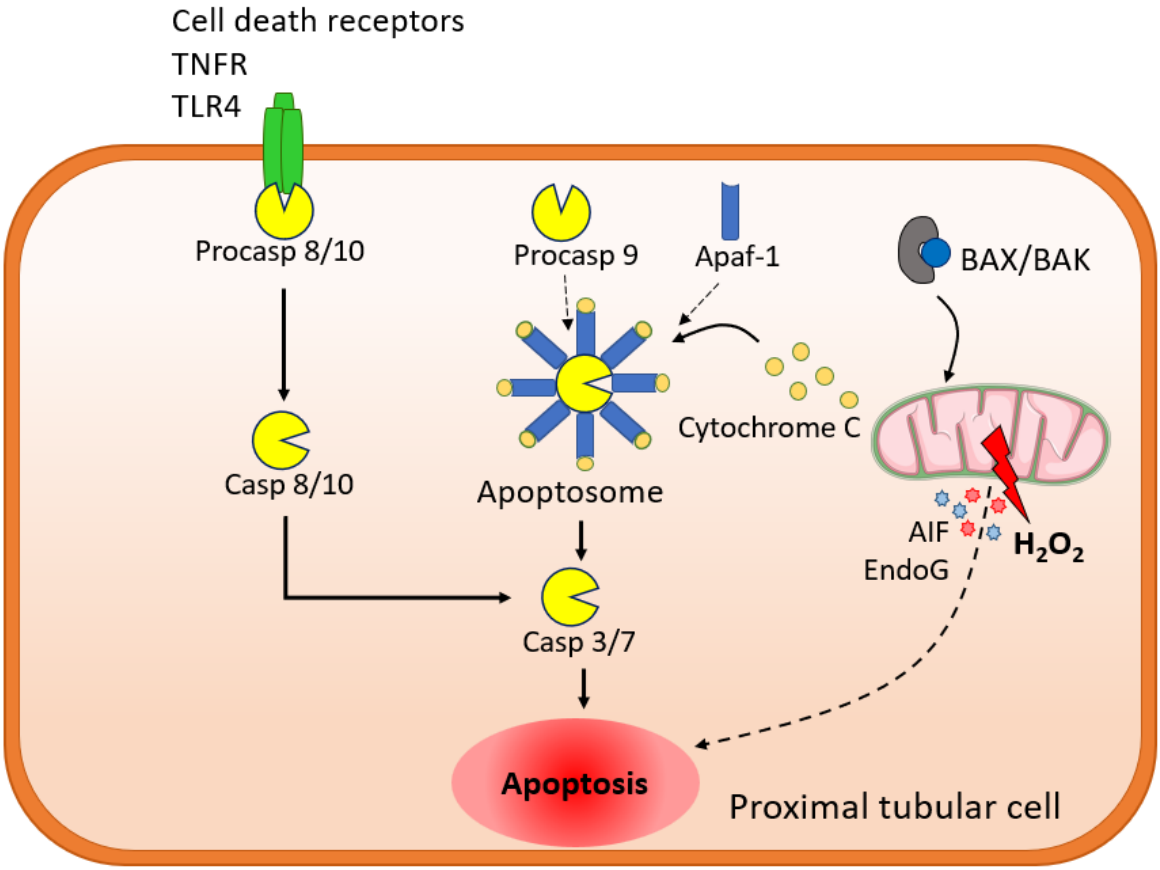

Figure 1-4 The regulation and downstream processes of apoptosis: Caspase-dependent apoptosis can be triggered by exogenous sources via membrane-bound receptors, such as cell death receptors, TNFR, and TLR4, in the extrinsic pathway, or stimulated through intracellular proteins, BAX and BAK, by radiation, oxidative stress, or chemical agents in the intrinsic pathway. Downstream of these events, caspase proteins are activated, leading to cytoplasmic enzyme activation and apoptosis. In caspase-independent apoptosis, apoptosis-inducing factor (AIF) and endonuclease G (EndoG) are released from the mitochondria and translocate into the nucleus for DNA fragmentation.

Apoptosis in kidney transplantation occurs after renal ischemic reperfusion injury. The severity of cell apoptosis can lead to long-term reduced kidney function. The study by Dong et al. demonstrated the relationship between the severity and frequency of IRI and the progression of kidney injury (Dong et al., 2019). In an IRI rat kidney model, severe tubular damage and cell apoptosis from long-duration IRI (45 minutes unilateral IRI) or repeated moderate-duration IRI (30 minutes unilateral IRI at a 7-day interval) led to the progression of acute kidney injury, with high levels of apoptosis shown by TUNEL staining and higher levels of fibrosis marker collagen I on immunohistochemistry. The study by Jain et al. (2020) demonstrated that donor kidneys exposed to cold ischemia had tubular cell apoptosis and

acute tubular necrosis in a transplanted mouse model (Jain et al., 2020). In contrast, there was no acute tubular necrosis or apoptosis in transplanted kidneys without cold ischemia. This study confirmed that IRI is the cause of apoptosis in kidney transplantation.

1.5.2 Kidney fibrosis

Kidney fibrosis is the overgrowth and scarring of kidney tissue due to excessive deposition of connective tissue components (Wynn, 2008; Panizo et al., 2021). Severe IRI can induce tubular cell damage and abnormalities in renal repair, leading to kidney fibrosis (Liang et al., 2018; Chen et al., 2022a). The transition to kidney fibrosis following IRI is mediated by the transforming growth factor-β (TGF-β)-Smad pathway (Okami et al., 2025). Since IRI is a common complication after kidney transplantation, it is essential to understand the basic mechanism of kidney fibrosis.

After IRI, kidney cells release fibrotic progenitor mediators and cytokines such as TGF-β1, IFN-γ, and interleukin-1β (IL-1β), which bind to their receptors on myofibroblasts and interstitial cells in the kidney (Zhao et al., 2022; Li et al., 2022a). Extracellular matrix deposition is activated and formed with fibrotic proteins such as collagen type I (COL I), elastin, fibronectin, and entactin (Kwiecinski et al., 2011; Yu et al., 2023). Excessive extracellular matrix deposition causes fibrosis. This mechanism is reversed by matrix metalloproteinase (MMP) activity, which leads to degradation of the extracellular matrix (Chen et al., 2011a; Zou et al., 2016) (**Figure 1-5**). Thus, inhibition of fibrotic progenitor mediators and promotion of MMP activity are strategies for antifibrotic treatment in a kidney transplantation model.

1.6 Exosomes and microvesicles

Intercellular communication is a hallmark of multicellular organisms which can be mediated by extracellular vesicles (EVs). EVs are membrane-bound vesicles involved in intercellular communication under physiological and pathological conditions. They can be divided into exosomes, microvesicles, and apoptotic bodies. In this chapter, I will focus on exosomes and microvesicles.

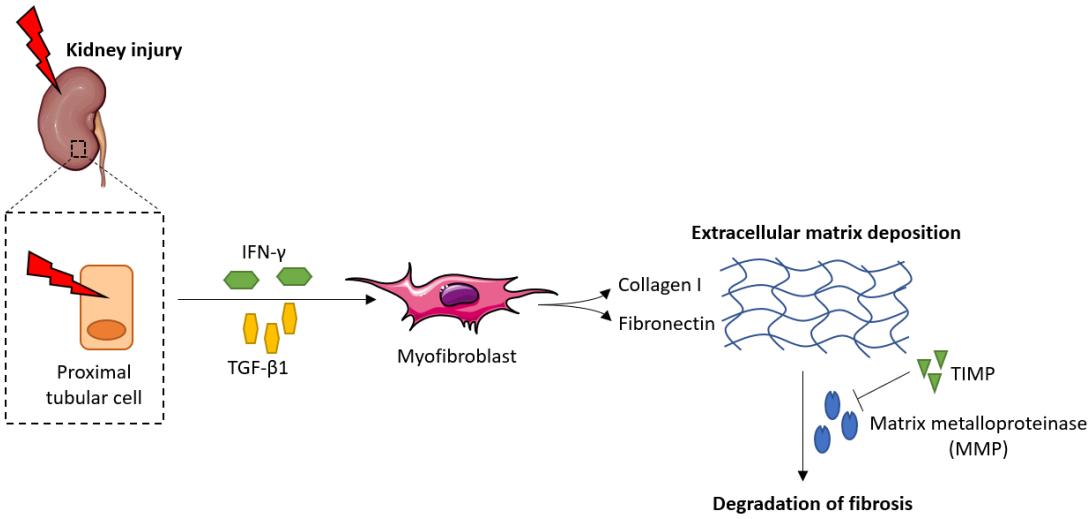

Figure 1-5 Schematic of fibrosis in kidney injury: After kidney injury, renal tubular cells release fibrotic progenitor mediators and cytokines such as TGF-β1, IFN-γ, and interleukin-1β (IL-1β) in response to cellular damage. Myofibroblasts secrete fibrotic proteins such as collagen type I, fibronectin, and entactin into the extracellular matrix. Excessive extracellular matrix deposition leads to pathological healing, or fibrosis. A proteolytic enzyme, matrix metalloproteinase, is activated to degrade extracellular matrix proteins.

An exosome is formed by the invagination of the cell membrane and the formation of an early sorting endosome. Therefore, the surface of exosomes contains components of cell-surface proteins and extracellular components. The size of an exosome is 30–100 nanometres. The regulation of exosome biogenesis involves the endosomal sorting complexes required for transport (ESCRT), tetraspanins, ceramide, and cholesterol lipid domains, which recruit factors for this pathway (Larios et al., 2020). Exosomes reach target cells through endocytosis or by fusing with the target cell membrane, and then release their cargo to activate target cell mechanisms.

Microvesicles are vesicular structures. The size of microvesicles ranges from 100 to 1000 nanometres. The formation of microvesicles occurs through the outward blebbing of the plasma membrane. Therefore, microvesicles have the composition of plasma membranes. They consist of a phospholipid bilayer and transmembrane proteins. The protein markers of microvesicles are annexin V, flotillin-2, selectin, integrin, and CD40 metalloproteinase (Jayachandran et al., 2012). Microvesicles can be extracted using the ultracentrifugation technique. They are considered carriers of proteins, mRNA, and microRNA for intercellular communication. The study by Skog et al. (2008) showed that glioblastoma-derived microvesicles contain angiogenic proteins such as angiogenin,

interleukin-6, interleukin-8, and VEGF, as identified using a human angiogenesis antibody array. Human brain microvascular endothelial cells (HBMVECs), the target cells of glioblastoma in this study, showed changes in tubule formation under electron microscope scanning after treatment with microvesicles compared to the group without microvesicle treatment (Skog et al., 2008). This demonstrated the function of microvesicles in intercellular communication.

In the kidney, the sources of extracellular vesicles are tubular cells and podocytes, which play a role in intercellular communication under both physiological and pathological conditions. Therefore, kidney researchers use these extracellular vesicles as markers of disease and as promising therapeutic agents in kidney disease and kidney transplantation.

1.6.1 Exosomes and the kidney

The content of exosomes excreted in the urine has been used as an indicator of injury in kidney transplantation and kidney diseases. Alvarez and colleagues demonstrated NGAL in urinary exosomes as a marker of delayed graft function (DGF) after kidney transplantation (Alvarez et al., 2013). This study collected urine samples from patients at 24, 48, and 72 hours after kidney transplantation and then extracted the exosome-rich fraction for measurement of neutrophil gelatinase-associated lipocalin (NGAL), a kidney injury marker, using semi-quantitation with western blot analysis. The DGF patients showed higher NGAL expression in urinary exosomes compared to patients without DGF. This implies the importance of exosome function during the development of the DGF process. Another study showed that urinary exosome mRNA of CD2-associated protein correlated with the degree of kidney disease (Lv et al., 2014). Urine exosomes in this study were purified by ultracentrifugation, and then the CD2-associated protein mRNA was extracted using an RNA extraction kit. The level of mRNA in urine exosomes correlates with clinical renal parameters-serum creatinine, blood urea nitrogen, and urine protein-and correlates with the severity of tubulointerstitial fibrosis and glomerulosclerosis. Therefore, the content of exosomes can be a potential source of kidney injury markers from urine exosomes in kidney transplantation and kidney diseases, with a non-invasive technique for sample collection.

1.6.2 Microvesicles and the kidney

Glomerular cells, tubulointerstitial cells, and endothelial cells in the kidney can release microvesicles after stress or damage. Therefore, these released microvesicles (MVs) can be used as indicators of kidney diseases or prognosis in kidney transplantation. Cai et al. (2020) showed that altered MV profiles correlate with diabetic nephropathy progression. In this study, urine samples from both healthy individuals and diabetic nephropathy patients were collected and analysed using flow cytometry. MVs were detected with Annexin V. The findings revealed an increased presence of podocyte-derived MVs in the urine of patients compared to those without nephropathy, indicating vascular damage in individuals with diabetic nephropathy (Cai et al., 2020). These data suggest the utility of MVs as non-invasive biomarkers for early detection and monitoring of the disease. Another study showed that microvesicles from adipose tissue-derived stem cells have therapeutic effects in Wistar rats (Mohammed et al., 2024). Rats were randomly divided into five groups: control with no treatment, control with sodium chloride, positive control with aluminium chloride treatment, positive control with adipose tissue-derived stem cells, and positive control with microvesicles from adipose tissue-derived stem cells. The results showed that microvesicles decrease proinflammatory cytokine IL-1β, apoptotic marker caspase-3, and collagen fibres. These findings indicate the potential of microvesicles as disease progression indicators and for therapeutic use in kidney disease.

Exosomes and microvesicles are useful in the prognosis of kidney disease and progression in kidney transplantation. Therefore, I used these extracellular vesicles in my studies.

1.7 Aims of this project

a) To demonstrate evidence of mesenchymal stem cell therapy in the existing scientific literature through a systematic review.

b) To generate kidney organoids, validate these kidney organoids, and use them as an injury model.

c) To generate kidney tubular cell cultures, validate these tubular cell cultures, and use them as a model to study kidney injury.

d) To examine the therapeutic effects of ADRC, including anti-apoptotic, anti-fibrotic progenitor, anti-oxidative, and proliferative properties in kidney tubular cells.

1.8 Hypothesis

I hypothesize that ADRCs have reparative effects by inhibiting apoptosis, reducing fibrosis, reducing oxidative stress, and reducing inflammation in cellular models of kidney IRI.

Chapter 2: Materials and methods

2.1 Methods for systematic reviews

This systematic review was conducted using the systematic review search engines Rayyan for collecting studies between 1991 and 2020. The studies were imported from seven databases including Medline, PubMed, ZETOC, Web of Knowledge, AMED, EMBASE, and Ovid databases. The studies with the terms “kidney”, “liver”, “lung”, “machine perfusion”, “mesenchymal”, “organ”, “perfusate”, “regenerative”, “solid”, “stem”, and “transplant” were identified and were assessed with specific selection criteria for quality assessment. The inclusion criteria for assessment were research article, non-in vitro research, ex-vivo research, and mesenchymal stem cells used in an organ transplant model. The exclusion criteria for assessment were literature reviews and abstract proceedings. The data were processed for replication from the Rayyan programme and then assessed by two researchers for validity. After assessment, data in exclusion criteria, data in replication, and not relevant to research questions were removed. The missing data were included in the final step by manual handling to complete this study (**Figure 2-1**).

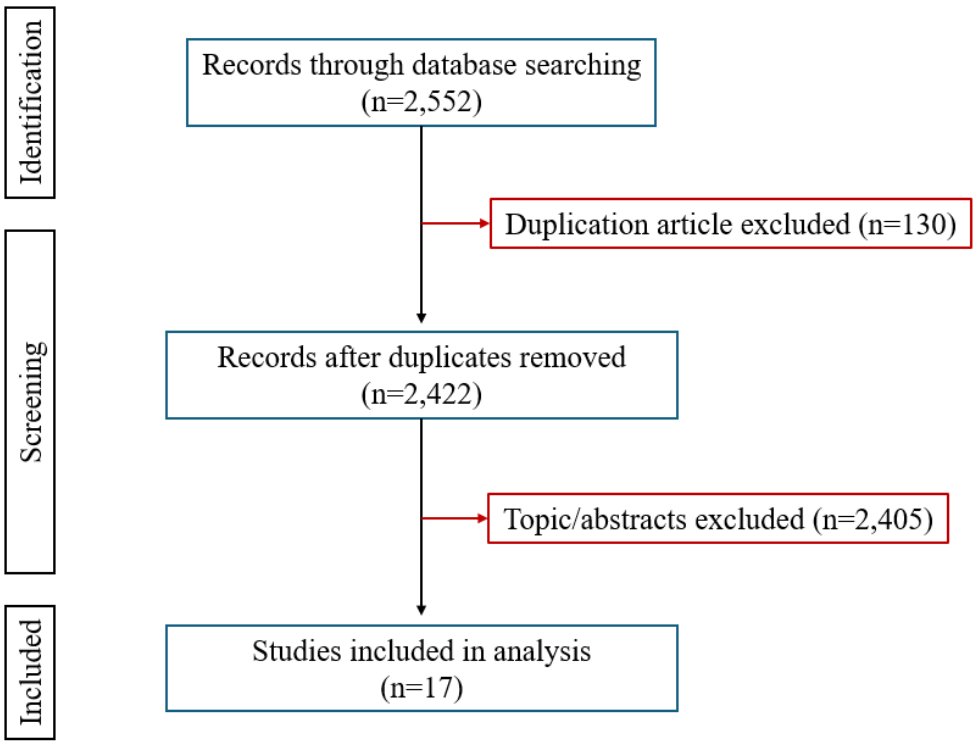

Figure 2-1 Diagram of systematic reviews with included search database and screening

2.2 Materials for laboratory work

Lists of cells, reagents, materials and buffer preparation in this project are shown in **Table 2-1** to **2-5**.

Table 2-1 kidney organoid validation primary and secondary antibodies for immunofluorescence staining

Antibodies	Structural marker	Raised in	Catalogue	Fluorochrome
Primary antibodies:				
Wilms' tumour 1 (Wt1)	Nephron progenitor	Mouse	ab212951	Non-conjugated
Pax2	Ureteric epithelium	Rabbit	ab218058	AF 647
Synaptopodin	Podocyte (glomeruli)	Mouse	sc515842	AF 488
Megalin (H-10)	Proximal tubule	Mouse	sc515772	AF 546
Secondary antibody:				
IgG-kappa	anti-mouse	Mouse	sc516176	CF 488
IgG	anti-rabbit	Mouse	sc516251	CFL 647

Table 2-2 Real-Time PCR Primers on NRK-52E cell experiment

Primer name	Full name/ other name	Marker	Primer sequence (5'-3')
KIM1-F	Kidney injury molecule-1	Tubular injury	AGAGAGAGCAGGAC ACAGGCTT
KIM1-R	Kidney injury molecule-1	Tubular injury	ACCCGTGGTAGTCCC AAACA
NGAL-F	Neutrophil gelatinase associated lipocalin	Tubular injury	GATGTTGTTATCCTT GAGGCCC
NGAL-R	Neutrophil gelatinase associated lipocalin	Tubular injury	CACTGACTACGACC AGTTTGCC
CASP3-F	Caspase 3	Apoptosis – execution pathway	AATTCAAGGGACGG GTCATG
CASP3-R	Caspase 3	Apoptosis – execution pathway	GCTTGTGCGCGTACA GTTTC
BAX-F	BCL2-like protein 4	Apoptosis – intrinsic pathway	AGATCACATTCACG GTGCTG
BAX-R	BCL2-like protein 4	Apoptosis – intrinsic pathway	CTTCAGAGGCAGGA AACAGG
CASP9-F	Caspase 9	Apoptosis – intrinsic pathway	ATGCAGGTCCCTGTC ATG
CASP9-R	Caspase 9	Apoptosis – intrinsic pathway	GCTTGAGGTGGTTGT GGA
SOD1-F	Superoxide dimutase	Oxidative stress	TTCCATCATTGGCCG TA
SOD1-R	Superoxide dimutase	Oxidative stress	AAGCGGCTTCCAGC ATTTC
GAPDH-F	Glyceraldehyde-3-phosphate dehydrogenase	Housekeeping	GGCAAGTTCAACGG CACAG
GAPDH-R	Glyceraldehyde-3-phosphate dehydrogenase	Housekeeping	CGCCAGTAGACTCC ACGACAT

Table 2-3 Lists of cells, reagents, and materials in organoid and NRK-52E cell culture laboratory

Name	Company	Catalogue number
Celase	Cytori	1235-01
StemSource Reagent B (Intravase)	Cytori	940/MB
EASY strainer 40 um	Greiner Bio-One	542-040
EASY strainer 70 um	Greiner Bio-One	542-070
Minimum essential medium (MEM)	Sigma Aldrich	M5650
Dulbecco's Modified Eagle's medium (DMEM)	Gibco	22320-022
Fetal bovine serum (FBS)	Gibco	10500-064
0.5% Trypsin-EDTA (10x)	Gibco	15400-054
Eppendorf 1.5 mL tube	Greiner bio-one	616 201
TC Insert, 12 Well, PET 8µm, TL	Sarstedt AG & Co. KG	83.3931.800
PKH26	Sigma Aldrich	PKH26GL-1KT
NRK-52E cell line	ATCC	CRL-1571
Dulbecco's phosphate-buffered saline (DPBS)	Gibco	14190-094
Penicillin-Streptomycin	Sigma	P0781

Table 2-4 Lists of reagents and materials in bench laboratory

Name	Company	Catalogue number
DNase I, Amplification Grade	Invitrogen	18068-015
QIAzol Lysis Reagent	QIAGEN	79306
RNase Zap	Invitrogen	AM9780
Precision Plus Protein™ (WB ladder)	Bio-Rad	1610377
Caspase-3 Assay Kit (Colorimetric)	Abcam	ab 39401
NovexTM WedgeWellTM 4-20% Tris-Glycine Gel	Invitrogen	XP04205BOX
Bovine serum albumin	Sigma	A7906-100G

Table 2-5 Lists of buffers preparation

Name	Laboratory techniques	Preparation
Immunofluorescence blocking buffer	Immunofluorescence staining	For 100 mL of immunofluorescence blocking buffer, 1. Add 5 g of normal goat serum into 100 mL of Dulbecco's phosphate-buffered saline (DPBS). 2. Add 0.3 mL of Triton®X-100 and then mixing the components.
Protein loading buffer (Laemmli buffer)	Western blot	For 25 mL of protein loading buffer, 1. Mixing of 1.47 g of Tris-HCl, 1.5 g of SDS and 1.2 mL of glycerol and warm at 40°C. 2. After dissolving the components, 2.25 mL of 2-mercaptoethonol and 7.5 of mg bromophenol blue were added. 3. Adjusted pH to 6.8 and add distilled water to 25 mL as a final volume.

2.3 Laboratory techniques for ADRC generation

2.3.1 Animal model and husbandry

Pregnant F344 rats at 13–14 gestation days were used for embryo collection. Both male and female rats were used for adipose tissue collection. All rats were euthanized with carbon dioxide gas. The study protocol was approved by the UK Home Office's ethical committee (protocol license number PPL70/8980). All procedures were performed under the approval of the University of Glasgow Home Office's ethical committee. The breeding and maintenance of rats were conducted under the guidelines of the University of Glasgow Home Office's ethical committee.

2.3.2 Adipose derived regenerative cell (ADRC) generation

Adipose tissues from the left and right inguinal areas were collected and pooled in cold DPBS, then minced with fine surgical scissors until the pieces were less than 4 millimetres in diameter. A concentration of 0.5 Wroblewski units/millilitre (WU/mL) collagenase enzyme (Celase®) was added to the minced tissue for 30-minute digestion. The digested solution was centrifuged, and the supernatant was discarded. DPBS was added to adjust the volume to 25 ml, and 0.125 mg of Intravase® was added. The cell suspension was centrifuged, and the resuspended pellet was filtered through a 70-micron cell strainer and then a 40-micron cell strainer. ADRC-rich pellets were counted using a NucleoCounter®. ADRCs were stored in liquid nitrogen for future use.

2.4 Laboratory techniques for kidney organoid generation

2.4.1 Collection of embryonic metanephros

Embryos were collected at E13.5 and E14.5 in Dulbecco's phosphate-buffered saline (DPBS). Individual embryos were removed with fine scissors and harvested in minimum essential medium (MEM). Each metanephros was dissected with two 26G needles under a stereomicroscope (Olympus model SZH10) and stored in MEM. Pooled metanephric tissue was centrifuged and then trypsinised in 10% trypsin (Sigma-Aldrich) for cell dissociation. After trypsinization, the cell suspension was inactivated with organoid media (Dulbecco's

Modified Eagle's Medium (DMEM) with 10% fetal bovine serum (FBS) and 1% penicillin-streptomycin). Kidney organoids were maintained in organoid media.

2.4.2 Kidney organoid creation

To generate kidney organoids, approximately 150,000 total embryonic cells were used to create each kidney organoid. The embryonic cell suspension was aliquoted into LoBind microcentrifuge tubes (Eppendorf). Tubes were centrifuged to create a compacted pellet and then cultured using an air-liquid interface culture technique. Kidney organoids were assigned to four treatment groups: control (media only), injured, ADRC-treated control, and ADRC-treated injured groups. Injured organoids were treated with 10 µM hydrogen peroxide for 60 minutes at 37°C and then washed twice with organoid media on organoid formation before cell culture, or were exposed to ADRCs for 14 days before being collected for downstream assays.

For treatment with ADRCs, cryopreserved ADRCs were thawed in a water bath, diluted in 10% FBS in DMEM, and then counted using a NucleoCounter®. PKH26 (Sigma-Aldrich protocol) was used for ADRC labelling before treating control and injured kidney organoids. ADRCs at 10,000 to 15,000 cells, or 10% of the embryonic cell number, were used for treatment in the ADRC-treated group in this study. ADRCs were added after grouping, and then ADRC-treated organoids were centrifuged to create a compact pellet (**Figure 2-2**).

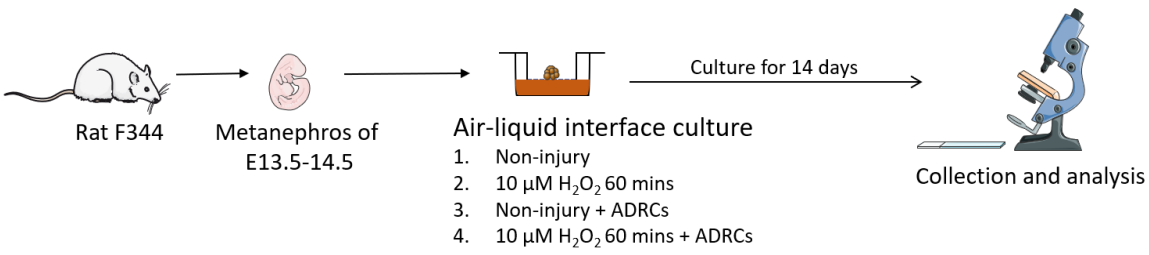

Figure 2-2 Experimental protocol for treatment in kidney organoids. Rat embryos were collected at E13.5–14.5 and then centrifuged to form a compacted pellet. Cell pellets were assigned to four treatment groups: non-injured (media only), injured, ADRC-treated non-injured, and ADRC-treated injured groups. Cell pellets were cultured for 14 days to differentiate into kidney organoids before collection and analysis.

2.5 Laboratory technique for proximal tubular cell culture

2.5.1 Normal rat kidney (NRK) cells

Normal rat kidney clone 52 (NRK-52E) cells are a continuous cell line derived from rat proximal tubular epithelial cells. This cell line was obtained from the European Collection of Authenticated Cell Cultures (ECACC), and passages between 8 and 10 were used in this experiment.

2.5.2. NRK-52E cell culture technique

2.5.2.1. Culture media preparation

Culture media for NRK-52E cells consisted of 10% fetal bovine serum (FBS) and 1% penicillin-streptomycin (P/S) in Dulbecco's Modified Eagle Medium (DMEM). To prepare the culture media, briefly, penicillin-streptomycin and fetal bovine serum (FBS) were thawed in a 37 degrees Celsius (°C) water bath for approximately 15 minutes prior to use. Five millilitres of penicillin-streptomycin and 50 ml of fetal bovine serum were added to a 500 ml bottle of DMEM. Media was aliquoted into 50 mL conical tubes until use.

2.5.2.2. Thawing cells

Pre-warmed culture media, a sterile rack, a 15 mL conical tube, and a T150 flask were transferred to a biosafety cabinet. Frozen cells were carried on dry ice from a liquid nitrogen container and warmed in a 37°C water bath by gently swirling until a small ice crystal remained. The whole contents of the thawed tube were pipetted into a 15 mL conical tube. Ten millilitres of culture media were gently pipetted dropwise at the side of the tube and gently resuspended by pipetting 2–3 times. The cell suspension was centrifuged at 150 x g for 5 minutes at room temperature. During centrifugation, 20 ml of culture media was added to the T150 flask. After centrifugation, the supernatant was discarded, and 2 ml of pre-warmed culture media was added to the 15 mL conical tube. The cell pellet was gently resuspended by pipetting, and the cell suspension was transferred to the prepared T150 flask. The flask was rotated forward-backward and left-right 4–5 times to evenly distribute the cells. The flask was incubated in an incubator set to 37°C and 5% carbon dioxide (CO_2). Culture media was changed every second day.

2.5.2.3. Changing culture media

Culture media was warmed in a 37°C water bath for 15–20 minutes prior to use. The T150 flask with cells was transferred to a biosafety cabinet. Old culture media was aspirated using vacuum aspiration, and 20–25 ml of fresh culture media was added to the flask. The flask was returned for incubation at 37°C / 5% CO_2.

2.5.2.4. Subculture

When the cells are approximately 80–90% confluent, subculture is required to maintain the cell line. Pre-warmed culture media, Dulbecco's phosphate-buffered saline (DPBS), and 0.05% trypsin were thawed in a 37°C water bath. A confluent cell culture flask was transferred to a biosafety cabinet with a new T150 flask labelled with the cell line name, passage number, date, and name of experimenter. Old culture media was aspirated, and the NRK-52E cells were washed with warmed DPBS twice. The cells were then treated with 2 ml of 0.05% trypsin, enough to sufficiently cover the entire surface area, and were incubated in a 37°C incubator for 1–2 minutes. The cells were checked for detachment under the microscope, and the dissociation reaction was subsequently inhibited by adding at least twice the volume of trypsin with culture media (10% FBS, 1% P/S, DMEM). The cell suspension was resuspended, aliquoted to a new flask using a 1:6 split ratio, and then incubated in a 37°C / 5% CO_2 incubator.

2.5.2.5. Freezing cells

NRK-52E cells are ready to be frozen when they are approximately 80–90% confluent. Freezing media can be prepared in advance and consists of 70% culture media, 20% fetal bovine serum (FBS), and 10% filtered dimethyl sulfoxide (DMSO). Steps of cell dissociation are the same as in the subculture dissociation technique. After inhibiting the cell dissociation reaction with FBS culture media, a total viable cell count and a total non-viable cell count were done using trypan blue exclusion and cell counting with a haemocytometer. The appropriate number of viable cells per cryovial tube should be 1,000,000 to 2,000,000 cells. The cell suspension was centrifuged at 150 x g for 5 minutes at room temperature. The supernatant was discarded, and freezing media was added to the cell pellet. The volume of freezing media is 1 ml per aliquot. The appropriately diluted cell pellet was resuspended by gently pipetting and aliquoted into pre-labelled 1.5 ml cryovial tubes. These tubes were kept

in a freezing container (Mr. Frosty®) and stored at -80°C overnight. After this slow cooling, the following day the cryovial tubes were transferred to a liquid nitrogen tank (approximately -196°C).

2.5.3 NRK-52E cell injury induction

Cells were cultured with 10% w/v fetal bovine serum and 1% w/v penicillin-streptomycin in Dulbecco's Modified Eagle Medium (DMEM) at 37°C in 5% CO_2, and cell adherence was disrupted using a 0.05% trypsin/EDTA solution. In a model validation experiment, cells were seeded onto 6-well plates and were 80% confluent for the experiment. Cells were treated with hydrogen peroxide at 0, 100, 300, and 500 µM concentrations with differing incubation times of 1, 2, 4, and 24 hours to induce injury and then were washed twice with Dulbecco's phosphate-buffered saline before collection at 24 hours after exposure to hydrogen peroxide. The suitable dose and incubation time were used for the ADRC treatment experiment (**Figure 2-3**).

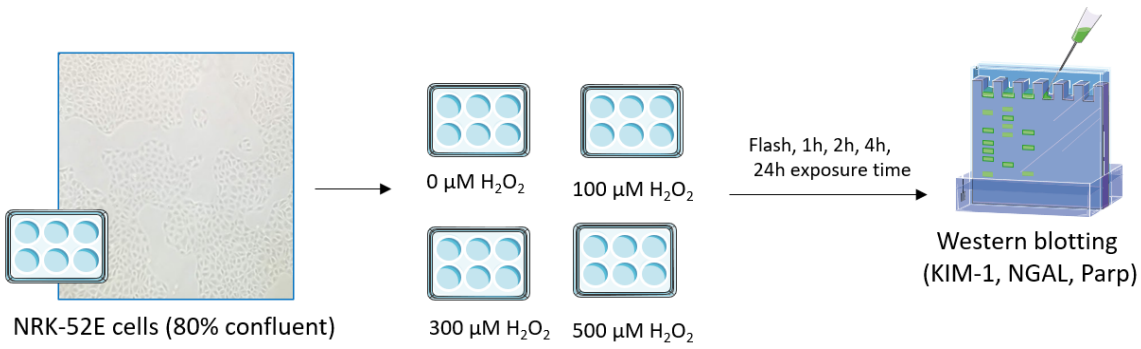

Figure 2-3 Experimental protocol for validation of injured NRK-52E cells. NRK-52E cells were seeded and collected at 80% confluence. These cells were then exposed to hydrogen peroxide at 0, 100, 300, and 500 µM with different incubation times, including 1, 2, 4, and 24 hours, for injury induction before being collected at 24 hours for laboratory analysis.

After model validation, a 4-hour induction with 500 µM hydrogen peroxide was used subsequently in this study. NRK-52E cells were seeded onto 6-well plates and were 80% confluent for the experiment. Four experimental groups were assigned and included: 1) non-hydrogen peroxide exposure, 2) non-hydrogen peroxide exposure with 10% ADRC treatment, 3) 500 µM hydrogen peroxide exposure for 4 hours, and 4) 500 µM hydrogen peroxide exposure for 4 hours with 10% ADRC treatment. These cells were then collected for analysis after 24 hours. (**Figure 2-4**).

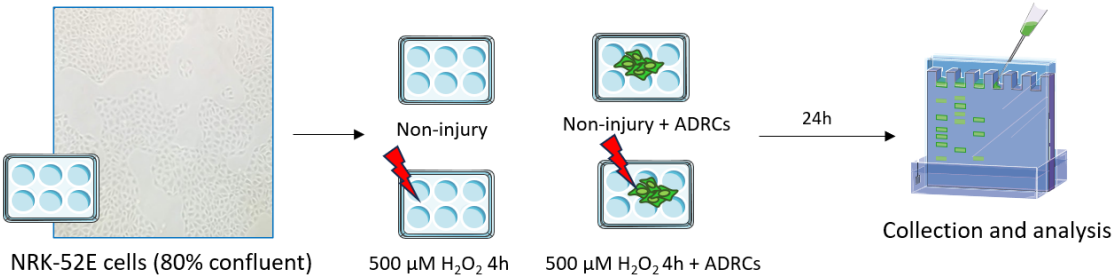

Figure 2-4 Experimental protocol for ADRC treatment of injured NRK-52E cells. NRK-52E cells were assigned to four experimental groups: non-injury, non-injury with ADRC treatment, hydrogen peroxide-induced injury, and hydrogen peroxide-induced injury with ADRC treatment.

2.6 Other biological assays

2.6.1 Immunohistology

Immunofluorescence staining is an immunological laboratory technique used for detecting specific proteins on a histological slide. Kidney organoid sample slides or NRK-52E cell sample slides were incubated with blocking buffer, which consisted of 5% normal goat serum and 0.3% Triton® X-100 in DPBS, for 60 minutes at room temperature. Primary antibody was applied, and samples were incubated overnight at 4°C in the dark. Samples were rinsed three times with DPBS for 5 minutes each at room temperature. Secondary antibody was applied for 1 to 2 hours at room temperature in the dark, and samples were washed three times with DPBS for 5 minutes each at room temperature. ProLong™ Gold Antifade reagent with 4′,6-diamidino-2-phenylindole (DAPI) was applied to the sample slides, which were then covered with a coverslip at room temperature overnight in the dark. Sample slides were kept at 4°C for longer storage.

2.6.2 Bicinchoninic acid (BCA) assay

Bicinchoninic acid (BCA) assay is a method to quantify protein concentration. This procedure followed the Pierce BCA Protein Assay Kit protocol (#23225; Thermo Fisher). A working solution was prepared by mixing solution A and solution B in a 50:1 ratio in a 10 mL conical tube. Frozen protein samples were thawed and 25 µL was loaded onto a microplate in duplicate. Then, 200 µL of the working reagent was added to each well using a multi-channel micropipette. The microplate was thoroughly mixed on a plate shaker at 350 rpm for 30 minutes and then incubated at 37°C for 30 minutes. The microplate was cooled to room temperature before measuring protein concentration with the SoftMax Pro program. For quantitation, sample protein concentration was compared to the protein standard.

2.6.3 Western blot analysis

Cells were treated with 50 µL of lysis buffer per well of a 6-well plate, then scraped using a cell scraper and transferred to new labelled Eppendorf tubes. Lysis buffer suspensions were sonicated for 5 seconds to disrupt cellular membranes and release the cell contents. The cell suspensions were then centrifuged at 13,000 x g for 10 minutes at 4°C to sediment cell debris. The supernatant was collected into a new Eppendorf tube, and the pellets were discarded. The supernatant can be stored at -20°C or -80°C for future use. The total protein of lysates was quantified using the bicinchoninic acid (BCA) protein assay (Pierce™ BCA Protein Assay Kit, Thermo Scientific, #23227), and absorbance was measured at 562 nanometres by spectrophotometry. Before running in the gel, a 30-µg total protein sample was prepared with distilled water. One volume of 6x loading buffer (Laemmli buffer) was added to five volumes of protein sample. The loading buffer included β-mercaptoethanol to break disulfide bonds in proteins and SDS to denature the proteins and add a negative charge. The samples were boiled at 95°C for 5 minutes in heated Eppendorf blocks in the fume hood to denature the proteins and then briefly centrifuged to eliminate condensation before western blotting or storage at -20°C.

2.6.4 Trypan blue exclusion test of cell viability

NRK-52E cells were treated with 200 µL of 0.05% trypsin per well of a 6-well plate. The solution covered the entire surface area, and plates were incubated in a 37°C incubator for 1 minute. The cells were checked for detachment under the microscope, and the dissociation

reaction was subsequently inhibited by adding 800 µL of culture media. The cell suspensions were stained with trypan blue at a 1:2 dilution. Viable and non-viable cells were counted using a haemocytometer under a microscope.

2.6.5 Nanoparticle tracking analysis

Cell culture media (supernatants) were used for nanoparticle analysis by ultracentrifugation with an exosome isolation technique. Crude exosomes and microvesicles were then measured using nanoparticle tracking analysis (Nanosight®). For exosome isolation, the following steps were taken: 100 µL of NRK-52E cell culture medium was collected and stored at -20°C. After thawing at room temperature, supernatants were transferred to a new Eppendorf tube and diluted with DPBS (1:20 dilution factor). The supernatant was separated using differential centrifugation, and pellets were discarded afterwards. Samples were first centrifuged at 480 x g at 4°C for 5 minutes to remove intact cells, and then centrifuged a second time at 2,000 x g at 4°C for 10 minutes to remove cell debris. Sample tubes were then weighed for balancing before using the ultracentrifuge. The volume of solution after ultracentrifugation decreased by approximately 30–40% from the original 1,000 µL due to evaporation. Supernatants were centrifuged with ultracentrifugation at 100,000 x g (42,906 rpm; radius of rotor 48.5 mm, Beckman TLA 100.4) at 4°C for 60 minutes for crude exosome and microvesicle extraction. After ultracentrifugation, crude exosome and microvesicle pellets were transferred to a new Eppendorf tube and adjusted to a 1,000 µL volume with DPBS. Crude exosome and microvesicle suspensions were stored at -80°C until further use.

2.6.6 Real Time Reverse transcription polymerase chain reaction (RT-PCR)

2.6.6.1 RNA extraction

Medium was aspirated from the NRK-52E cell culture plate. The cells were washed twice with cold sterile DPBS and the culture plate was kept on ice. Cells were lysed with 500 µL of Qiazol per well of a 6-well plate and 750 µL per 60 millilitre Petri dish. Cells were homogenized by pipetting and transferred to Eppendorf tubes. These samples can be kept at -80°C for long-term storage. To each Qiazol sample, 200 µL of chloroform was added and gently shaken for 15 seconds. Sample suspensions were incubated at room temperature for 2 minutes for phase separation. Sample suspensions were centrifuged at 12,000 x g for 15 minutes at 4°C. After centrifugation, sample suspensions separated into three phases: an aqueous phase containing RNA, an interphase containing protein and DNA, and an organic

phase containing DNA. The aqueous phase of the samples was transferred to new Eppendorf tubes, avoiding the interphase to prevent DNA contamination. To each aqueous phase sample, 500 µL of isopropanol was added, inverted 15–30 times, and then incubated at room temperature for 15 minutes. After incubation, aqueous samples were centrifuged at 12,000 x g for 10 minutes at 4°C. Supernatants were carefully discarded using a P200 pipettor. Pellets were washed with 500 µL of cold 75% ethanol in nuclease-free water and centrifuged at 7,500 x g for 5 minutes at 4°C. The RNA samples appeared as a white pellet. Supernatants were carefully discarded using a P200 pipettor. These tubes were air-dried by inverting the tube until no residual ethanol remained. Dried RNA samples were dissolved in 100 µL DNase-free water before quantifying concentration with a spectrophotometer (Nanodrop™).

2.6.6.2 DNase I treatment

To remove DNA contaminants from RNA samples, RNA samples were treated with DNase I. A digestion mix was prepared from four components: 1 µg of RNA sample, 1 µL of 10X DNase I reaction buffer, 1 µL of DNase I (1 unit/µL), and DEPC-treated water to adjust the volume to 10 µL. The volume of each reagent was adjusted based on the amount of RNA. Reaction tubes were prepared with 1 µL of digestion mix and incubated for a maximum of 15 minutes. The DNase I enzymatic reaction was activated by adding 1 µL of 25 mM EDTA solution to the reaction mix. Therefore, the total volume of the reaction was 11 µL. The DNase reaction was stopped by heating at 65°C for 10 minutes, and then the reaction tubes were transferred to ice.

2.6.6.3 cDNA synthesis

Template RNA was annealed with random hexamers and dNTPs, and then reverse transcriptase was added to generate cDNA from the RNA samples. The total volume in a single reverse transcription reaction in this procedure was 20 µL, and the total reaction volume was increased by multiplying by the number of samples. To create annealed RNA, 1 µL of 50 µM random hexamers and 1 µL of 10 mM dNTPs were added to the template RNA from the 11 µL reaction mix in the previous reaction. The reaction components were mixed, briefly centrifuged, and heated at 65°C for 5 minutes. The reaction was then stopped by incubating on ice for at least 1 minute while waiting to be mixed with the reverse transcription reaction master mix. To create the master mix, 4 µL of 5x SuperScript™ IV buffer, 1 µL of 100 mM DTT, 1 µL of RNaseOUT recombinant RNase inhibitor, and 1 µL of 200 units/µL SuperScript IV reverse transcriptase were mixed and briefly centrifuged. The annealed RNA and the reverse transcription reaction master mix were combined by

pipetting and incubated with gradually increasing temperature. Incubation times for the combined components included three phases: incubation at 23°C for 10 minutes, incubation at 50–55°C for 10 minutes, and then incubation at 80°C for 10 minutes to inactivate the reaction. The cDNA template was kept at -20°C or -80°C for long-term storage.

2.6.6.4 Real time PCR

The cDNA templates were thawed and kept on ice during this procedure. These templates were adjusted to a concentration of 10 ng/µL by diluting with DNase-free water. A master mix of primers was prepared for one 10-µL reaction by combining four components: 5 µL of 2X Fast SYBR® Green master mix, which is a fluorescence marker for generated DNA strands; 300 nM of forward primer solution; 300 nM of reverse primer solution; and 1.4 µL of nuclease-free water as a diluent. The cDNA templates were loaded at the bottom of each well in duplicate on an optical plate, and the master mix of primers was then loaded on top of the templates. The optical plate was sealed with a sealing film and briefly centrifuged at 3,000 rpm for 5 seconds. Air bubbles were checked and removed. The PCR reaction of cDNA templates was performed using a real-time PCR machine (QuantStudio™). The maximum cycle number was set at 40. Melting-curve analysis was used to identify the specificity of the primers (**Figure 2-5**).

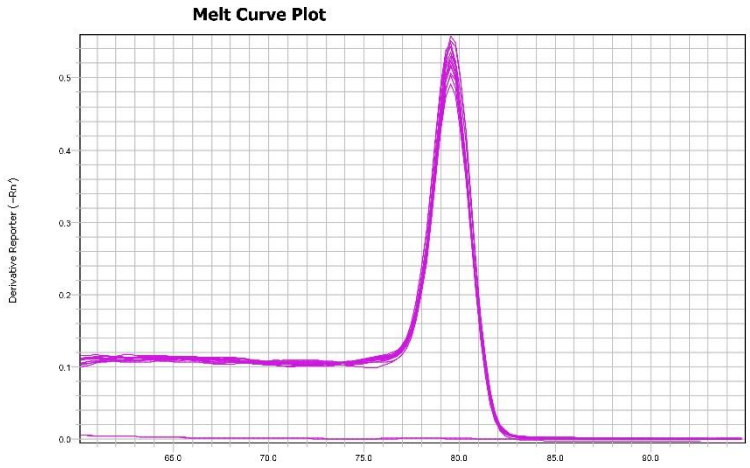

Figure 2-5 An example of melting-curve analysis of GAPDH. GAPDH is the housekeeping gene used as a reference gene in RT-PCR assays for gene expression analysis in this study.

2.6.7 Flow cytometry

NRK-52E cells were cultured and treated with four different treatments. ADRCs were applied directly to NRK-52E cells in BrdU and 7-AAD experiments and were applied through transwell membranes in the Ki-67 antibody experiment. The cells were collected using 0.05% trypsin in EDTA and kept in Eppendorf tubes on ice. Samples were washed twice with cold DPBS for 5 minutes each. Supernatants were carefully discarded using a pipette. Sample volumes were adjusted to 50 µL with cold DPBS. An eFluor 780 fluorescence viability dye was used at 0.5 µL in 50 µL per sample. Stained cells were vortexed immediately and incubated for 30 minutes on ice in the dark. The cells were washed twice with cold DPBS for 5 minutes each. One million stained cells per tube were used, resuspended with 4% paraformaldehyde in DPBS for 15 minutes, washed twice with cold DPBS, and then resuspended in cold 1% BSA in DPBS. Cells were stored at -20°C before running the experiment the following day. Cell samples were thawed at room temperature and washed twice with cold DPBS for 5 minutes each. The cell suspensions were incubated with 70% ethanol for 30 minutes on ice, then washed twice with cold DPBS by centrifugation, and resuspended in cold 2% BSA in DPBS. Primary antibody was added to these samples, and samples were incubated on ice in the dark for 30 minutes. Samples were washed twice with cold DPBS for 5 minutes. Secondary antibody was added to the samples, and samples were incubated on ice in the dark for 20 minutes. Fluorescence-stained samples were washed twice with cold DPBS by centrifugation and filtered through a 40 µM strainer to remove artifacts. These cells were run on a FACS Canto flow cytometer, and recorded events were set to capture 10,000 cells at medium flow.

2.6.7. Caspase-3 activity assay

NRK-52E cells from four experimental groups were cultured and collected using the 0.05% trypsin procedure as described in 2.5.1.4. The caspase-3 activity assay followed the caspase-3 assay kit (colorimetric) protocol (Abcam; ab39401). Briefly, the cells were normalized to 5,000,000 cells in every sample. Cell suspensions were resuspended in 50 µL of chilled cell lysis buffer and incubated for 10 minutes. Cell suspensions were centrifuged at 10,000 x g for 1 minute, and supernatants were transferred to new Eppendorf tubes on ice. These sample supernatants were stored at -80°C. Sample supernatant protein concentrations were measured, and then samples were loaded into a 96-microwell plate at a concentration of 100 µg protein per 50 µL cell lysis buffer for each well. Cell lysis buffer suspensions, 2X reaction

buffer, and dilution buffer were equilibrated to room temperature before starting the procedure. All samples, positive control, and blank (2X reaction buffer) were duplicated in this procedure. Fifty microlitres of 2X reaction buffer and samples were loaded into blank and sample wells. A master mix was prepared using 50 µL of 2X reaction buffer with 0.5 µL of dithiothreitol (DTT) per reaction and then 50 µL was loaded into each well. An amino acid sequence DEVD-pNA substrate, which is a substrate of caspase-3, was added to the reaction. This peptide substrate is cleaved to free p-nitroaniline (pNA), a colorimetric substrate, and was quantified by spectrophotometric detection (Peterson et al., 2010). Five microlitres of a 4 mM DEVD-pNA substrate was added to each well. The microplate was gently shaken and incubated at 37°C in an incubator for 120 minutes. The microplate was measured using a spectrophotometer at an optical density (O.D.) of 400–405 nanometres. The absorbance of samples and positive control was subtracted by the absorbance of the blank before calculating fold change relative to the positive control.

2.7 Graphic illustration

The figures in this thesis were drawn using Microsoft PowerPoint 365, and some images adapted from Servier Medical Art (https://smart.servier.com/), licensed under CC BY 4.0 (https://creativecommons.org/licenses/by/4.0/).

2.8 Statistical analysis

Data are presented as mean ± standard error of the mean. Statistical analysis was performed with the Mann-Whitney U-test to compare between two experimental groups and with the Kruskal-Wallis H test with Dunn's multiple comparisons test as a post-hoc analysis to compare more than two experimental groups, using GraphPad Prism 8, with $P<0.05$ and $P<0.01$ considered statistically significant.

Chapter 3: Systematic review: therapeutic effects of mesenchymal stem cells in preclinical and clinical studies

3.1 Introduction

Kidney transplantation is the gold standard treatment for end-stage kidney disease (ESKD). The need for increasing numbers of kidney transplants is gradually rising over time. This drives donor policy to accept organs from expanded criteria donors (ECD) in efforts to increase the pool of available donor organs. However, this may increase the risk to recipients by providing more 'marginal' kidneys from ECDs. The main consequence of ECD is an increased risk of delayed graft function (DGF). Risk factors for DGF include expanded criteria donors (ECD), donation after circulatory death (DCD) donors, prolonged warm (WIT) or cold ischaemia time (CIT), and recipient sensitization (Summers et al., 2015). In this context, ischaemic reperfusion injury (IRI) is identified as a primary cause of DGF. Therefore, the focus of kidney transplantation research is to mitigate IRI and its associated events.

Regenerative cell therapy is a new therapeutic option to restore graft health after IRI. These cells are a heterogeneous population and include mesenchymal stem cells, other progenitor cells, fibroblasts, T-cells, and macrophages. Mesenchymal stem cells have demonstrated efficacy in both preclinical and clinical studies. In preclinical research, adipose mesenchymal stem cell treatment reduces apoptotic cell numbers, total urinary protein, and pro-inflammatory cytokines, while enhancing anti-inflammatory cytokines and anti-apoptotic regulators in an ischemia-reperfusion injury (IRI) rat model. Additionally, mesenchymal stem cells from adipose tissue restore damage and necrosis in renal tubular epithelial cells, leading to decreased expression of pro-inflammatory cytokines and fibrotic progenitor mediators such as tumour growth factor (TGF)-β, tumour necrosis factor (TNF)-α, interleukin (IL)-6, and interferon (IFN)-γ in surgical IRI rats (Zhang et al., 2017). In a clinical study, mesenchymal stem cells enhance urine output, improve microvascular perfusion, decrease expression of the kidney injury biomarker NGAL, downregulate the inflammatory cytokine interleukin (IL)-1β, and upregulate the anti-inflammatory cytokine IL-10 in kidney transplantation (Hosgood et al., 2018). Previous research highlights the therapeutic effects of mesenchymal stem cells. In this chapter, the impact of mesenchymal stem cells on a solid organ model through systematic analysis is explored. The study of mesenchymal stem cells on a liver transplantation model was included to expand the

literature search to the effects on other solid organ transplantation models, particularly as liver transplantation also entails IRI injury and need for organ preservation and to increase the number of studies in this chapter.

3.2 Aim

To investigate the potential therapeutic effects of mesenchymal stem cells in solid organ transplant models.

3.3 Results and interpretation

Overall, 2,522 records were identified (**Figure 3-1**). After removal of 130 duplicates, 2,422 abstracts were screened against eligibility criteria, and 2,405 records were excluded. A total of 17 studies were included in the final analysis. The main results of kidney and liver transplantation model studies in this systematic review are shown in **Tables 3-1** and **3-2**.

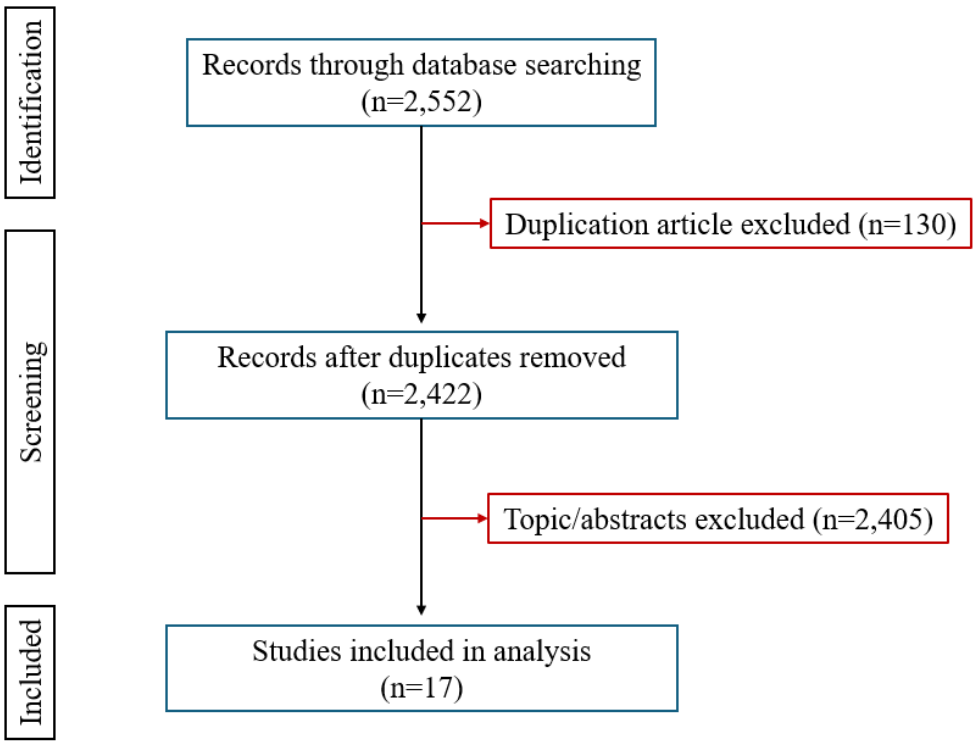

Figure 3-1 Diagram of systematic reviews with included search database and screening.

Table 3-1 Characteristics and main results of kidney transplantation model studies

Theme	Study	Subject Model	Sample size	Source of MSCs	Objectives	Main Outcome Measures	Key Findings
Kidney	Gregorini et al., 2017	Sprague-Dawley rats	15	Sprague-Dawley rats	Assess role of MSC-derived ECV 4 hours of hypothermic perfusion	1) Degree or ischaemic damage, 2) Lactate production, 3) Glucose consumption	• ECV can preserving enzymatic processes for protect IRI.
	Sierra Parraga et al., 2019	Porcine	15	Human and porcine	Assess the impact of normothermic perfusion conditions on peri-renal adipose-derived MSC	1) MSC viability, 2) ROS production, 3) Endothelial Cell Adhesion	• Human MSC more resistant to perfusate suspension and freeze-thawing process. • MSC-endothelial cells adhesion was reduced by perfusate. • Increase in pro-inflammatory cytokines with perfusate.
	Pool et al., 2019	Porcine	12	Human	Feasibility of delivering MSCs during 7 hours of normothermic perfusion	1) Localization of MSC, 2) Cell viability	• MSC localized to glomerular capillaries in a dose-dependent manner. • Viability reduced to 10% following perfusion.
	Brasile et al., 2019	Human	10	Human	Delivery of MSC via exsanguinous metabolic support (non-RBC based perfusion) for 24 hours	1) Cytokine production, 2) Histological analysis, 1) Functional parameters	• Increased ATP synthesis • Reduced IL-6 and IL-10 • Increase in markers of mitosis. • No change in functional parameters.
	Pool et al., 2020	Porcine	15	Human	Assess impact of MSC delivery during 7 hours of normothermic perfusion.	2) Lactate production, 3) NGAL, 4) Cytokine production, 1) Renal blood flow	• No different in functional outcomes (i.e. blood flow, urine output) • Reduced levels of lactate, NGAL and NAG
	Emily R Thompson et al., 2020	Human	10	Human	Bone marrow derived MSC delivered to untransplantable kidney grafts perfused for 7 hours	2) Functional parameters, 3) Markers for IRI	• Improved urine output • NGAL reduced, but no difference evident in KIM-1 • Improved medullary blood flow. • Anti-inflammatory IL-10 increased in MSC group. • MSC localized to glomeruli.

Table 3-2 Characteristics and main results of liver transplantation model studies

Theme	Study	Subject Model	Sample size	Source of MSCs	Objectives	Main Outcome Measures	Key Findings
Liver	Rigo et al., 2018	Wistar rats	19	Human liver stem cells	Human liver stem cell-derived extracellular vesicles (EV) delivered via normothermic perfusion for four hours.	1) Bile production, 2) Oxygen consumption and transaminase levels 3) Histopathology	• Reduced evidence of necrosis and apoptosis • AST and ALT less elevated in EV treatment group. • No difference in bile production. • Protective against hypoxic injury.
	Laing et al., 2020	Human	6	Multipotent adult progenitor cells (MAPC®)	Delivery of multi-potent adult progenitor cells (MAPC) during normothermic perfusion for 6 hours via portal vein or hepatic artery	1) Functional parameters, 2) Organ viability, 3) Lactate levels, 4) Cytokine production	• MAPC delivery upregulated cytokines including IL-4, IL-5, Il-6, IL10 and MCP-1. • Delivery via hepatic artery appeared to improve delivery of cells to vascular endothelium compared to portal vein delivery.
	Yang, Cao, Sun, Hou, et al., 2020	Sprague-Dawley rats	10	Sprague-Dawley rats	Delivery of BM-MSC to livers via normothermic perfusion for up to 8 hours	1) Histopathology, 2) Functional parameters	• Less vacuolar degeneration, sinusoid congestion and inflammatory cell infiltrate with MSC treatment. • Reduced mitochondrial damage, inhibition of macrophage. Activation with MSC treatment. • Improved bile production and lactate clearance.
	Yang, Cao, Sun, Lin, et al., 2020	Sprague-Dawley rats	20	Sprague-Dawley rats	Delivery of BM-MSC to livers via normothermic perfusion for up to 8 hours with corroboration of findings against IAR20 in vitro model	Downstream mechanism analysis, histological analysis.	• Reduced ROS production, mitochondrial damage and increased the mitochondrial membrane potential. • Downregulated the activation of JNK-NF-kappa-B and upregulated AMPK activation.

3.3.1 Anti-inflammation properties of mesenchymal stem cells

The study by Pool et al. (2020) was conducted in porcine kidneys perfused for 7 hours with 10,000,000 cells of cultured human adipose-derived MSCs or 10,000,000 cells of cultured human bone marrow-derived MSCs using normothermic machine perfusion (NMP) (Pool et al., 2020). The concentrations of proinflammatory cytokines IL-6 and IL-8 in the MSC-treated groups were lower than those in the control group, and the lowest levels of IL-6 and IL-8 were found in the adipose-derived MSC-treated group. These findings demonstrated that MSCs can mitigate inflammation by decreasing IL-6 and IL-8 production in the kidney. There are few studies comparing bone marrow- and adipose-derived MSCs (Ammar et al., 2015; Yoshida et al., 2023). The survivability of post-treatment MSCs, their persistence within the injured environment, and the persistence of soluble MSC-derived factors were not addressed in this study, and the cross-species experiment between human MSCs and porcine kidneys might raise questions about the immune response to using human MSCs in porcine kidneys.

Thompson et al. (2020) investigated the effects of stem cells in human kidneys by using commercial multipotent adult progenitor cells (MultiStem®) with normothermic machine perfusion (Thompson et al., 2020). The proinflammatory cytokine IL-1β was downregulated in the stem cell-treated group, and the potent anti-inflammatory cytokine IL-10 was upregulated compared to the group without stem cell treatment. In addition, neutrophil recruitment was decreased in the group with stem cell treatment. This indicated the potential anti-inflammatory property of stem cell treatment in a clinical study. This ex vivo study did not observe long-term outcomes and used a sample size of 5 samples per group, which might affect the statistical power.

The study by Brasile et al. (2019) was conducted with exsanguinous metabolic support in paired human kidneys with warm perfusion for 24 hours (Brasile et al., 2019). The proinflammatory IL-1β and IL-6 in the mesenchymal stem cell treatment group were lower than in the control. Taken together, these studies corroborate the hypothesis that MSCs serve as anti-inflammatory agents in injured kidneys.

3.3.2 Mesenchymal stem cell improving cell regeneration and reducing cellular apoptosis

Proliferating cell nuclear antigen (PCNA) is a ring-shaped DNA clamp in eukaryotes that encircles a DNA parent strand and interacts with DNA polymerase III during DNA replication (Kubota et al., 2013; Strzalka and Ziemienowicz, 2011).

Brasile et al. (2019) investigated the effect of MSCs on cellular regeneration in human kidneys with warm perfusion (Brasile et al., 2019). The results showed that MSC-treated kidneys had higher positive signals of PCNA in immunofluorescence staining and a higher presence of mitotic figures in toluidine blue staining compared to control kidneys. These results indicated the effect of MSCs on cellular regeneration in kidneys. This study demonstrated strength in its design by comparing paired kidneys from the same donor and using different dosages of MSCs. However, there were only 5 pairs of human kidneys, and the study assessed only the immediate effects of MSCs. Longer MSC exposure times within the kidney should be investigated.

Rigo et al. (2018) demonstrated an anti-apoptotic effect of MSCs in normothermic hypoxic liver in male Wistar rats with normothermic machine perfusion (Rigo et al., 2018). Extracellular vesicles of human liver stem cells were used in this study, and TUNEL assay was used to detect cellular apoptosis. The histology revealed that the apoptosis index in the extracellular vesicle-treated group was lower than that in the untreated group. This visualization indicated the anti-apoptotic property of MSCs through extracellular vesicle shedding. This study used an ex vivo hypothermic liver model to mimic IRI in liver transplantation. However, an in vivo model should be studied to confirm the anti-apoptotic property and safety of MSCs. Moreover, there was no mention of the apoptotic mechanism, for example, caspase activation of apoptosis.

3.3.3 Anti-oxidative properties of mesenchymal stem cells

Gregorini et al. (2017) investigated the effects of extracellular vesicles and mesenchymal stem cells in Fischer F344 rats during cold ischaemic time (4 hours at 4°C) (Gregorini et al., 2017). The study groups included kidneys perfused with Belzer solution (BS), BS with 3 million bone marrow mesenchymal stem cells from EGFP-transgenic Sprague–Dawley rats, and BS with extracellular vesicles from mesenchymal stem cells. Malondialdehyde (MDA),

a marker of oxidative stress, was quantified using the HPLC method. The results showed that MDA levels were higher in BS kidneys compared to the BS with MSCs and BS with EV groups. This study did not explore dose optimization of MSCs and EVs from MSCs, nor did it assess the long-term effects of EVs and MSCs. Therefore, the effect of the persistence of EVs within injured kidney tissue was not observed.

Sierra Parraga et al. (2019) investigated the effect of normothermic machine perfusion on human and porcine mesenchymal stem cells (Sierra Parraga et al., 2019). Reactive oxygen species (ROS) production in MSCs from both species increased after 30 and 120 minutes of perfusion incubation, as measured using a reactive oxygen species (ROS) detection reagent (CellRox®, ThermoFisher) in flow cytometry. This result showed that perfusion fluid affects ROS production in the first hour after thawing. The strength of this study lies in the use of human MSCs from kidney adipose tissue and the use of clinically relevant perfusion fluid; however, signalling pathways related to ROS production were not investigated. Moreover, this study was done in in vitro human umbilical vein, which makes it difficult to justify the effect of MSCs in a practical setting.

In contrast to previous studies, Pool et al. (2020) showed no difference in MDA levels between experimental groups in porcine kidneys (Pool et al., 2020). This indicates the uncertain effects of the anti-oxidative properties of MSCs.

3.3.4 Anti-fibrosis of mesenchymal stem cells

Transforming Growth Factor-β1 (TGF-β1) is a main driver in tissue fibrosis. It is upregulated in injured tissue, and its downstream effects lead to scarring (Tang et al., 2018). Another factor driving tissue fibrosis is hypoxia-inducible factors (HIFs). HIF is a transcription factor that is normally degraded by the 26S proteasome under normoxic conditions; however, its active form accumulates under hypoxic conditions (Roth and Copple, 2015; Moon et al., 2009). HIF regulates cytokines and factors that promote fibrosis, for example, plasminogen activator inhibitor-1 (PAI-1), vascular endothelial growth factor (VEGF), transforming growth factor-β1 (TGF-β1), and fibroblast growth factor 2 (FGF-2). In a study conducted by Rigo et al. (2018), rat kidneys preserved with a normothermic machine perfusion technique showed a decrease in mRNA expression of HIF-1 and TGF-β1 after treatment with extracellular vesicles from human liver mesenchymal stem cells compared to kidneys perfused without extracellular vesicles (Rigo et al., 2018). This study shows upstream

regulation of fibrosis by mesenchymal stem cells in injured liver through the HIF-1 and TGF-β1-associated pathway.

The study by Pool et al. (2020) used hepatocyte growth factor (HGF) as an anti-fibrotic cytokine in porcine kidneys with an ex vivo normothermic machine perfusion technique (Pool et al., 2020). HGF is a protein that attenuates liver fibrosis by inhibiting collagen type I and IV synthesis and reducing TGF-β1 expression (Kwiecinski et al., 2011; Xia et al., 2006). The group found that hepatocyte growth factor was increased in mesenchymal stem cell-treated groups compared to the group without MSC treatment. This result showed the anti-fibrotic effect of MSCs through the HGF-associated pathway. In this study, there was research showing that miRNA-29 is involved in extracellular matrix synthesis (Kwiecinski et al., 2011). More specific pathways should be addressed.

3.4. Discussion

This systematic review showed that the therapeutic effects of MSCs are associated with multiple mechanisms. These roles have been documented in this systematic review and other studies.

3.4.1 The effect of MSCs on cellular apoptosis

The findings in this systematic review revealed that the therapeutic mechanism of MSCs may be potentially associated with extracellular vesicles. Extracellular vesicles (EVs) are membrane-bound vesicles secreted by cells (Kwon, 2019). EVs serve as cargo for intercellular communication. The EVs of MSCs contain several cytokines, including TNF-stimulated gene 6 protein (TSG-6), prostaglandin E2 (PGE2), insulin-like growth factor 2 (IGF-2), indoleamine 2,3-dioxygenase (IDO) metabolite kynurenine, vascular endothelial growth factor (VEGF), and basic fibroblast growth factor (bFGF) (Fu et al., 2021). These cytokines help injured tissue to repair. Another study administering human adipose-derived mesenchymal stem cells attenuated cell and tissue injury in cisplatin-induced kidney injury (Yao et al., 2015). This group demonstrated that human MSCs inhibited the activation of p38 MAPK, which resulted in downregulation of BAX and upregulation of BCL2 in the apoptotic pathway. This reduced apoptosis and promoted cell proliferation. These studies confirmed the cellular apoptotic protection through BAX and BCL2 regulation by MSCs,

either in whole cell or EV administration. However, this study used cisplatin to induce acute kidney injury.

3.4.2 The effect of MSCs on anti-inflammation

This systematic review revealed that MSCs downregulated proinflammatory cytokines IL-1β, IL-6, and IL-8, and upregulated the anti-inflammatory cytokine IL-10. These effects of MSCs led to reduced inflammation in the damaged organ or injured tissues. Administration of chemical IL-1β antagonists, anakinra and parthenolide, reduced cardiac graft inflammation and cellular recruitment in rat cardiac transplantation (Jones et al., 2021). IL-10 modified mRNA administration prolongs allograft survival in face transplantation without immunosuppression (Aviña et al., 2023), with lymphocyte infiltration and proinflammatory T-helper 1 cells decreased and anti-inflammatory regulatory T-cells increased. These supporting studies show the impact of proinflammatory and anti-inflammatory cytokines on graft or organ transplantation. MSCs can modulate IL-1β, IL-6, IL-8, and IL-10 cytokines to alleviate inflammation in organ transplantation.

3.4.3 The effect of MSCs on oxidative stress

This systematic review showed that MSCs decreased ROS and MDA production to reduce oxidative stress. Another study showed that MDA levels at day 1 and day 7 after kidney transplantation is a useful predictor of delayed graft function and 1-year graft function, respectively (Fonseca et al., 2014). Another study used two antioxidative enzymes, superoxide dismutase (SOD) and catalase (CAT), to form enzyme-polymer nanocomplexes, which were administered in an IRI liver model in mice (Yan et al., 2022). The results showed that nanoparticles of SOD and CAT can improve hepatic injury. These findings support the impact of oxidative stress on organ transplantation, and MSCs can reduce oxidative stress; therefore, MSCs might improve the outcomes of organ transplantation.

3.4.4 The effect of MSCs on tissue fibrotic progenitors

Fibrosis is a compensatory response to inflammation and injury, with excessive accumulation of extracellular matrix (Zhao et al., 2022). Development of fibrosis involves interactions between cytokines and cells. Among those cytokines and factors, HGF and TGF-β play a role in the fibrotic pathway, as mentioned in this systematic review.

HGF and its target, mesenchymal–epithelial transition factor (c-MET), have an anti-fibrotic effect by antagonizing TGF-β-induced fibrosis. There are several modes of action for the anti-fibrotic effect. Firstly, HGF/MET activation promotes the export of Smad7 and Smurf1 proteins from the nucleus to the cytoplasm, and then those proteins block activation of Smad2/3 of TGF-β signalling pathways (Chakraborty et al., 2013; Ma et al., 2014). Secondly, HGF induces metalloproteinase-9 (MMP-9) production to degrade extracellular matrix protein surrounding myofibroblasts (Mizuno et al., 2005; Atta et al., 2014). Thirdly, HGF plays a role in preventing epithelial to mesenchymal transition (EMT), which helps prevent fibrosis (Nakamura and Mizuno, 2010). This implies that MSCs attenuate fibrotic progenitors through an HGF-MET-related mechanism.

Transforming growth factor beta (TGF-β) serves as a primary factor driving fibrosis (Meng et al., 2016). The mechanism of TGF-β-driven fibrosis is related to the Smad signalling pathway (Heldin and Moustakas, 2012; Wu et al., 2022). Several studies showed that TGF-β is involved in organ fibrosis such as kidney fibrosis, liver fibrosis, cardiac fibrosis, and lung fibrosis (Higgins et al., 2018; Katz et al., 2016; Yue et al., 2017; Tirunavalli et al., 2023). The blockade of TGF-β prevents or ameliorates fibrotic progenitors. Therefore, TGF-β has been considered a therapeutic target for prevention of tissue fibrotic progenitors, and decreasing TGF-β should help prevent kidney fibrosis in kidney transplantation.

3.5 Strengths and limitations

This systematic review shows the strengths of the research studies. Firstly, most of the research used human MSCs. These studies can be translated to human medicine for future medical applications. Secondly, some studies used ex vivo kidneys from both animals and discarded human kidneys in study design. This mimics the clinical condition. Thirdly, functional parameters or clinical parameters were included in these studies, for example,

NGAL, eGFR, and renal blood flow. These showed the feasibility of using and monitoring MSCs in clinical practice.

The limitations of studies in this systematic review include the inclusion of various species, methods, and outcomes. Regarding species, Gregorini et al. (2017) and Yang et al. (2020) used rat models, and Sierra Parraga et al. (2019) used a porcine model in their studies. The sources of MSCs vary from rats, porcine, and human. Some studies used different sources of MSCs and animal models, for example, the studies of Pool et al. (2019, 2020) used human MSCs in a pig model, and Rigo et al. (2018) used human MSCs in a rat model. It is hard to justify the effect of MSCs from different sources and models, and the cross-species experiment between human MSCs and animal kidneys might raise questions about immune response. Regarding methods, ex vivo models were used in the studies of Rigo et al. (2008) and Thomson et al. (2020), and in vivo models were used in other studies. The biomarkers in these studies were different. These parameters include metabolic parameters, cellular injury parameters, kidney function parameters, and histopathological parameters. This makes it hard to compare results from these studies. Justifying the properties of MSCs is challenging due to these variations. Future studies with consistent outcome measurements are needed for better justification

3.6 Summary

This systematic review demonstrated the multipurpose effects of MSCs on organ transplantation models. MSCs showed more positive effects than negative effects. They can protect against cellular apoptosis through BAX and BCL2 regulation, modulate IL-1β, IL-6, IL-8, and IL-10 cytokines to alleviate inflammation, decrease ROS and MDA production to reduce oxidative stress, and attenuate fibrosis through HGF- and TGF-β-related mechanisms. This shows the potential of MSCs to improve outcomes in organ transplantation in clinical applications.

Chapter 4: Effect of adipose derived regenerative cells on rat kidney organoids

4.1 Introduction

Human kidney organoids were first generated from induced pluripotent stem cells (PSCs) by Takasato et al. in 2015 (Takasato et al., 2015). Since that time, kidney organoids have been generated as a potential new complex structural model for disease. This three-dimensional (3D) model can theoretically be used as a powerful tool to mimic the structure, physiology, and disease of the kidney. Kidney organoids can be generated from PSCs, adult stem cells, and progenitor cells. Multicellular interactions and responses can be observed in this model.

Kidney organoids present an attractive model for the studies described within my thesis for a number of reasons. Firstly, kidney organoids can create a complex renal structure (Jun et al., 2018; Kang et al., 2019). Intercellular interactions, communication, and responses can be observed. Aspects of kidney function can be studied with multiple cellular responses occurring in glomerular cells and renal tubular cells. Moreover, multicellular renal tubular responses after injury induction can be studied. Secondly, kidney organoid culturing time is longer than general monolayer cell culture; therefore, cellular reactions can be assessed over a longer period, with kidney organoids expected to show long-term cellular responses.

In vitro ADRC studies have previously been performed in monocellular layers, which lack intercellular communication/responses (Collino et al., 2020; Jin et al., 2019). Although IRI in the kidney particularly affects proximal tubular cells, intercellular communication between proximal tubular cells and surrounding cells should be observed. Since overproduction of reactive oxygen species (ROS) from hydrogen peroxide is similar to the overproduction of ROS in the ischaemic phase of IRI in the kidney, hydrogen peroxide was used in this study to mimic oxidative stress and induce intrinsic pathway stimulation of apoptosis. The studies in this chapter might reveal therapeutic effects of ADRCs through multiple cellular responses in kidney organoids after injury induction with hydrogen peroxide.

However, these studies were severely affected by the COVID-19 pandemic. Few rats could be kept during the COVID-19 lockdown because of husbandry limitations due to staff

availability. In addition, lockdown restrictions on access to the laboratory, restrictive laboratory practices, and social distancing all impacted this project. Therefore, following studies validating cellular markers of the organoids, the experiments assessing the therapeutic effect of ADRCs were limited to assessing the diameter of kidney organoids and extracellular vesicle extrusion. The diameter of kidney organoids was used to quantify the protective effects or anti-apoptotic properties of ADRCs, and extracellular vesicle extrusion was used as a marker of kidney injury.

4.2 Aims

The aims of this chapter are to:

1. Validate kidney organoids in rats with adult kidney protein markers.
2. Validate a kidney injury model using organoids with hydrogen peroxide induction.
3. Investigate the therapeutic effect of ADRCs in a kidney organoid model.

4.3 Hypothesis

ADRCs have anti-apoptotic properties that preserve injured kidney organoids in a setting of oxidative stress.

4.4 Results

4.4.1 Rat adult kidney protein expression in naïve and injured kidney organoids

Kidney organoids in this study were generated as described in Chapter 2.4.2. Briefly, kidney organoids were produced using E13.5 metanephros and then assigned to four treatment groups: control (media only), injured, ADRC-treated control, and ADRC-treated injured groups. Injured organoids were treated with 10 μM hydrogen peroxide for 60 minutes. ADRC-treated organoids were exposed to ADRCs, which were 10% of the embryonic cell number, for 14 days before collection for downstream assays.

Non-treated kidney organoids and 10 μM hydrogen peroxide-treated kidney organoids were stained with immunofluorescence and assessed for the presence of specific adult kidney proteins: synaptopodin, megalin, and Wilms' tumour 1. Synaptopodin, a renal podocyte protein, was expressed in both control and injured kidney organoids. This protein can also be found in dendritic processes in the brain (Mundel et al., 1997). Megalin is a receptor abundantly expressed in the brush border, endocytic vesicles, and dense topical tubules of the apical membrane of proximal tubular cells. This protein was shown in both control and injured kidney organoids in this study (**Figure 4-1**). These findings confirm adult kidney protein expression in these rat kidney organoids and suggest that these organoids have utility as a kidney model for appropriately designed experiments.

4.4.2. Exosome and microvesicle shedding of healthy and injured rat kidney organoids

The injured rat kidney organoids showed similar shedding of exosomes and microvesicles, as non-injury organoids. In this nanoparticle study (n=3-5), there was no significant difference between healthy and injured organoids over time. In exosome and microvesicle shedding analysis, there was a fluctuation in concentration over time (**Figure 4-2**). In exosome concentration analysis, the highest concentration of exosome was $5.67x10^9$ ($\pm3.34x10^9$) particles per mL in the healthy group and was $6.78x10^9$ ($\pm3.24x10^9$) particles per mL in the injury group on day 3. The lowest concentration was $2.86x10^9$ ($\pm5.14x10^8$) particles per mL in the healthy group on day 12 and $3.12x10^9$ ($\pm9.43x10^8$) particles per mL in the injury group on day 5. In microvesicle concentration analysis, the highest concentration of microvesicle was $2.51x10^{10}$ ($\pm1.75x10^{10}$) particles per mL in the healthy group on day 3 and was $2.12x10^{10}$ ($\pm7.67x10^9$) particles per mL in the injury group on day 3. The lowest concentration was $1.2x10^9$ ($\pm9.58x10^8$) particles per mL in the healthy group on day 7 and $1.47x10^9$ ($\pm1.13x10^9$) particles per mL in the injury group on day 10.

The injured rat kidney organoids showed similar shedding of exosomes and microvesicles as non-injured organoids. In this nanoparticle study (n=3-5), there was no significant difference between healthy and injured organoids over time. In exosome and microvesicle shedding analysis, there was a fluctuation in concentration over time (**Figure 4-2**). In exosome concentration analysis, the highest concentration of exosomes was $5.67x10^9$ ($\pm3.34x10^9$) particles per mL in the healthy group and $6.78\ x10^9$ ($\pm3.24x10^9$) particles per mL in the injury group on day 3. The lowest concentration was $2.86x10^9$ ($\pm5.14x10^8$)

particles per mL in the healthy group on day 12 and $3.12x10^9$ ($\pm 9.43x10^8$) particles per mL in the injury group on day 5.

In microvesicle concentration analysis, the highest concentration of microvesicles was $2.51x10^{10}$ ($\pm 1.75x10^{10}$) particles per mL in the healthy group on day 3 and $2.12x10^{10}$ ($\pm 7.67x10^9$) particles per mL in the injury group on day 3. The lowest concentration was $1.2x10^9$ ($\pm 9.58x10^8$) particles per mL in the healthy group on day 7 and $1.47x10^9$ ($\pm 1.13x10^9$) particles per mL in the injury group on day 10.

4.4.3. The therapeutic effect of ADRCs on the rat kidney organoid model

In this study, two effects of ADRCs were investigated-the regulatory effect of ADRCs on extracellular vesicle extrusion and the anti-apoptotic effect of ADRCs on organoid health using the diameter of rat kidney organoids.

4.4.3.1 Effects of ADRCs on exosomes and microvesicles extrusion

This study assessed the regulatory effect of ADRCs on extracellular vesicle extrusion into culture media, and there was a variation in extracellular vesicles, exosomes, and microvesicles extruded from healthy and injured kidney organoids (with or without ADRCs). The concentrations of extracellular vesicles shed from healthy organoids, injured organoids, healthy organoids with ADRC treatment, and injured organoids with ADRC treatment on day 7 were $3.03x10^9 \pm 9.16x10^8$, $3.77x10^9 \pm 9.93x10^8$, $2.27x10^9 \pm 1.07x10^8$, $2.8x10^9 \pm 7.81x10^8$ particles per mL, respectively ($p<0.05$, $n=5$). Similar results were observed on day 14. The concentrations of extracellular vesicles extruded were $4.12x10^9 \pm 3.83x10^8$, $4.66x10^9 \pm 8.99x10^8$, $3.07x10^9 \pm 4.73x10^8$ and $3.56x10^9 \pm 4.86x10^8$ from healthy organoids, injured organoids, healthy organoids with ADRC treatment, and injured organoids with ADRC treatment, respectively (**Figure 4-3**). The concentration of microvesicles in healthy organoids was significantly lower than that in injured organoids on day 12 ($1.4x10^{10} \pm 6.05x10^8$ vs $1.7x10^{10} \pm 1.72x10^8$ particles per mL, $p<0.05$, $n=3$) (**Figure 4-4**). However, there was no difference between the ADRC treatment group and their control group. Therefore, there was no effect of ADRCs on the rat kidney organoid model.

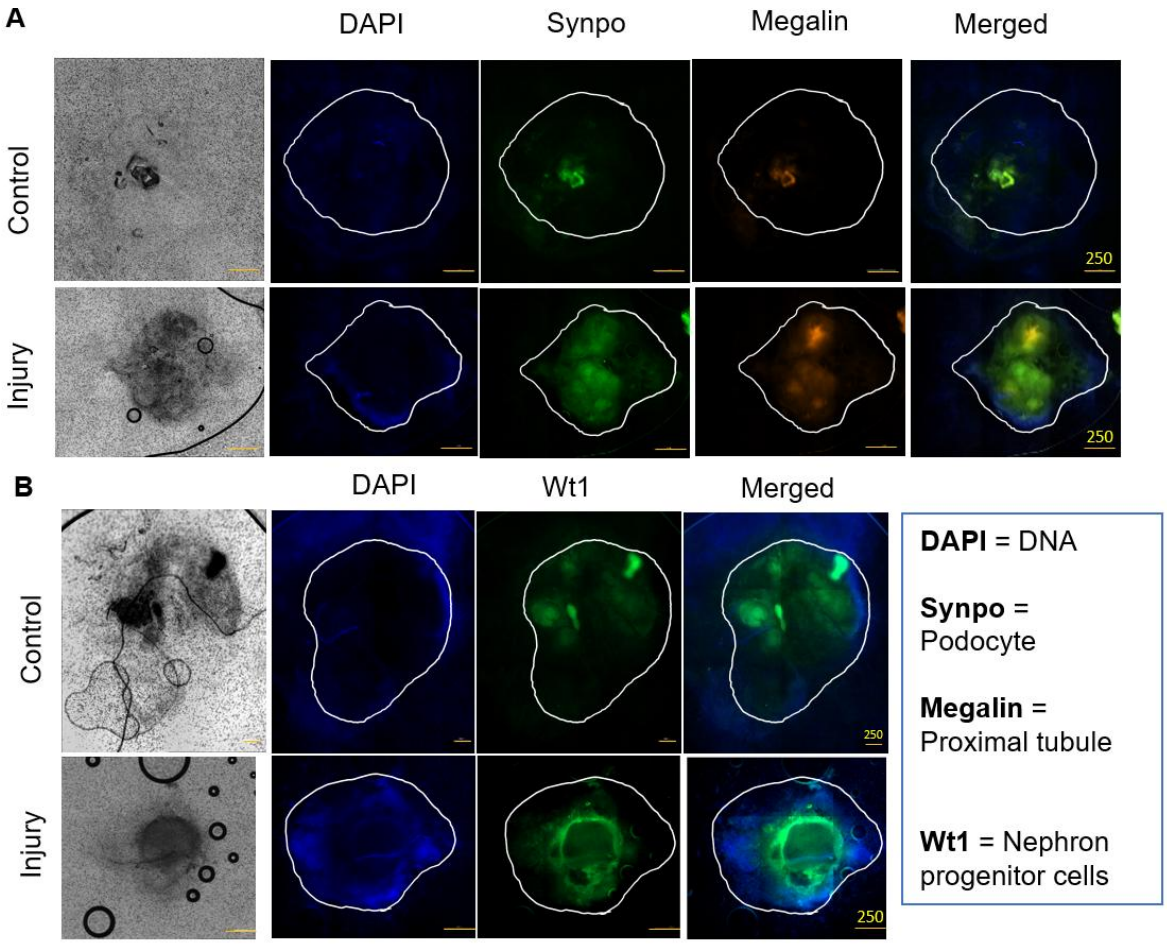

Figure 4-1 A representative images of kidney developmental markers (n=3) after hydrogen peroxide treatment of kidney organoids. Specific kidney protein expressions were shown on normal and 10 µM hydrogen peroxide-treated kidney organoids at day 14 of culturing in immunofluorescent staining. Two adult kidney proteins, Synaptopodin (Synpo) and megalin proteins, were expressed in both normal and injured kidney organoids. Wilms' tumour 1 (Wt1) protein, a transcription factor of mesenchymal-to-epithelial transition during kidney development, was expressed in both normal and injured kidney organoids. Scale bar (yellow), 250 µM.

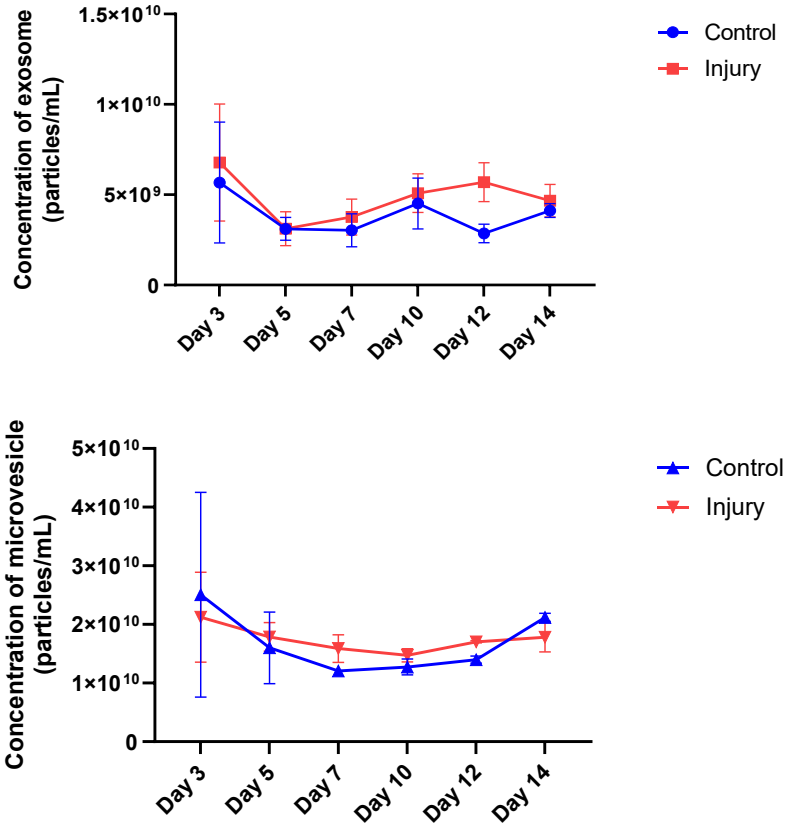

Figure 4-2 The concentration of exosomes and microvesicles in rat kidney organoid culture media. The concentrations of exosomes (30–100 nm) and microvesicles (100–1000 nm) are depicted from day 3 to day 14 of culturing in the control group and the 10 μM hydrogen peroxide-treated kidney organoid group. Quantified data are expressed as mean (± SEM, n=3–5). Data were analysed with two-way ANOVA.

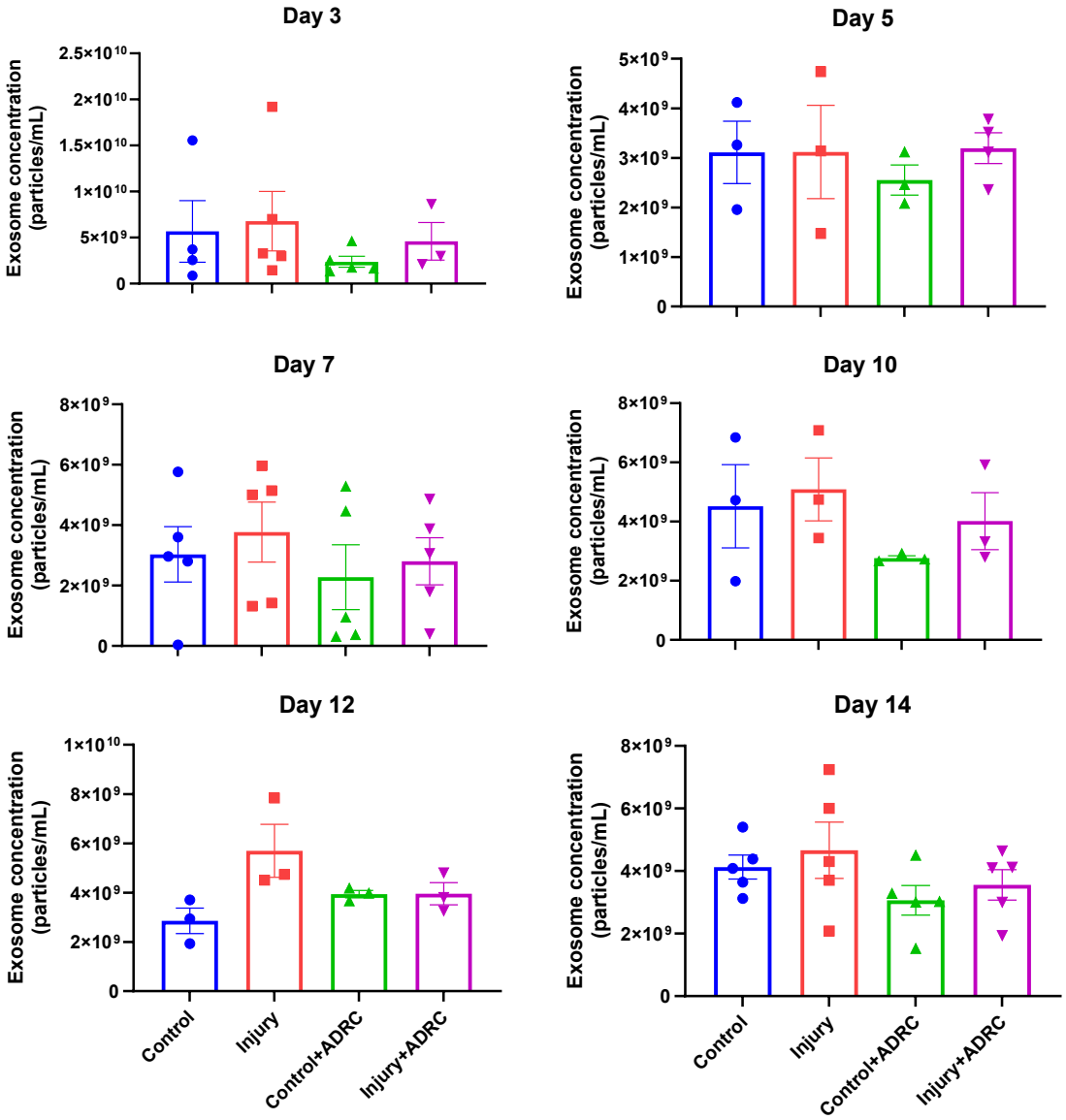

Figure 4-3 The concentration of exosomes in rat kidney organoid culture media in ADRC-treated groups. The concentration of exosomes from day 3 to day 14 of culturing in experimental groups. Quantified results are expressed as mean (± SEM, n=3–5). Statistical analysis was performed with the Kruskal-Wallis H test with Dunn's multiple comparisons test. *p<0.05.

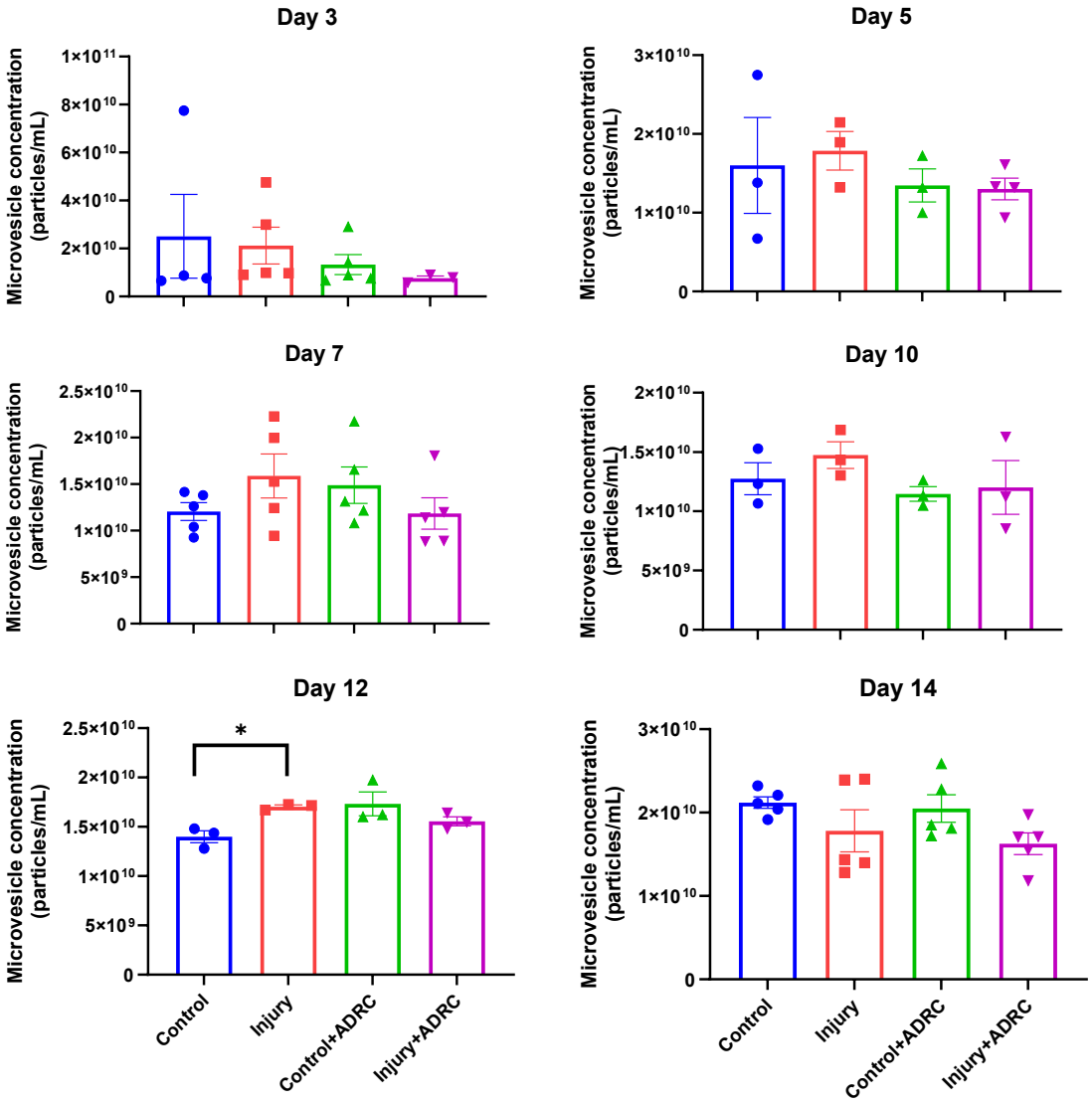

Figure 4-4 The concentration of microvesicles in rat kidney organoid culture media in ADRC treated groups. The concentration of microvesicles from day 3 to day 14 of culturing in experimental groups. Quantified results expressed as mean (± SEM, n=3-5). Statistical analysis was performed with the Kruskal-Wallis H test with Dunn's multiple comparisons test. *p<0.05.

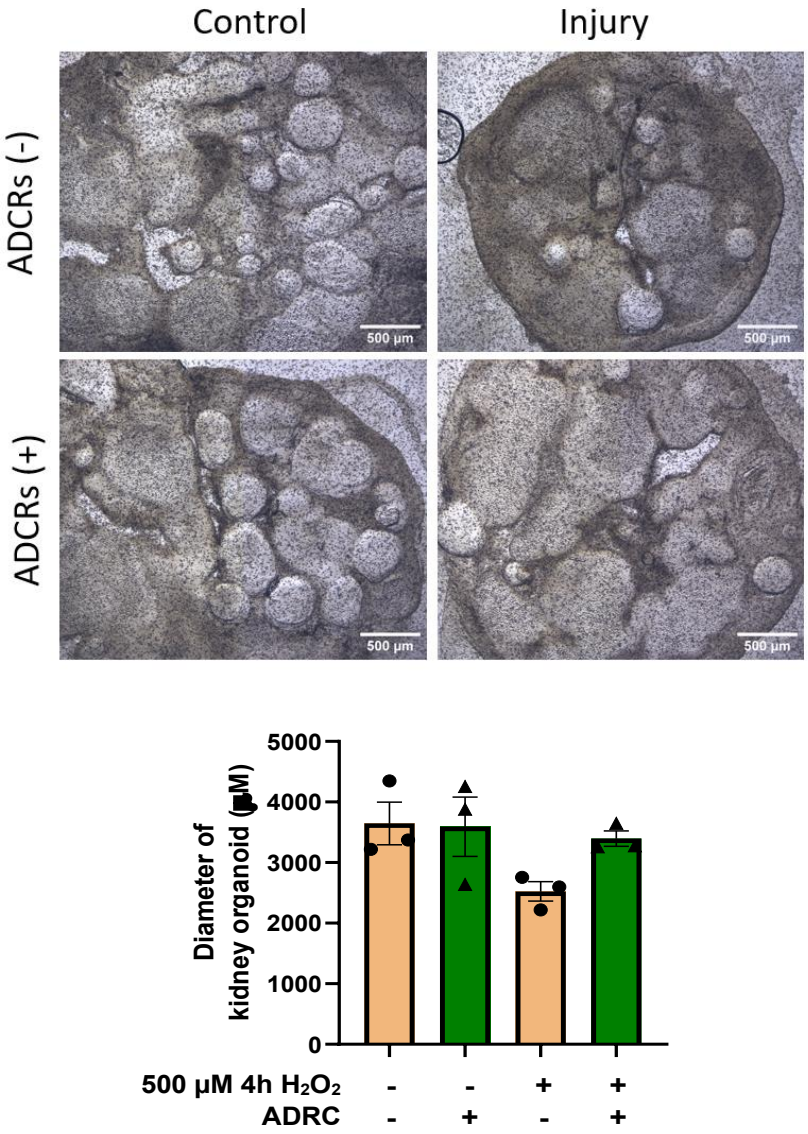

Figure 4-5 Diameter size of rat kidney organoids at day 14. The diameter of rat kidney organoids at day 14 of culturing after treatment with ADRCs with or without injury induction using hydrogen peroxide. These pictures show rat kidney organoids in 4 treatment groups: normal kidney organoids, normal kidney organoids with ADRC treatment, injured organoids, and injured kidney organoids with ADRC treatment. The diameters of kidney organoids were significantly greater in the ADRC-treated group relative to the non-ADRC-treated group. Quantified results are expressed as mean (± SEM, n=3). Statistical analysis was performed with the Kruskal-Wallis H test with Dunn's multiple comparisons test. Scale bar, 500 µM.

4.4.3.2. The effect of ADRCs on size of rat kidney organoids

Representative images showed rat kidney organoids in four treatment groups: healthy kidney organoids, healthy kidney organoids with ADRC treatment, injured organoids, and injured kidney organoids with ADRC treatment (**Figure 4-5**). The diameters of the kidney organoids at day 14 of culturing were as follows: healthy organoids, 3,646 ± 353.2 μM; injured organoids, 2,525 ± 160 μM; healthy organoids with ADRC treatment, 3,592 ± 488.3 μM; and injured organoids with ADRC treatment, 3,396 ± 126.9 μM (n=3). There was no significant difference between the ADRC-treated groups and their respective controls. Therefore, ADRC treatment had no statistically significant effect on the preservation of kidney organoid size in the presence of IRI.

4.5 Discussion

Kidney organoids represent exciting novel models that potentially expand research methods for the study of kidney anatomy, physiology, and response to stressors. In this study, both non-injured and injured kidney organoids were investigated with specific protein markers, first to validate their expression of conventional markers of adult human renal cells. Furthermore, the therapeutic effects of ADRCs on the response of the kidney organoid model to injury were assessed using measurements of extracellular vesicle extrusion and kidney organoid diameter.

In this study, the three-dimensional organoid culture of rat metanephros expressed markers of nephrogenesis and markers of adult kidney tissue. Embryonic kidneys arise from the intermediate mesoderm (IM). The metanephros is considered the origin of the functional kidney during embryonic development. Osr1 and Wt1 are expressed by the posterior intermediate mesoderm as the origin of the metanephros (Taguchi et al., 2014). Pax2 and Lim1 are used as intermediate mesoderm markers in mouse embryos (Bouchard et al., 2002; Tsang et al., 2000). These markers are also used for mapping kidney tubular cells from PSCs. Wt1 protein is expressed within the posterior area of the intermediate mesoderm (Morizane and Bonventre, 2017). In a study by Kato and Mizuno (2017), Wt1 and synaptopodin were expressed in developing podocytes in mouse embryos (Kato and Mizuno, 2017). In my studies, expression of Wt1 protein in kidney organoids confirmed that these organoids were developed from metanephros or kidney tissue origin and confirmed correct laboratory techniques and skill during the microdissection collection of metanephros from embryos. In

a study by Nielsen et al. (1998), megalin expression was shown in renal proximal tubular cells (Nielsen et al., 1998). In the studies in this chapter, expression of adult kidney tissue markers, synaptopodin and megalin, represents the development of organoids to express markers of adult kidney tissue. A similar result was illustrated in the study of Xinaris et al. (2012), which generated kidney organoids from E11.5 mouse kidney that were later implanted into a mouse kidney as a primitive model of kidney transplantation. Synaptopodin and megalin were observed in immunofluorescence staining in these organoids (Xinaris et al., 2012). My study showed that hydrogen peroxide-induced kidney organoids have the potential to be a model of IRI and an in vitro rat kidney transplant model.

Extracellular vesicle concentration of kidney organoids was used as a marker of kidney injury to the organoids in this study. Extracellular vesicles are subdivided into exosomes, microvesicles, and apoptotic bodies. These subtypes differ in size, biogenesis, and composition. A study by Dominguez et al. (2018) showed that injection of exosomes can reduce oxidative stress and reduce apoptosis in IRI kidney in rats (Dominguez et al., 2018). In contrast to the beneficial effect of exosomes, Guo et al. (2019) stated that microvesicles are shed from hypoxia-induced or oxidative stress-induced cells and the shedding process involves the caspase-3 pathway of apoptosis (Guo et al., 2019). The level of microvesicles in ADRC-treated kidney organoids in my study was higher than in injured kidney organoids over time. This implies that ADRCs could attenuate cellular apoptosis in kidneys.

This study investigated two effects of ADRCs on kidney injury with H_2O_2: 1) regulation of extracellular vesicle extrusion and 2) reduced cell death or promoted proliferation of rat kidney organoids with ADRC treatment. I used kidney organoid size to determine the maintenance of cell size due to proliferation and/or lack of cell death, suggesting anti-apoptotic properties. The size of kidney organoids did not differ between control and ADRC-treated control organoids. However, the kidney organoid diameter of untreated injured organoids was numerically smaller than the diameter of ADRC-treated injured organoids. Since this study induced injury in kidney organoids too early, future studies with hydrogen peroxide-induced injury in aged kidney organoids should be conducted to confirm the results of this study.

4.6 Strengths and limitations

The kidney organoid model in this study showed that it can express various markers of complex adult kidney structures and can respond to injury in a manner similar to normal kidney responses. Other studies have shown that kidney organoids can express various adult kidney proteins, for example, nephrin (a podocyte marker), *Lotus tetragonolobus* lectin (LTL, a marker for proximal tubule), E-cadherin (a marker of distal tubule), and platelet endothelial cell adhesion molecule (CD31, a marker of endothelial cells) (Suhito et al., 2022; Bejoy et al., 2023). These results imply the potential of kidney organoids to mimic *in vivo* models.

Regarding the injury response of kidney organoids, the concentration of microvesicle shedding from injured kidney organoids in this study was higher than that from healthy organoids at day 12 post-culture. This showed that an injured kidney organoid can respond to an injury inducer. The study by Gupta et al. (2022) showed that a human iPSC-derived kidney organoid can be injured by using 5 μM cisplatin and then expressed KIM-1 (an injured tubular marker) and gamma H2A.X Variant Histone (γH2AX), a marker of DNA damage, at LTL+ proximal tubular marker structures (Gupta et al., 2022). This indicates that a kidney organoid is a potentially reliable model for testing injury and can mimic kidney disease.

The use of kidney organoids in research still has limitations. Firstly, there are several methods to generate kidney organoids. The lack of uniformity in methods for generating kidney organoids could affect the uniformity of kidney organoid structure (Morizane and Bonventre, 2017). Secondly, IgG isotype controls should be used as negative controls to distinguish between specific and non-specific antibody binding. This negative control provides an assessment of non-specific background staining (Zhou et al., 2013; Agrelo et al., 2020). Thirdly, specific kidney injury markers such as KIM-1 and NGAL should be tested in this study to confirm and locate injured structures. The study by Jun et al. (2018) demonstrated that kidney injury molecule-1 (KIM-1) and neutrophil gelatinase-associated lipocalin (NGAL), tubular injury markers, were observed in kidney tubular organoids with cisplatin-induced renal injury (Jun et al., 2018). However, in the present study, I was unable to detect KIM-1 in the organoid media using an ELISA assay. The possible causes are a low level of KIM-1 in the organoid media, a very low number of renal tubular cells in kidney

organoids, or hydrogen peroxide did not induce sufficient injury in kidney organoids to promote KIM-1 secretion.

These will be challenges for modelling human disease with organoid models. However, induced PSC-origin organoids represent another method of organoid production that can address this ethical issue.

4.7 Suggestion for further study

I would suggest, in terms of organoid generation, injury induction, and selection of laboratory techniques, the following improvements. For organoid generation, embryonic kidney markers and adult kidney markers should be assessed on E13.5 embryos as a control group for comparing the progression of embryonic and adult protein expression during organoid culture over time. Human iPSCs as an organoid origin should be used to better mimic human cellular studies.

For injury induction, the treatment of hydrogen peroxide at day 0 of organoid culturing should be avoided because this can lead to misinterpretation between protecting organoid development and protecting injured organoids. The treatment of hydrogen peroxide should be applied to kidney organoids at the adult stage, which was day 14 of organoid culturing in present study. In addition, culturing kidney organoids under hypoxic conditions can be considered as an alternative injury induction technique to mimic kidney transplantation.

Further analysis of cell death reduction and proliferative properties should be performed, for example, using TUNEL assays to detect apoptotic DNA fragments, a dextran uptake assay to detect the percentage of apoptotic cells, or RT-PCR of caspase 3 as an apoptotic marker. Alternatively, an antibody against the nuclear protein Ki67 could be used as a proliferation assay (Grassi et al., 2019; Garreta et al., 2019; Ye et al., 2011). Other laboratory techniques such as RT-PCR, immunohistochemistry, and immunofluorescence staining should be used to detect injury markers such as caspase-3, KIM-1, and γH2AX (Takasato et al., 2015; Morizane et al., 2015b).

Other functional assays in kidney organoids should also be tested. The dextran uptake assay is used to investigate the accumulation of tubular cells in kidney organoids (Takasato et al., 2015; Freedman et al., 2015). Dextran has a wide range of molecular weights. The

uptake of fluorescence-tagged dextran mimics tubular reabsorption in adult tubular cells. Renal endocrine function is essential for kidney homeostasis. The renin production assay can be performed by using qPCR for renin gene expression detection, and immunofluorescence or immunohistochemistry for renin protein expression detection (Shankar et al., 2021). These functional assays could be used to clarify that kidney organoids have normal kidney cellular activity.

4.8 Summary

The studies in this chapter demonstrate the origin of kidney organoids and their potential to differentiate into kidney tissue expressing markers of adult kidney cells. Treatment of these organoids with ADRCs in an H_2O_2 model of kidney injury showed some beneficial effects, with evidence that the ADRCs exhibit some anti-apoptotic properties and/or promote proliferation.

Chapter 5: Effect of adipose derived regenerative cells on NRK-52E cells

5.1 Introduction

As discussed in previous chapters, ADRCs have been proposed as having potential therapeutic effects in preclinical and clinical studies. It has been suggested that ADRCs may prevent injury, reduce inflammation, reduce fibrosis, and decrease free radical production in the injured kidney in both in vivo and clinical studies.

5.1.1 In Vitro model of kidney injury

The most affected structures in kidneys after ischaemic reperfusion injury (IRI) in the setting of kidney transplantation are proximal tubular cells because of their high energy requirements for membrane transport of metabolites, oxidative phosphorylation, and anaerobic glycolysis (Sharfuddin and Molitoris, 2011; Basile et al., 2012; Barin-Le Guellec et al., 2018). In preclinical kidney research, there are several cell lines of proximal tubular cells. Cell cultures that are widely used include the normal rat kidney proximal tubular cell line (NRK-52E), the human proximal tubular epithelial cell line HK-2, or primary cell cultures that are directly derived from renal tubular epithelial cells. All could be used to mimic an injured kidney model from different species (Lee et al., 2019; Collino et al., 2020).

In the studies described in this chapter, the rat cell line NRK-52E was used. There are several reasons for using NRK-52E cells in this study. Firstly, several studies have already been published using NRK-52E as an in vitro injured kidney model (Sáenz-Morales et al., 2006; Ogata et al., 2012; Kim et al., 2022; Sauvant et al., 2009). Secondly, to avoid inter-species immune effects, using cell cultures from rats can diminish those effects. Therefore, a rat cell line was an appropriate choice for this study. Thirdly, a continuous cell line was selected instead of using primary cell lines. Continuous cell lines are cell lines that have acquired the ability to proliferate indefinitely, while primary cell lines are directly isolated from human or animal tissue and have limited proliferation. Continuous cell lines show uniformity of cellular responses, while primary cell lines show various cellular responses, may be difficult to generate, and there are limits to using passaged cell growth as a laboratory culture technique. Lastly, this study was designed to investigate the principal therapeutic effect of ADRCs after IRI. IRI studies in rats have been performed in several

research publications (Chen et al., 2011b; Lin et al., 2016; Lim et al., 2021; Tseng et al., 2021). Generation of rat-derived ADRCs from rats was accessible for the studies described in this chapter. Therefore, NRK-52E cells were the rat proximal tubular cell line used in the experiments described in this chapter. Other studies have previously demonstrated that this cell line is a well-established proximal tubular model for IRI studies (Barin-Le Guellec et al., 2018; Kishi et al., 2019).

For injury induction, I used hydrogen peroxide as an injury reagent to mimic clinical kidney cell responses. Studies of cellular responses after ischaemic reperfusion injury show that increasing reactive oxygen species and induction of apoptotic pathways occur. Hydrogen peroxide induction can increase intracellular oxygen species (Wijeratne et al., 2005; Park et al., 2017), which in some ways reflects the oxidative stress observed in clinical IRI. Therefore, hydrogen peroxide was used as a cheap, readily available, and clinically appropriate injury induction reagent for this research.

5.1.2 Detection of tubular injury in kidneys

Injury to the kidney can be detected by using kidney injury biomarkers such as NGAL and KIM-1. NGAL is a protein in the lipocalin family. It was initially found in activated human neutrophils and is expressed in the stomach, liver, and injured epithelial cells (Cowland and Borregaard, 1997). The study by An et al. (2013) showed the protective mechanism of NGAL shedding, in which exogenous NGAL reduced apoptosis in ischaemic reperfusion injury in a surgical model of IRI in rat kidneys through mitochondrial apoptotic pathways (An et al., 2013). KIM-1 (kidney injury molecule 1) is a transmembrane glycoprotein, also known as T cell immunoglobulin mucin domain (TIM)-1. It is upregulated in injured proximal tubules or kidney disease. KIM-1 has also been used as a biomarker of nephrotoxicity, which was approved by the Food and Drug Administration (FDA) and the European Medicines Agency (EMEA) (Dieterle et al., 2010). Both NGAL and KIM-1 proteins have a protective effect on injured renal epithelial cells in acute kidney injury and are used as clinical kidney injury markers.

5.1.3 Detection of cell death and cell proliferation in kidneys

Cell death is an inevitable and passive finale of life. The ultrastructures of cell death change depending on the type of cell death. During normal development, apoptosis, or programmed

cell death (also known as regulated cell death), manifests as cytoplasmic shrinkage, nuclear condensation, and retention of membrane and organelle integrity (Galluzzi et al., 2018; Fuchs and Steller, 2015). In contrast, accidental cell death, which is caused by physical, chemical, or mechanical damage, manifests as cell swelling and rupture. These manifestations can be useful for distinguishing the cause of cell death by morphology. Cell death is typically discussed as apoptosis, necroptosis, and ferroptosis. Necroptosis and ferroptosis result in the release of proinflammatory signals surrounding the cell and lead to inflammatory cellular responses. In contrast to these types of cell death, apoptosis is silent to the immunological response (Bertheloot et al., 2021). My systematic review showed that mesenchymal stem cells have an anti-apoptotic effect. Therefore, this led me to focus on apoptosis in the studies described in this chapter.

In research, we can detect cell death by various methods. Nuclear morphology changes after cellular necrosis or apoptosis, so the assessment of fluorescence nuclear staining can detect the difference between healthy cells and dead cells (Pliss et al., 2010; Ferlini et al., 1996; Singh, 2000). The leakage of intracellular enzymes such as lactate dehydrogenase (LDH) through the breakdown of the cellular membrane during necrosis can also be a marker of cell death (Chan et al., 2013; Pliss et al., 2010). The permeability of the plasma membrane changes after necrosis, so impermeable fluorescent dyes such as the DNA-binding dye propidium iodide (PI) can stain necroptotic cells (Fu et al., 2023; Vitale et al., 1993; Sawai and Domae, 2011; Tsurusaki et al., 2022). Cellular apoptosis can be measured by using annexin V to detect the externalization of phosphatidylserine on the plasma membrane (Sawai and Domae, 2011; Kawai et al., 2018; El-Habta et al., 2021). In addition, specific markers of signalling pathways of cellular death such as caspase, BAX, and BAK can be measured for apoptotic cell death (Zhong et al., 2021; Wang et al., 2020; Kawai et al., 2018).

Cell proliferation is the increase in cell numbers, which can be measured as cell number as a function of time and is regulated by cellular growth and the cell cycle (Fajas-Coll et al., 2014; Yang et al., 2014). There is a balance between the cell cycle and cell proliferation, given that over a million cells die each day. The key to the sustainability of life is the regulation of the complex processes of cell regeneration and cell repair to ensure proper growth and survival of multicellular structures. Therefore, cell proliferation is a compensatory response to cell injury or cell death (Yang et al., 2014). In research, cell proliferation can be detected using cell proliferation markers, for example, Ki-67,

proliferating cell nuclear antigen (PCNA), or minichromosome maintenance genes (Whitfield et al., 2006; Miller et al., 2018).

As mentioned in the previous chapter, oxidative stress plays a role in ischaemic reperfusion injury (IRI) and can lead to apoptotic cell death. Therefore, here I focus on apoptosis, proliferation, oxidative stress, and assessment of some apoptotic markers.

5.1.4 Detection of fibrotic progenitors in kidneys

Kidney fibrosis is the overgrowth and scarring of kidney tissue due to excessive connective tissue component deposition (Huang et al., 2023). This pathological process is responsible for kidney injury resulting from maladaptive repair and leads to kidney malfunction. There are several fibrotic progenitor markers such as Lif, TGF-β, and NF-κB (Antar et al., 2023).

After kidney injury, injured tubular cells express Lif, a cellular cytokine, to activate myofibroblasts in fibrosis. A study demonstrated the role of Lif as a fibrotic progenitor in myofibroblast activation in an IRI rat model, and the activation is mediated via the ERK and STAT3 pathways (Xu et al., 2022). This Lif biomarker can be used for non-invasive detection of kidney fibrosis in diabetic nephropathy (Kim et al., 2021). Therefore, Lif can be used as a fibrotic progenitor marker.

TGF-β signalling is a primary factor with a major role in the development of fibrosis. It increases the proliferation of fibroblasts, the production of myofibroblasts, extracellular matrix production, and inhibits collagenolytic enzymes (Ren et al., 2023). This cytokine transduces its signalling through type 2 TGF-β receptor (TβR2) activation in myofibroblasts, activates Smad 2/3, and then translocates into the nucleus to accelerate the accumulation of extracellular matrix (ECM) and apoptosis (Tang et al., 2018; Heldin and Moustakas, 2012). In addition, TGF-β also activates mitogen-activated protein kinases (MAPKs), including extracellular-signal-regulated kinase-1 and -2 (ERK1/2), c-Jun N-terminal kinase (JNK), and p38 MAPK (Mu et al., 2012; Lee et al., 2015). Therefore, TGF-β can be used as a fibrotic progenitor marker as a reflection of these cellular processes.

As mentioned above, these markers are related to the severity of kidney fibrosis and kidney inflammation. In the studies in this chapter, Lif and TGF-β were used as fibrotic progenitor markers to detect fibrotic progenitor preponderance in an *in vitro* model. Moreover, a study showed that ADRCs contain fibroblasts as a component (Vijay et al.,

2020; Nunes et al., 2013). Collagen type I and elastin gene expression were tested as a paracrine effect of the kidney cells after injury induction. This chapter studies the effect of ADRCs on cellular responses, particularly anti-apoptotic or proliferative properties. These studies might reveal therapeutic effects of ADRCs on those cellular responses in NRK-52E cells after injury induction with hydrogen peroxide.

5.2 Aims

The aims of this chapter are to:

1. validate hydrogen peroxide as a method for inducing injury in rat proximal tubular cells,
2. investigate the potential therapeutic effects of ADRCs in injured proximal tubular cells, and
3. investigate cellular responses of injured proximal tubular cells after ADRC treatment.

5.3 Hypothesis

ADRCs have injury-reducing, anti-apoptotic, anti-oxidative, and fibrosis-reducing effects on injured NRK-52E cells.

5.4 Results

5.4.1 Injury NRK-52E cell validation

5.4.1.1 KIM-1 and NGAL protein expression on hydrogen peroxide induced injury NRK-52E cells

Kidney injury markers were used in this study to indicate the severity of injury response in renal tubular cells. Increasing levels of kidney injury markers suggest greater kidney cellular damage. Anti-kidney injury molecule-1 (KIM-1) antibody and anti-neutrophil gelatinase-associated lipocalin (NGAL) antibody were used to detect protein levels of these markers in western blot analysis. NRK-52E cells were exposed to hydrogen peroxide at different concentrations-0 μM, 100 μM, 300 μM, and 500 μM-and for different exposure times: flash exposure, 1 hour, 2 hours, 4 hours, and 24 hours (n=5–6) (**Figure 5-1**). The results showed

that the levels of these kidney injury markers increased relative to the concentration and exposure time to hydrogen peroxide.

Kidney injury molecule-1 (KIM-1) protein levels increased relative to the concentration and exposure time to hydrogen peroxide. In 100 μM hydrogen peroxide exposure, KIM-1 protein expression after exposure to hydrogen peroxide gradually increased in the group with flash exposure (1.24±0.23-fold change, $p>0.05$), 1 hour (1.46±0.29-fold change, $*p=0.048$), 2 hours (0.86±0.23-fold change, $*p=0.048$), 4 hours (3.4±0.27-fold change, $**p=0.002$), and 24 hours (3.4±0.9-fold change, $**p=0.002$) compared to the control group. In the 300 μM hydrogen peroxide exposure experiment, KIM-1 protein expression was similar between flash exposure (0.97±0.11-fold change, $p>0.05$) and 1 hour (0.72±0.11-fold change, $p>0.05$) versus the control group. An elevation of KIM-1 protein expression was found after exposure to hydrogen peroxide for 2 hours (0.86±0.23-fold change, $*p=0.048$), 4 hours (10.52±8.7-fold change, $*p=0.048$), and 24 hours (7.6±5.9-fold change, $**p=0.002$). Similar to the 300 μM hydrogen peroxide exposure experiments, KIM-1 protein expression in the 500 μM hydrogen peroxide exposure experiment was no different between flash exposure (0.85±0.09-fold change, $p>0.05$) and 1 hour (17.18±10.32-fold change, $p>0.05$).

Studying exposure groups versus the control group showed peak KIM-1 with 24-hour hydrogen peroxide exposure time. There were significant increases in KIM-1 expression in the groups with 2-hour (39.24±12.35-fold change, $*p=0.048$), 4-hour (50.5±12.01-fold change, $*p=0.002$), and 24-hour (220.8±16.28-fold change, $*p=0.002$) exposure times versus the control group. This showed that there was no change in KIM-1 expression at short exposure times. However, 24-hour exposure at 500 μM hydrogen peroxide seems to harm the cells and might cause the death of NRK-52E cells.

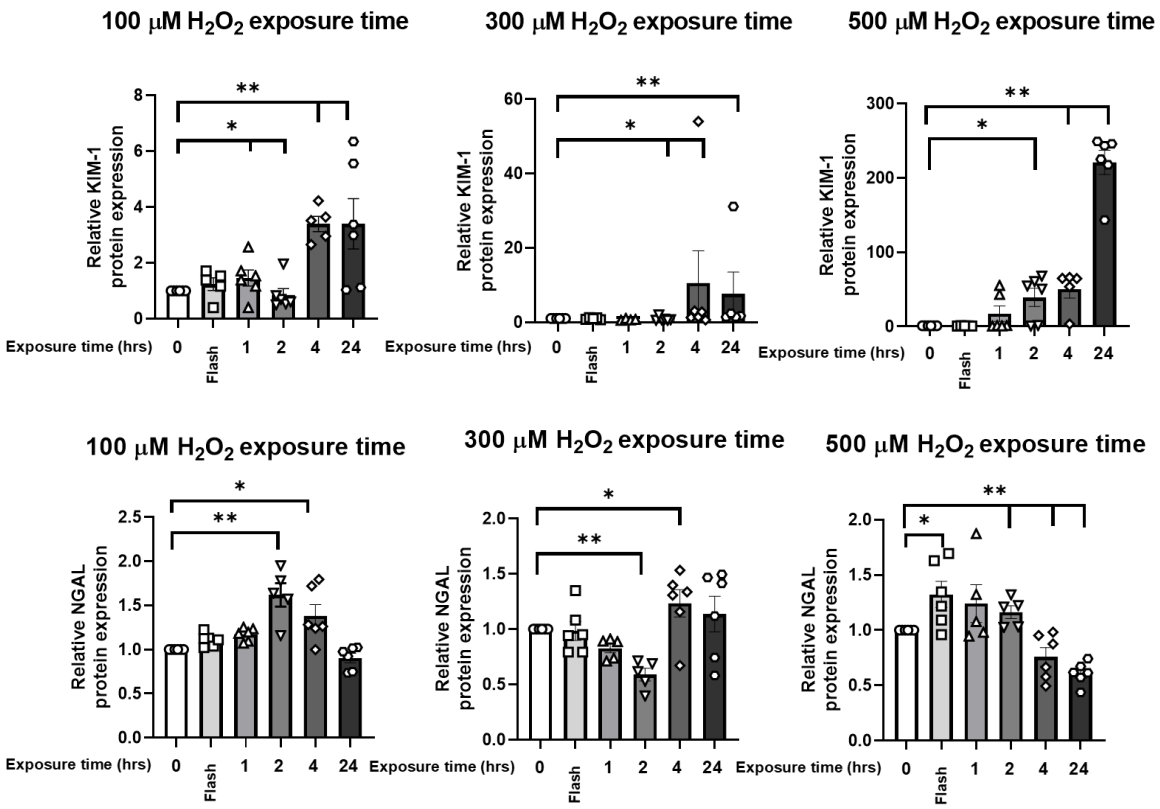

Figure 5-1 Protein profiling of KIM-1 and NGAL expression after NRK-52E cell treatment with hydrogen peroxide. Kidney injury molecule-1 (KIM-1) and neutrophil gelatinase-associated lipocalin (NGAL) protein expression at different hydrogen peroxide concentrations and exposure times in NRK-52E cells was assessed using western blot analysis. Data are means ± SEM (n=5-6). Data compared to control were analysed with the Mann-Whitney U test. *p<0.05, **p<0.01.

Neutrophil gelatinase-associated lipocalin (NGAL) protein expression in this study was variable. In the 100 µM hydrogen peroxide exposure experiments, NGAL protein expression peaked at the 2-hour exposure time and then gradually decreased to control levels at the 24-hour exposure time. There was similar NGAL protein expression when comparing the control group to flash exposure (1.11±0.03-fold change, $p>0.05$), 1 hour (1.17±0.03-fold change, $p>0.05$), and 24 hours (0.9±0.05-fold change, $p>0.05$) exposure times. Elevations of NGAL expression were observed in the groups with 2-hour (1.62±0.13-fold change, $*p=0.002$) and 4-hour (1.3±0.13-fold change, $*p=0.048$) exposure times. In the 300 µM hydrogen peroxide exposure experiments, NGAL expression was variable. Similar NGAL expression was observed in the group with flash exposure compared to control (0.99±0.09-fold change, $p>0.05$) and 1 hour (0.83±0.04-fold change, $p>0.05$), was significantly decreased at 2 hours (0.59±0.06-fold change, $**p=0.002$) exposure time, and then significantly increased at 4 hours (1.23±0.12-fold change, $*p=0.048$) exposure time versus control. It then slightly dropped at 24 hours (1.14±0.16-fold change, $p>0.05$) exposure time. In the 500 µM hydrogen peroxide exposure experiments, the trend of NGAL levels was slightly increased after flash exposure and then gradually decreased over exposure time. NGAL protein expression was significantly increased after treatment with flash exposure (1.32±0.12-fold change, $*p=0.048$), 1 hour (1.24±0.17-fold change, $p=0.057$), and 2 hours (1.16±0.06-fold change, $**p=0.002$) exposure times versus the control group. There was then a decrease in NGAL expression at 4 hours (0.76±0.08-fold change, $**p=0.002$) and 24 hours (0.61±0.04-fold change, $**p=0.002$) exposure times versus control. This implied that NGAL expression in NRK-52E cells is sensitive to high concentrations of hydrogen peroxide. There was no significant difference between the 1-hour exposure time and the control group at 500 µM hydrogen peroxide.

5.4.1.2 Parp protein expression in hydrogen peroxide-induced injury in NRK-52E cells

Poly ADP-ribose polymerase (Parp-1) is a DNA-dependent nuclear enzyme. Elevated Parp can promote necrosis, autophagy, or AIF-induced parthanatos (Weaver and Yang, 2013). Activated caspase-3 can cleave Parp-1; then, cleaved Parp-1 can inhibit uncleaved Parp-1, thereby promoting apoptosis. Therefore, Parp-1 can be used as a cellular apoptotic marker.

In these experiments, poly ADP-ribose polymerase (Parp) protein expression was variable (**Figure 5-2**). In 100 µM hydrogen peroxide exposure, most exposure times resulted in lower Parp protein expression. There was a significantly decreased Parp expression in groups with flash exposure (0.54±0.06-fold change, ***p=0.002*, n=6), 1-hour (0.65±0.04-fold change, ***p=0.002*, n=6), 2-hour (0.69±0.06-fold change, ***p=0.002*, n=6), and 24-hour (0.6±0.05-fold change, ***p=0.002*, n=6) exposure times. In 300 µM hydrogen peroxide exposure, most Parp protein expression levels were lower after exposure to hydrogen peroxide. There were significantly lower Parp protein expression levels in the 1-hour (0.57±0.05-fold change, ***p=0.002*, n=6), 4-hour (0.63±0.1-fold change, ***p=0.002*, n=6), and 24-hour (0.46±0.06-fold change, ***p=0.002*, n=6) exposure groups versus the control group. In addition, there was a trend of decreased Parp expression in the 2-hour (0.62±0.1-fold change, *p=0.08*, n=6) exposure group. Parp protein expression in the 500 µM hydrogen peroxide exposure treatment groups was similar in protein level except for those with 4-hour exposure time (1.41±0.18-fold change, ***p=0.002*, n=6). This experiment shows that exposure to 500 µM of hydrogen peroxide for 4 hours did not increase Parp protein expression.

To conclude this experiment, a 500 µM hydrogen peroxide exposure for 4 hours does not alter Parp protein expression in NRK-52E cells and therefore is not a reliable indicator of apoptosis under these conditions. Higher concentrations or longer exposure times, as well as other apoptotic protein markers such as caspase-3, BAX, and BAK, should be tried.

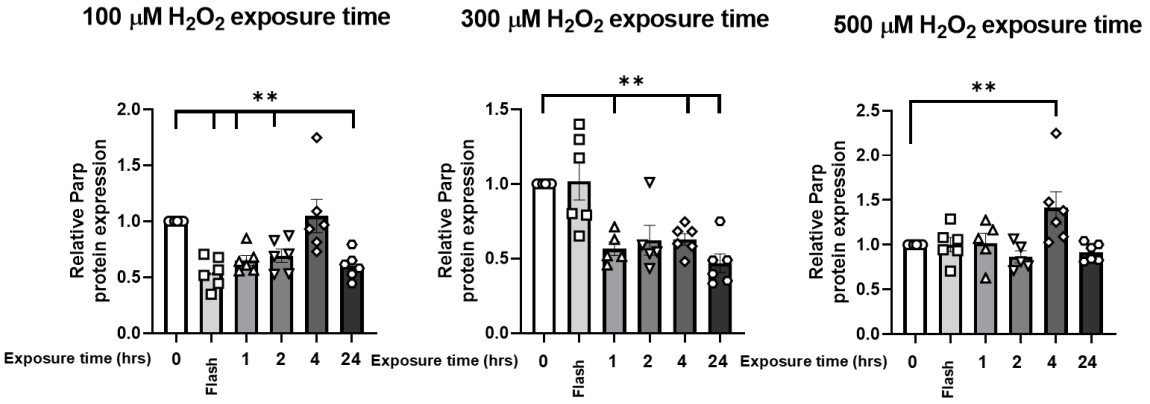

Figure 5-2 Protein profiling of Parp expression after NRK-52E cell treatment with hydrogen peroxide. Poly ADP-ribose polymerase (Parp) protein expression at different hydrogen peroxide concentrations and exposure times in NRK-52E cells was assessed using western blot. Data are means ± SEM (n=6). Data compared to control were analysed with the Mann-Whitney U-test. **p<0.01.

5.4.1.3 Viable and non-viable NRK-52E cells after 500 μM hydrogen peroxide exposure for 4 and 24 hours

To evaluate a suitable exposure time for 500 μM hydrogen peroxide, viable and non-viable cell counts were performed using the trypan blue exclusion test. NRK-52E cells were treated with or without 500 μM hydrogen peroxide for 4 hours and 24 hours in a 6-well plate (n=6) (**Fig 5-3 and 5-4**).

In viable cell counts, the viable cell number in the control group at 4 hours was 790,833 (±36,479) cells. After treatment with hydrogen peroxide for 4 hours, there was a significant decrease (528,333 ±42,302 cells, ***p=0.009,* n=6) in viable cell number. A similar pattern was found at the 24-hour observation: viable cells in the injured group were significantly lower (***p=0.002*) than those in the non-injured group. Viable cell count in the non-injured group and injured group was 935,000 (±29,721) cells and 343,333 (±37,565) cells, respectively. In addition, there was a significant difference in viable cell number between the non-injured group at 4 hours and 24 hours (**p=0.013*), and there were significant differences in viable cell number between injured cells at 4 hours and 24 hours exposure time (***p=0.009*). Viable cell number in the non-injured group was higher over time; however, viable cell number was lower over time after treatment with 500 μM hydrogen peroxide.

In non-viable cell counts, there were similar non-viable cell numbers between the non-injured and injured groups at 4 hours of cell culture. Non-viable cell numbers in the non-injured group and injured group were 38,333 (±8,233) cells and 37,500 (±5,881) cells, respectively. However, non-viable cell number at 24 hours of cell culture was significantly higher than at 4 hours of cell culture in both groups. Non-viable cell number in the non-injured group at 24 hours was 212,500 (±23,229) cells, which was significantly lower than in the injured group (326,667±38,398 cells, *$p=0.032$, n=6) at the same cell culture time. There was no difference in non-viable cell number between non-injured and injured groups at 4 hours of observation, but non-viable cells were higher at 24 hours of observation in both groups.

In conclusion, 500 µM hydrogen peroxide reduced viable NRK-52E cells after 4 hours (93.3%) and continued to decrease viable cells at 24 hours (51.41%). Therefore, the effect of 500 µM hydrogen peroxide on viable and non-viable NRK-52E cells was time-dependent. To select a suitable exposure time for hydrogen peroxide, the very low viable cell number at 24 hours exposure time was of concern. Therefore, the 4-hour incubation with 500 µM hydrogen peroxide was selected as the incubation time for further experiments.

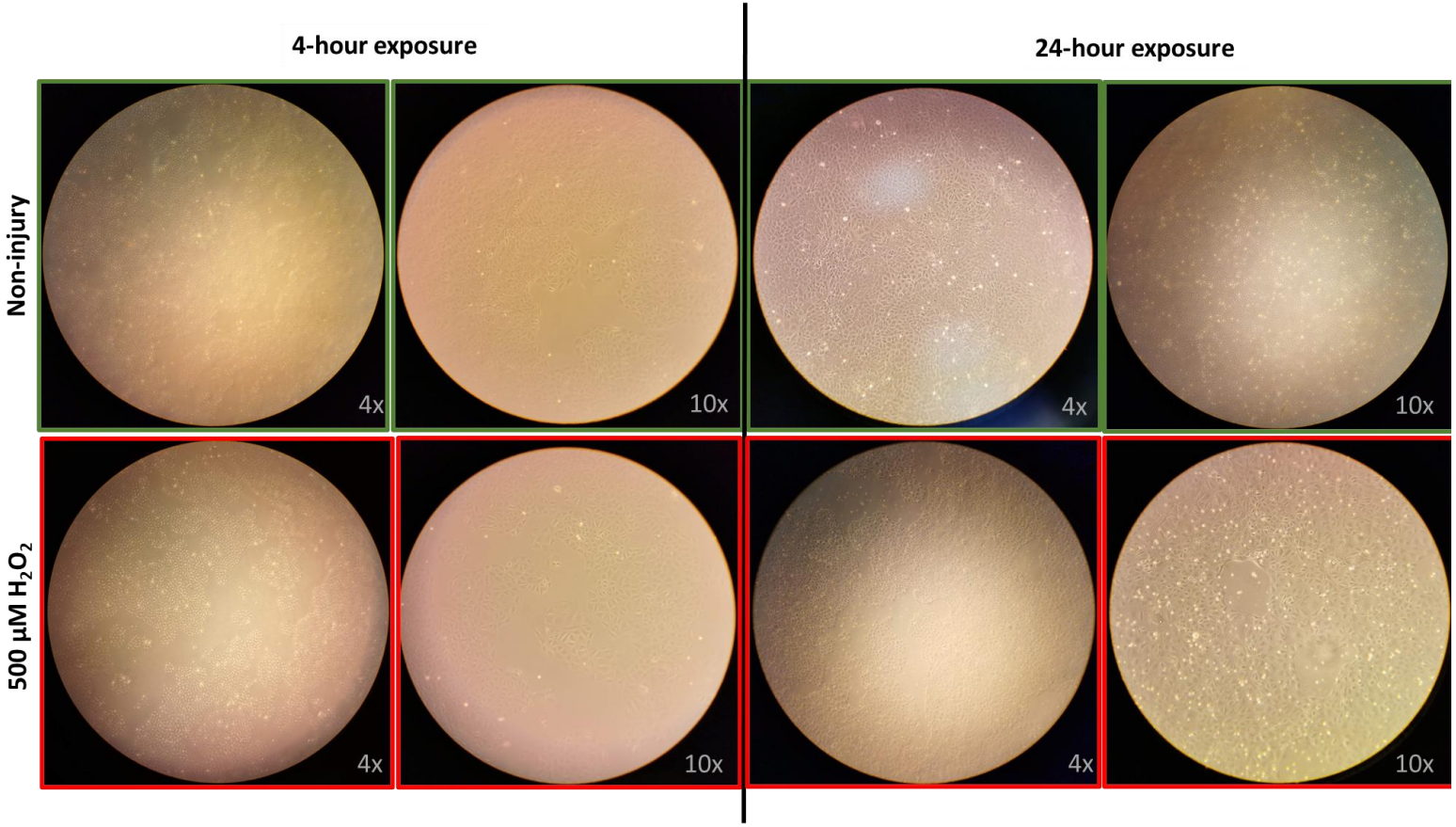

Figure 5-3 Cell growth at 4 and 24 hours after 500 µM hydrogen peroxide treatment on NRK-52E cells. Representative images of cultured NRK-52E cells under optimal conditions (non-injury) and with 500 µM hydrogen peroxide at 4 hours and 24 hours under a light microscope. Cell confluence in the same group increased over time, and the non-injured NRK-52E cell confluency was higher than that of the injured NRK-52E cells at both 4 hours and 24 hours of culture (4x and 10x magnification, n=6).

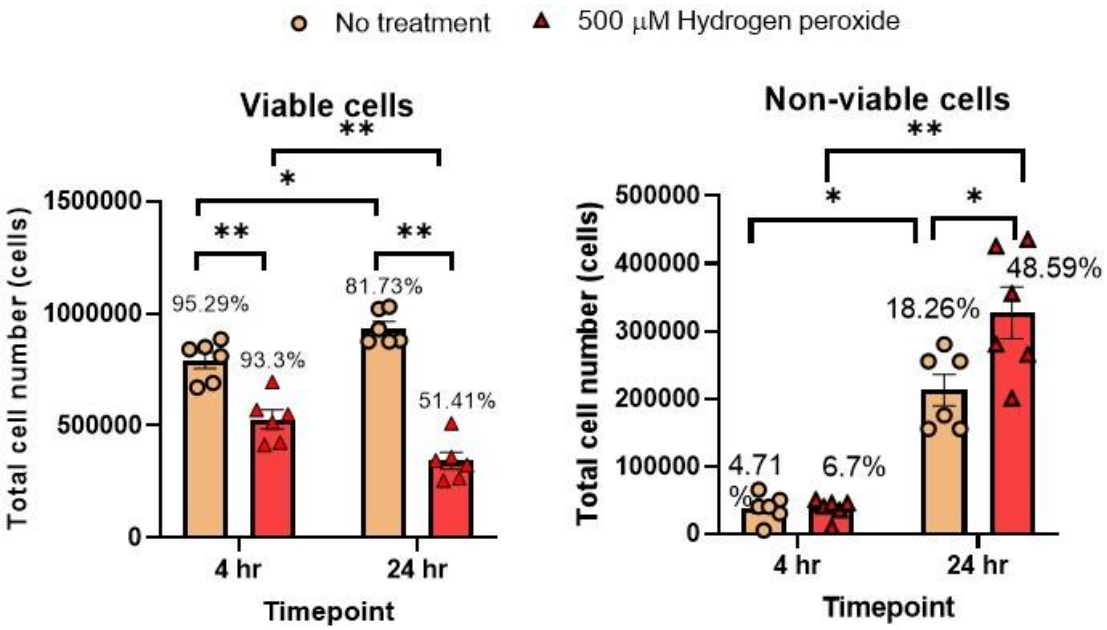

Figure 5-4 Total cell count comparing 500 µM hydrogen peroxide and control on NRK-52E cells. Viable and non-viable cell counts at the selected concentration (500 µM hydrogen peroxide-treated NRK-52E cells) were performed using the trypan blue exclusion test of cell viability. Data are means ± SEM (n=6). Data were analysed with the Mann-Whitney U-test. *p<0.05, **p<0.01.

5.4.1.4 Caspase-3 activity of NRK-52E cells after incubation with 500 µM hydrogen peroxide for 4 hours

Caspase-3 is a common enzyme used in research studies. Procaspase-3 is activated by either the death cell receptor or the mitochondrial apoptotic cascade. To measure the activity of caspase-3, the colorimetric peptidic substrate acetyl-Asp-Glu-Val-Asp p-nitroanilide was used for detection (Peterson et al., 2010). In this experiment, caspase-3 activity in the non-injury group was significantly higher than in the oxidative stress induction group (0.0136 ± 0.0008 O.D. vs 0.0113 ± 0.0005 O.D., respectively, $p=0.018$, n=11) (**Figure 5-5**). This showed that active caspase-3 was decreased by 500 µM hydrogen peroxide for 4 hours.

This result demonstrates that a concentration of 500 µM hydrogen peroxide and an incubation time of 4 hours represent a suitable induction of injury for further experiments.

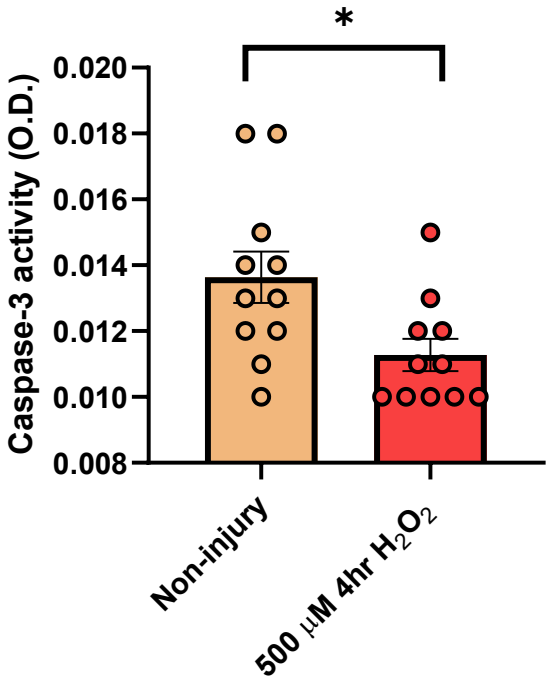

Figure 5-5 Comparison between caspase-3 activity in non-injury and 500 µM hydrogen peroxide-induced groups in NRK-52E cells. Data are means ± SEM (n = 11). Data were analysed with the Mann-Whitney U test. *$p < 0.05$.

5.4.2 Effects of ADRCs on NRK-52E cells

These studies evaluate the effects of ADRCs on several aspects of the response to injury induction, including assessment of tubular injury, cell viability, anti-apoptotic properties, proliferation, anti-oxidation, and anti-fibrotic properties.

5.4.2.1 Effects of ADRCs on NGAL and KIM-1 mRNA expression in injured NRK-52E cells

To evaluate the effect of ADRCs on tubular injury, NGAL and KIM-1 gene expression-both highly expressed in kidney injury-were used as indicators of the response to injury. In this study, transcriptional expression of these genes was measured using the qPCR technique.

NGAL mRNA relative expression was downregulated after treatment with ADRCs in the injured group (**Fig. 5-6**). The relative expression of NGAL in the control group was upregulated compared to the group exposed to hydrogen peroxide (0.72 ± 0.13 vs 1.02 ± 0.03 $2^{-\Delta\Delta Ct}$, respectively; $*p = 0.038$, n = 11). The relative expression in the injured group was significantly downregulated after ADRC treatment (1.02 ± 0.03 vs 0.69 ± 0.12 $2^{-\Delta\Delta Ct}$, respectively; $**p = 0.0075$, n = 12) and did not differ from the non-injured group with ADRC treatment (0.82 ± 0.09 $2^{-\Delta\Delta Ct}$). This indicates that the effect of ADRCs can be observed in the injured group and that ADRC treatment can return NGAL expression levels to normal.

Despite the changes in NGAL mRNA relative expression, there was no difference in KIM-1 mRNA expression among the non-injured group, injured group, non-injured group with ADRC treatment, and injured group with ADRC treatment (0.81 ± 0.4, 0.61 ± 0.33, 1.12 ± 0.56, 0.19 ± 0.11 $2^{-\Delta\Delta Ct}$, respectively) (**Fig. 5-6**). This shows that KIM-1 mRNA expression was not a sensitive marker in this context; however, it suggests that KIM-1 can be used as an indicator of injury, which may be clearer with a larger sample size. This experiment also showed that ADRCs had limited impact on KIM-1 expression and that hydrogen peroxide does not appear to induce KIM-1 mRNA expression.

These results suggest that ADRC treatment may have some effect against tubular injury by decreasing NGAL mRNA expression and returning it to naïve levels. However, KIM-1 mRNA expression was not a sensitive marker for 500 μM hydrogen peroxide exposure for 4 hours.

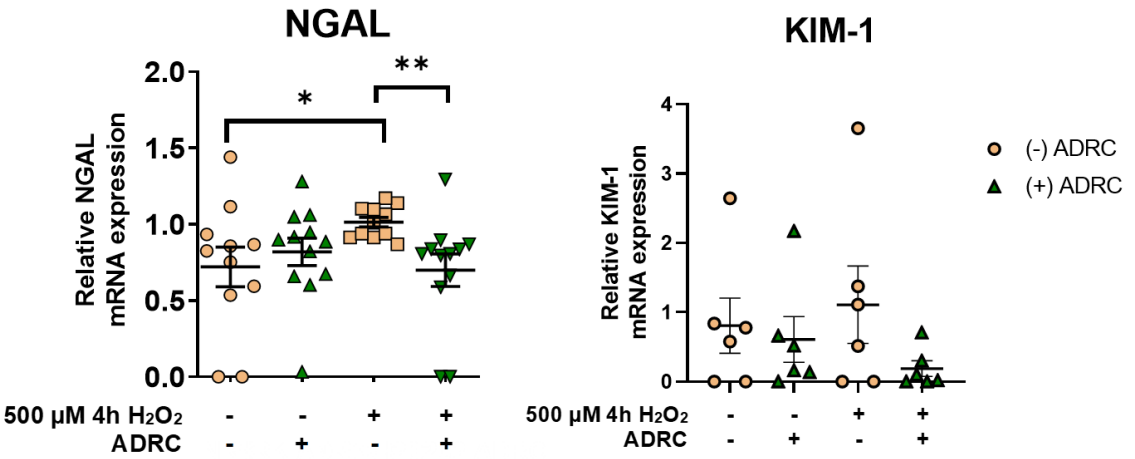

Figure 5-6 mRNA expression of NGAL and KIM-1 tubular injury markers after ADRC treatment in NRK-52E cells. Data are presented as means ± SEM (n = 11–12, NGAL; n = 6, KIM-1). Statistical analysis was performed using the Kruskal-Wallis H test with Dunn's multiple comparisons test. *$p < 0.05$, **$p < 0.01$.

5.4.2.2 Effects of ADRCs on microvesicle concentration in cultured injured NRK-52E cells

This study measured the supernatant of culture media using nanoparticle tracking analysis. To clarify the definition of microvesicles, particles with sizes between 150 and 1,000 nanometres were classified as microvesicles. Particles were measured in both the plain supernatant and concentrated supernatant via exosome isolation techniques (see Chapter 2.6.5). In this experiment, there was no difference in microvesicle concentration among the control, control with ADRC treatment, injury, and injury with ADRC treatment groups (9.22 $\pm$0.87 x10^9, 8.63 $\pm$0.99 x10^9, 9.69 $\pm$1.19 x10^9, 9.51 $\pm$1.04 x10^9 particles/mL respectively, *p>0.05,* n=6) (**Fig 5-7**).

Similar to the previous study of KIM-1 mRNA expression, 500 µM hydrogen peroxide for 4 hours did not induce microvesicle shedding in NRK-52E cells, with or without ADRC treatment. This study showed that these conditions are not strongly associated with microvesicle shedding, nor are microvesicles a sensitive indicator of these injury induction conditions.

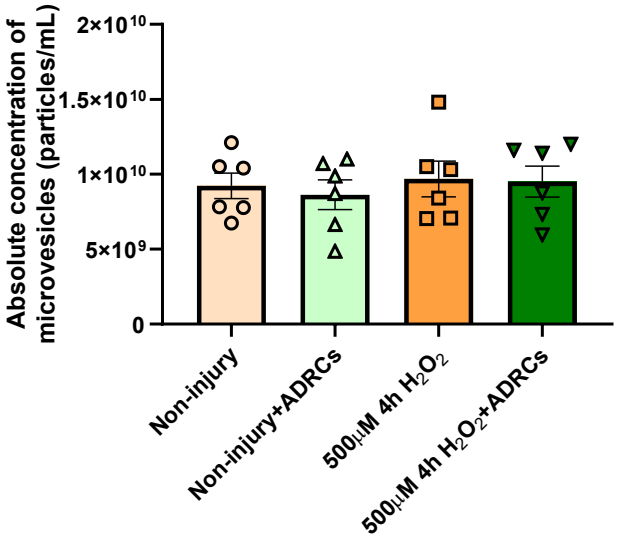

Figure 5-7 Microvesicle concentrations after ADRC treatment in injured and non-injured NRK-52E cells. Microvesicle concentrations were measured using nanoparticle tracking analysis. Data are presented as means ± SEM (n = 6). Statistical analysis was performed using the Kruskal-Wallis H test with Dunn's multiple comparisons test.

5.4.2.3 Effect of ADRCs on viable cells in injured NRK-52E cells using trypan blue exclusion assay

To evaluate the effects of ADRCs on cell survival, total cell count was measured using a trypan blue exclusion assay (**Fig. 5-8**). The number of viable cells in the hydrogen peroxide induction group was significantly lower than in the control group ($p = 0.02$). However, there was no difference in the number of viable cells between the naïve group and the naïve group with ADRC treatment (1,800,417 ± 350,452 vs 2,037,500 ± 214,646 cells, respectively; $p > 0.05$, n = 6), and there was no difference in the number of viable cells between the injury group and the injury group with ADRC treatment (602,500 ± 75,075 vs 805,000 ± 73,428 cells, respectively; $p > 0.05$, n = 6). These results show that ADRCs had no effect on NRK-52E cell viability in either normal cells or cells exposed to oxidative damage with 500 µM hydrogen peroxide for 4 hours.

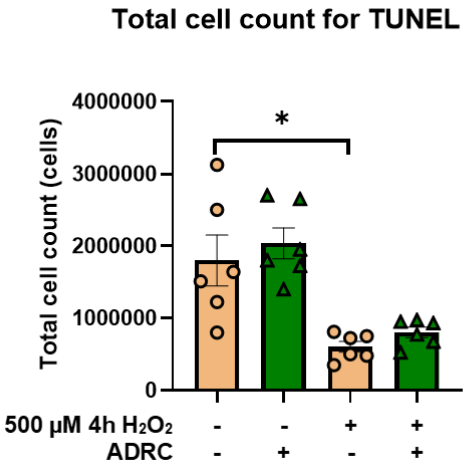

Figure 5-8 Total cell count after ADRC treatment in injured and non-injured NRK-52E cells. Total cell number of normal and injured NRK-52E cells with or without 500 µM hydrogen peroxide treatment was determined using the trypan blue exclusion assay under a light microscope. The cell growth area was 1.6 cm^2. Data are presented as means ± SEM (n = 6). Statistical analysis was performed using the Kruskal-Wallis H test with Dunn's multiple comparisons test. *$p < 0.05$.

5.4.2.4 Effects of ADRC treatment on caspase-3 activity and mRNA expression of BAX, Casp-3 and Casp-9 in injured NRK-52E cells

To investigate the anti-apoptotic properties of ADRCs, specific apoptotic marker genes were used in this study. BAX and caspase-9 are markers of the intrinsic pathway of apoptosis, while caspase-3 is a marker of the common pathway of apoptosis. These markers are commonly used in anti-apoptotic studies. Increased expression or activity of these apoptotic markers indicates upregulation of apoptosis.

A caspase-3 activity assay was used to observe caspase-3 activation. Higher caspase-3 activity indicates a stronger signal in the apoptotic pathways. The results showed that the injured group with ADRC treatment had decreased caspase-3 activity compared to healthy NRK-52E cells (0.001 ± 0.0005 vs 0.014 ± 0.0008 O.D., respectively, n = 11), and the injured group with ADRC treatment also had decreased caspase-3 activity compared to the healthy group with ADRC treatment (0.001 ± 0.0005 vs 0.012 ± 0.0005 O.D., respectively, n = 11). However, there was no difference between the healthy group and the injured group (0.001 ± 0.0005 vs 0.011 ± 0.0004 O.D., respectively, n = 11) (**Fig. 5-9**).

mRNA expression of BAX, caspase-3, and caspase-9 was also measured in this study to evaluate the effect of ADRCs on cellular signalling in the apoptotic pathway (**Fig. 5-10**). In the BAX mRNA expression experiments, there was no difference among the control, control with ADRC treatment, injury, and injury with ADRC treatment groups (0.53 ± 0.25, 0.9 ± 0.48, 1.74 ± 0.69, 1.25 ± 0.47 $2^{-\Delta\Delta Ct}$, respectively, n = 6). Similar results were observed for caspase-9 and caspase-3 mRNA expression. There was no difference among the naïve, naïve with ADRC treatment, injury, and injury with ADRC treatment groups (1.04 ± 0.1, 0.91 ± 0.9, 1.16 ± 0.11, 0.59 ± 0.11 $2^{-\Delta\Delta Ct}$, respectively, n = 9–11) in the caspase-9 experiment, and no difference among these four groups in the caspase-3 experiments (1.09 ± 0.23, 0.92 ± 0.11, 0.95 ± 0.08, 1.18 ± 0.14 $2^{-\Delta\Delta Ct}$, respectively, n = 9–11). These results showed that there was no anti-apoptotic effect of ADRCs on injured NRK-52E cells as observed in these experiments.

To summarize the assessment of the anti-apoptotic properties of ADRCs in these experiments, mRNA expression of apoptotic markers was not different across the four experimental groups. No anti-apoptotic properties of ADRCs were observed, and there was a rather limited impact of 500 μM hydrogen peroxide exposure for 4 hours on both healthy

and oxidative stress-induced NRK-52E cells as assessed by caspase-3 activity. The cause of cell death in this experiment might be due to necroptosis or pyroptosis. The cause of cell death should be studied further in the future.

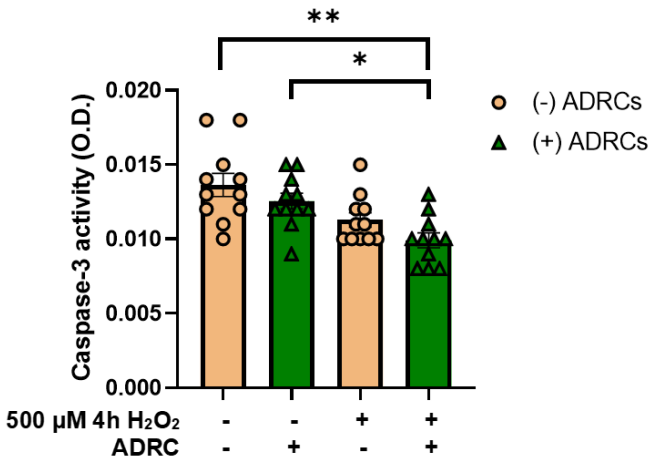

Figure 5-9 Caspase-3 activity after ADRC treatment in injured and non-injured NRK-52E cells. Caspase-3 activity assay of normal and 500 µM hydrogen peroxide-induced injured NRK-52E cells with or without ADRC treatment. Data are presented as means ± SEM (n = 11). Statistical analysis was performed using the Kruskal-Wallis H test with Dunn's multiple comparisons test. *$p < 0.05$, **$p < 0.01$.

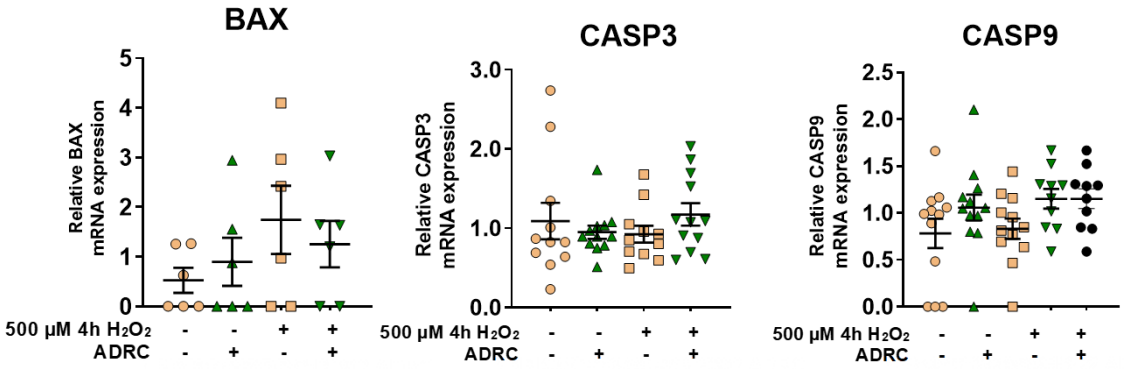

Figure 5-10 Apoptotic gene expression after ADRC treatment in injured and non-injured NRK-52E cells. Apoptotic marker gene expression is shown in normal and 500 µM hydrogen peroxide-induced injured NRK-52E cells with or without ADRC treatment. Data are presented as means ± SEM (n = 6 for BAX gene expression; n = 12 for CASP3 and CASP9 gene expression). Statistical analysis was performed using the Kruskal-Wallis H test with Dunn's multiple comparisons test.

5.4.2.5 The effect of ADRCs on dead cell markers, live cell markers, and proliferation markers in injured NRK-52E cells

5-bromo-2'-deoxyuridine (BrDU) and 7-aminoactinomycin D (7-AAD) were used for proliferation experiments. BrDU is a thymidine analogue that is incorporated into the 3'-OH ends of DNA fragments and then probed with an anti-BrdU antibody to detect apoptotic cells (Gavrieli et al., 1992; Liang et al., 2023). Higher BrDU intensity indicates higher cellular apoptosis. 7-AAD is a fluorescent viability dye that binds to DNA, incorporating into GC-rich regions; however, it cannot penetrate intact cell membranes. Therefore, it stains only non-viable or dead cells. Positive 7-AAD staining refers to dead cells. In this experiment, BrDU and 7-AAD were assessed using flow cytometric analysis. Each dot in the flow cytometric dot plot represents an event or a positive cell for a given marker after screening by gating strategy (**Fig. 5-11**). Ki-67, a proliferative marker, was also used in this flow cytometric experiment under the same experimental conditions.

Live cell markers in the injury group increased after treatment with ADRCs (**Figs. 5-12 and 5-13).** The percentage of BrDU-positive cells in the control group was not different from that in the hydrogen peroxide-induced injury group (7.47 ± 0.95% vs 11.94 ± 3.15%, respectively, $p > 0.05$, n = 6). After ADRC treatment, there was no change in the percentage of BrDU positivity in the injured group compared to the non-injured group (14.17 ± 0.68% vs 11.94 ± 3.15%, $p > 0.05$, n = 6). Although the dead cell marker in the naïve group was not different from that in hydrogen peroxide-induced injured cells, there was a trend toward decreased dead cell marker expression in ADRC-treated injured cells compared to injured cells alone ($p = 0.08$). In live cell analysis, the percentage of BrDU-negative and 7-AAD-positive cells in the control group was not different from that in the injured group (24.58 ± 3.19% vs 27.43 ± 3.46%, respectively, $p > 0.05$, n = 6). ADRC treatment in the injured group significantly increased the percentage of live cells compared to the injured group (52.17 ± 1.15% vs 27.43 ± 3.46%, respectively, $p = 0.0022$, n = 6). In addition, there was no difference between the control and the control treated with ADRCs (24.58 ± 3.19% vs 30.28 ± 5.29%, respectively, $p > 0.05$, n = 6). These results may imply a protective effect of ADRCs on oxidative stress-induced cells.

In proliferation experiments, the percentage of Ki-67-positive cells changed after oxidative stress induction, but an effect of ADRCs was not observed in this experiment (Figs. 5-14 and 5-15). Ki-67 positivity in the injured group was significantly lower than in the

control group (13.58 ± 0.51% vs 25.62 ± 0.62%, respectively, $p = 0.002$, n = 6). However, the percentage of proliferative marker-labelled cells did not differ between the control and the control with ADRC treatment (25.62 ± 0.62% vs 25.4 ± 1.23%, respectively, $p > 0.05$, n = 6), nor between the injury group and the injury group treated with ADRCs (13.58 ± 0.51% vs 12.18 ± 0.61%, respectively, $p > 0.05$, n = 6). Therefore, ADRCs did not impact the proliferation of injured NRK-52E cells as assessed by this assay.

To conclude these experiments, ADRC treatment showed some protective effects at 48 hours of cell culturing but did not show an impact on cellular proliferation of NRK-52E cells exposed to oxidative injury. This experiment also confirms the results of the trypan blue exclusion assay (**Fig. 5-8**).

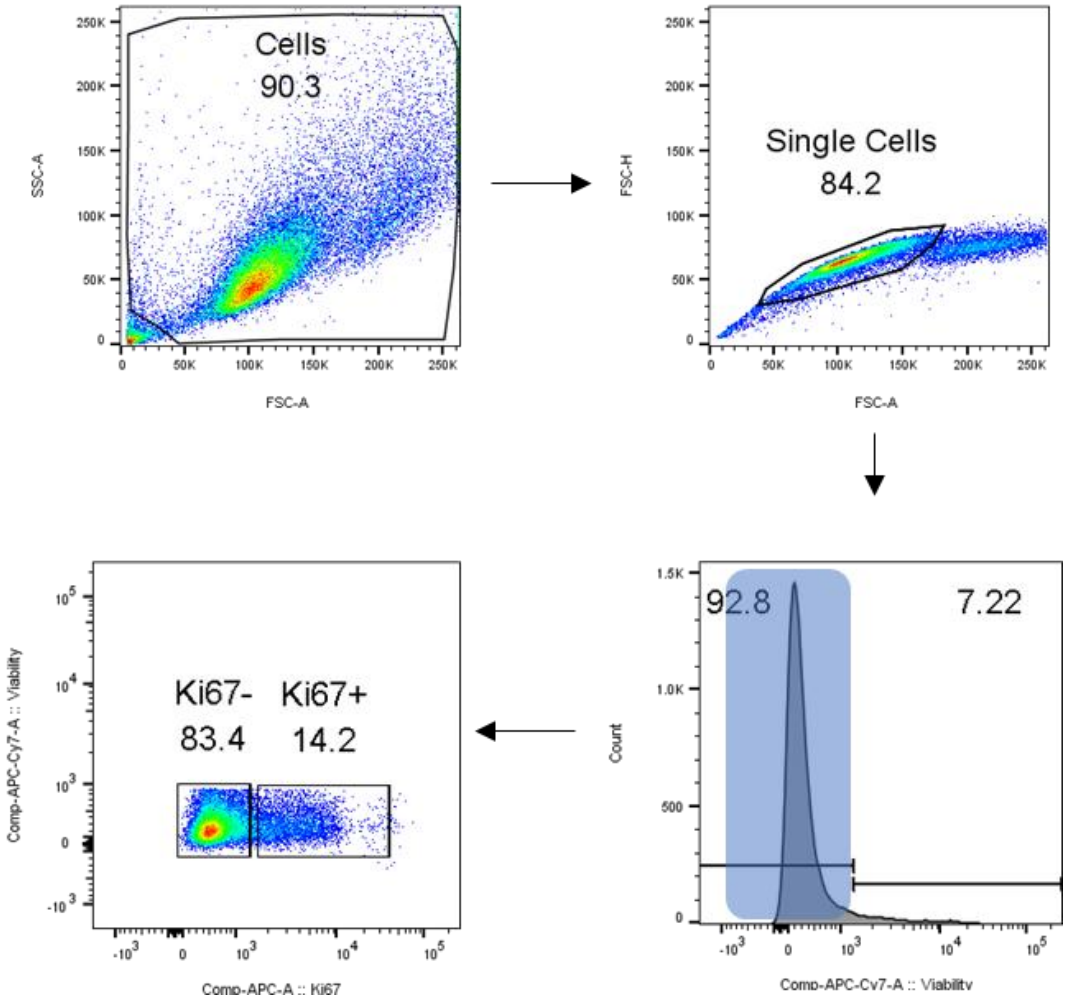

Figure 5-11 Gating strategy of cellular marker protein in NRK-52E cells. Forward scatter (FSC) intensity measures the diameter of the cells, while side scatter (SSC) intensity measures cell granularity. Cell debris, which has low FSC and SSC intensity, was excluded from this experiment. Cells showing a linear relationship between forward scatter area (FSC-A) and forward scatter height (FSC-H), indicating singlets, were gated and subsequently measured for fluorescence intensity of cell viability in a histogram. Cells stained with viability dye and identified as viability dye positive were classified as dead cells. Live cells were gated and plotted using two-parameter density plots to distinguish cell populations.

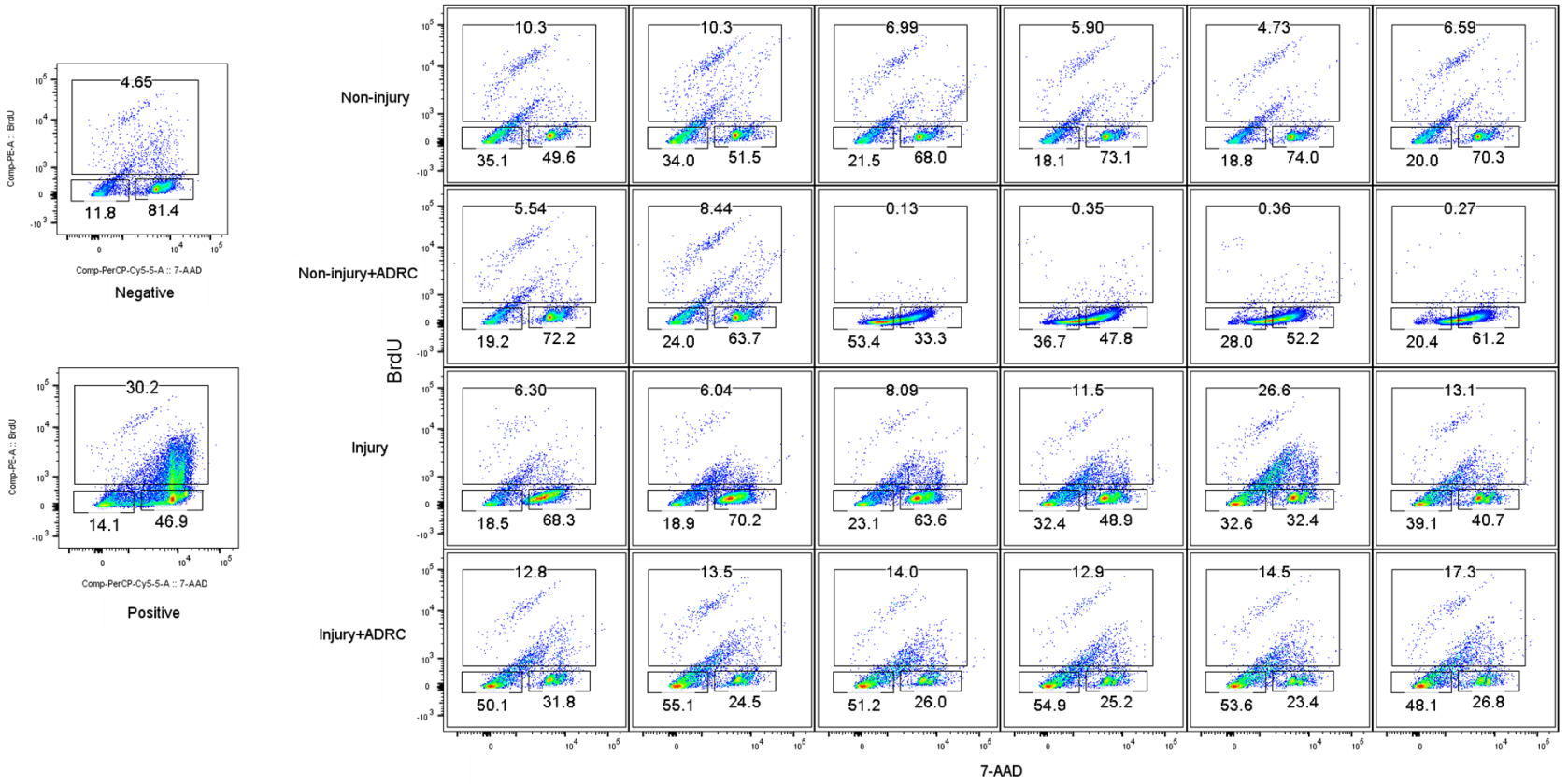

Figure 5-12 Scatter plots of dead cell marker (anti-7-AAD) into apoptotic marker (anti-BrdU) after ADRC treatment in NRK-52 cells. The upper gate identifies cells positive for BrDU, an apoptotic marker. The lower left gate identifies cells positive for the live cell marker, while the lower right gate identifies cells positive for the dead cell marker (n = 6).

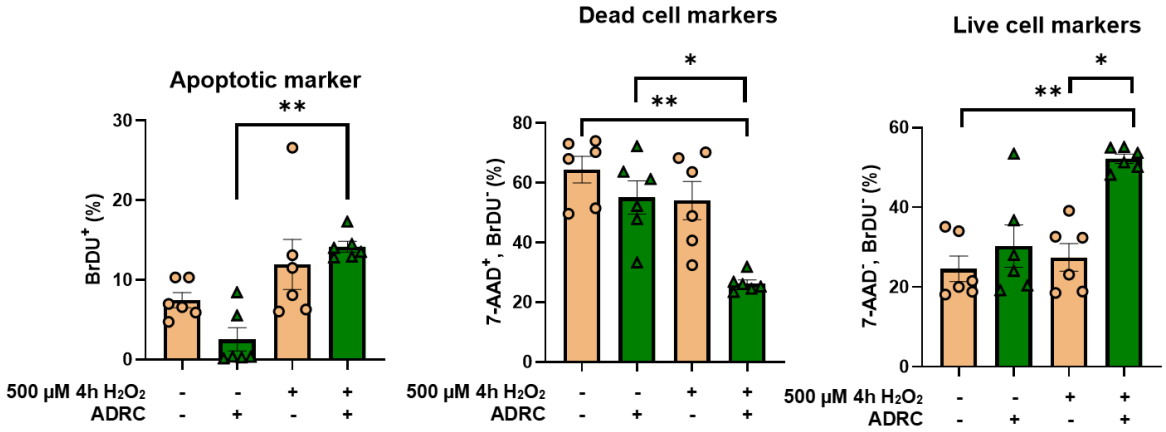

Figure 5-13 TUNEL assay analysis of apoptotic, dead cell, and live cell markers after ADRC treatment in NRK-52E cells. Apoptotic, dead cell, and live cell markers were assessed in the TUNEL assay of apoptosis using flow cytometry. Data are presented as means ± SEM (n = 6). Statistical analysis was performed using the Kruskal-Wallis H test with Dunn's multiple comparisons test. *$p < 0.05$, **$p < 0.01$.

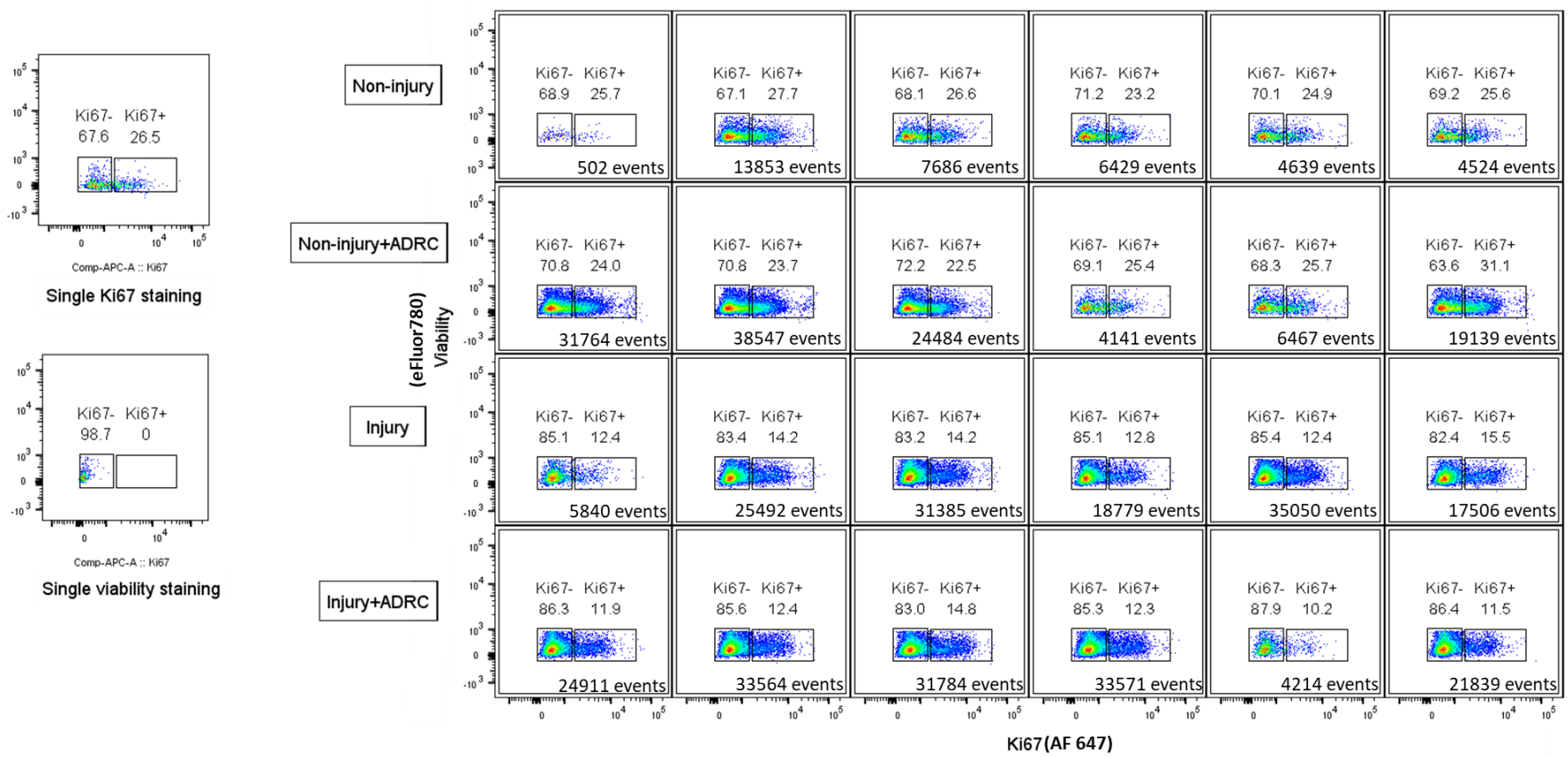

Figure 5-14 Scatter plots of proliferative marker (anti-Ki67) into Fixable Viability Dye (eFluor™ 780) after ADRC treatment in NRK-52 cells. Cells in the left gate were identified as non-proliferative, while cells in the right gate were identified as proliferative (n = 6).

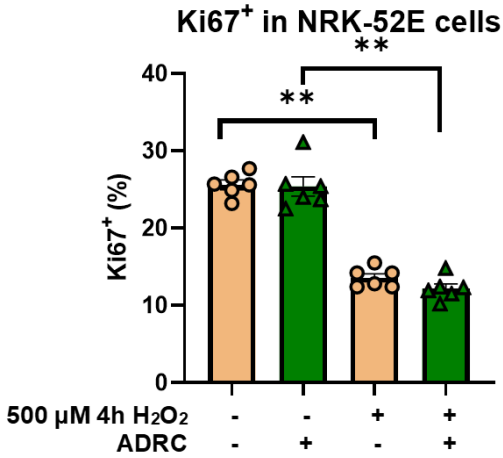

Figure 5-15 Flow cytometry analysis of a proliferative marker after ADRC treatment in NRK-52E cells. Ki-67 protein was used as a proliferative marker. Data are presented as means ± SEM (n = 6). Statistical analysis was performed using the Kruskal-Wallis H test with Dunn's multiple comparisons test. *$p < 0.05$.

5.4.2.6 The effect of ADRCs on mRNA expression of superoxide dismutase-1 in injured NRK-52E cells

Superoxide dismutase (SOD)-1 is an intracellular enzyme that catalyses the conversion of superoxide into oxygen and hydrogen peroxide. SOD-1 mRNA was used as a marker of oxidation in this experiment. The results showed that there was no difference among the four experimental groups: control, control with ADRC treatment, injury, and injury with ADRC treatment (1.33 ± 0.34, 1.20 ± 0.18, 1.05 ± 0.06, 1.17 ± 0.16 $2^{-\Delta\Delta Ct}$, respectively; n = 12) (**Fig. 5-16**). This experiment on NRK-52E cells showed that SOD-1 was not sensitive to hydrogen peroxide induction and that ADRCs had no effect on SOD-1 gene expression.

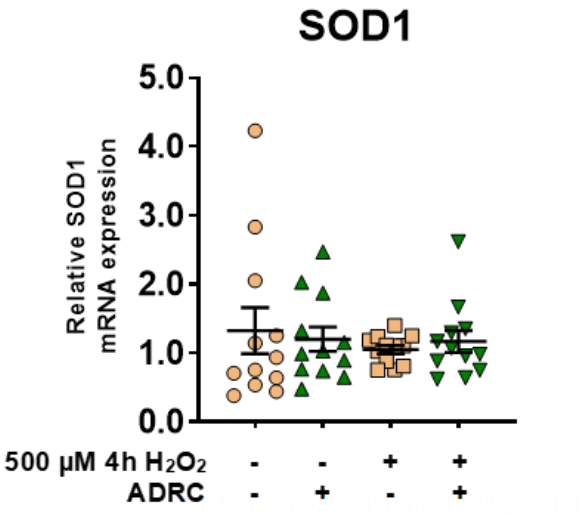

Figure 5-16 mRNA expression of SOD-1 after ADRC treatment in NRK-52E cells. mRNA expression of superoxide dismutase (SOD)-1 is shown in normal and 500 μM hydrogen peroxide-induced injured NRK-52E cells with or without ADRC treatment. There was no significant difference among the four experimental groups. Data are presented as means ± SEM (n = 12). Statistical analysis was performed using the Kruskal-Wallis H test with Dunn's multiple comparisons test.

5.4.2.7 The effects of ADRCs on Lif gene, transforming growth factor beta gene, and nuclear factor kappa B gene, collagen type I gene, and elastin gene expressions in injured NRK-52E cells

There are several fibrotic progenitor markers involved in fibrotic processes. Collagen type I, elastin, fibronectin, and entactin are protein components of the extracellular matrix. The accumulation of these proteins is commonly found in fibrotic tissues, and they were used as fibrotic markers in this study. Transforming growth factor (TGF-β), nuclear factor kappa B (NF-κB), and leukaemia inhibitory factor (Lif) are involved in fibrogenesis. In these experiments, Lif, TGF-β, and NF-κB mRNA were used as fibrotic progenitor markers.

Lif mRNA expression was altered after hydrogen peroxide induction, and ADRCs restored Lif mRNA expression to the naïve state (**Fig. 5-17**). There was no difference among the control, control with ADRC treatment, injury, and injury with ADRC treatment groups (0.5 ± 0.22, 0.4 ± 0.19, 1.58 ± 0.52, 0.76 ± 0.3 $2^{-\Delta\Delta Ct}$, respectively, n = 6). Similar to the Lif experimental result, TGF-β mRNA expression was not different among the four experimental groups: control, control with ADRC treatment, injury, and injury with ADRC treatment (0.53 ± 0.27, 0.34 ± 0.16, 1.14 ± 0.4, 0.81 ± 0.26 $2^{-\Delta\Delta Ct}$, respectively, n = 6). In the NF-κB experiments, there was no difference among the control, control with ADRC treatment, injury, and injury with ADRC treatment groups (0.5 ± 0.22, 0.59 ± 0.27, 1.46 ± 0.51, 1.02 ± 0.33 $2^{-\Delta\Delta Ct}$, respectively, n = 6).

ADRCs did not alter collagen type I mRNA expression between the injured group and the injured group with ADRC treatment (**Fig. 5-18**). Collagen type I mRNA expression in the injured group was significantly lower than in the control group (0.67 ± 0.09 vs 0.94 ± 0.1 2-ΔΔCt, respectively, $p = 0.001$, n = 12). After treatment with ADRCs, there was no difference between the ADRC-treated group and their control. In the elastin mRNA expression studies, there was no difference among the control, control with ADRC treatment, injury, and injury with ADRC treatment groups (1.21 ± 0.22, 0.88 ± 0.09, 0.61 ± 0.08, 1.16 ± 0.16 $2^{-\Delta\Delta Ct}$, respectively, n = 12).

To conclude, these experiments showed no effect of ADRCs on fibrotic progenitor markers or fibrotic markers.

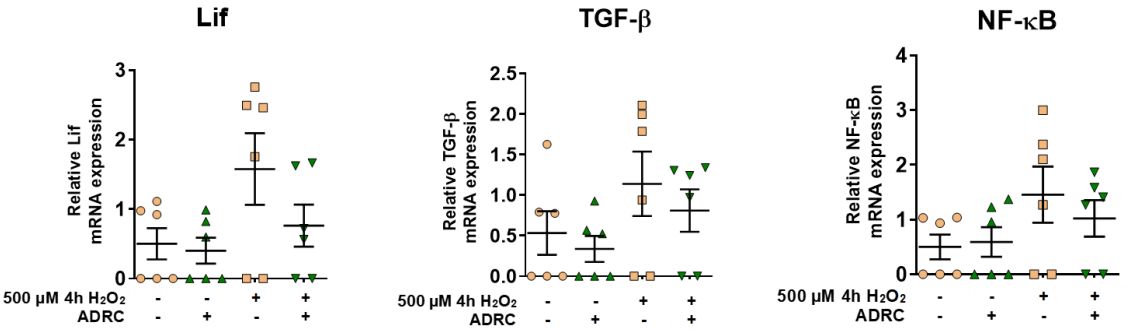

Figure 5-17 mRNA expression of fibrotic progenitors after ADRC treatment in NRK-52E cells. Leukaemia inhibitory factor (Lif) gene, transforming growth factor beta (TGF-β) gene, and nuclear factor kappa B (NF-κB) gene expressions in NRK-52E cells were determined using RT-PCR. Data are presented as means ± SEM (n = 6). Statistical analysis was performed using the Kruskal-Wallis H test with Dunn's multiple comparisons test.

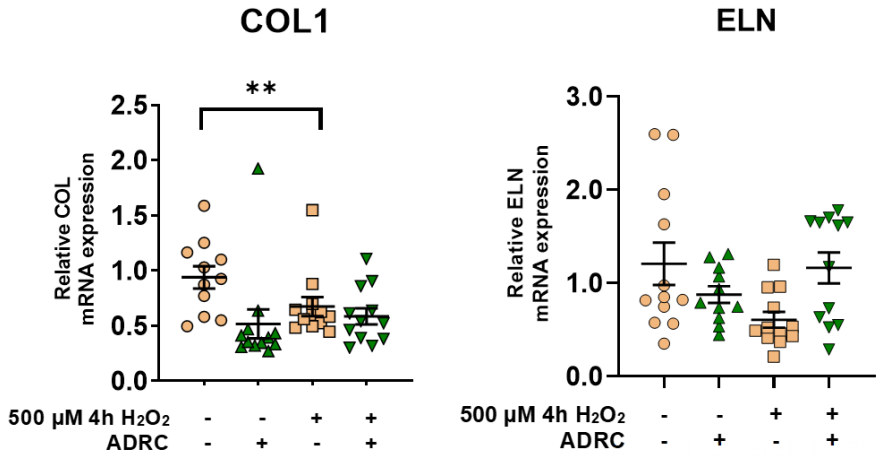

Figure 5-18 mRNA expression of collagen type I (COL1) and elastin (ELN) progenitors after ADRC treatment in NRK-52E cells. Type I collagen (COL1) and elastin (ELN) gene expression in NRK-52E cells was determined using RT-PCR. Data are presented as means ± SEM (n = 12). Statistical analysis was performed using the Kruskal-Wallis H test with Dunn's multiple comparisons test. $^{**}p < 0.01$.

5.5 Discussion

Proximal tubular cells are targets for kidney ischemia-reperfusion injury due to their high oxygen demand. Therefore, proximal tubular cell culture is a well-established model for experimental kidney injury (Piret and Mallipattu, 2020; Khundmiri et al., 2021). In this study, the results showed that ADRCs decreased fibrotic progenitor markers and had protective effects on NGAL expression and cell viability in NRK-52E cells exposed to 500 μM hydrogen peroxide for 4 hours. However, an apoptotic protective effect of ADRCs was not observed. This study demonstrates some of the potential therapeutic effects of ADRCs in an *in vitro* setting.

5.5.1 Pro-survival properties of ADRCs

This study demonstrated that ADRCs can increase live cell markers and showed a trend toward decreasing dead cell markers in NRK-52E cells. These results suggest that the decrease in dead cell markers is unlikely to be due to the influence of apoptotic pathways.

Anti-apoptotic effects of ADRCs have been shown in previous studies. For example, the study conducted by Li et al. (2019) demonstrated that exosomes extracted from Sprague-Dawley rat mesenchymal stem cells exhibited anti-apoptotic effects by inhibiting the expression of caspase-9, cleaved caspase-3, BAX, and BCL2 protein in the ischemia-reperfusion injury group, as shown by western blot analysis (Li et al., 2019b). In my study, there was no difference in the gene expression of BAX, caspase-3, and caspase-9. The possible differences in results could be due to the surgical rat model in Li's study having higher protein expression than the *in vitro* model, and the gene expression analysis by qPCR having a short time window for detecting gene expression.

Another technique to detect apoptosis is the TUNEL assay. The study by Zhang et al. (2017) showed lower levels of apoptotic markers in the TUNEL assay and higher anti-apoptotic BCL2 protein in ADRC-treated IRI kidneys in Sprague-Dawley rats subjected to 40 minutes of renal ischemia (Zhang et al., 2017). Since the TUNEL assay in Zhang's study was performed using immunohistochemistry in a surgical rat model, this may account for the differences in outcomes compared to my study. The possible anti-apoptotic effect of ADRCs based on my study and literature review is shown in **Figure 5-19**.

Since my study showed a trend toward decreasing dead cell markers in the injured group with ADRC treatment, but this was not triggered via the apoptotic pathway, other possible pathways could include caspase-independent apoptosis or ferroptosis.

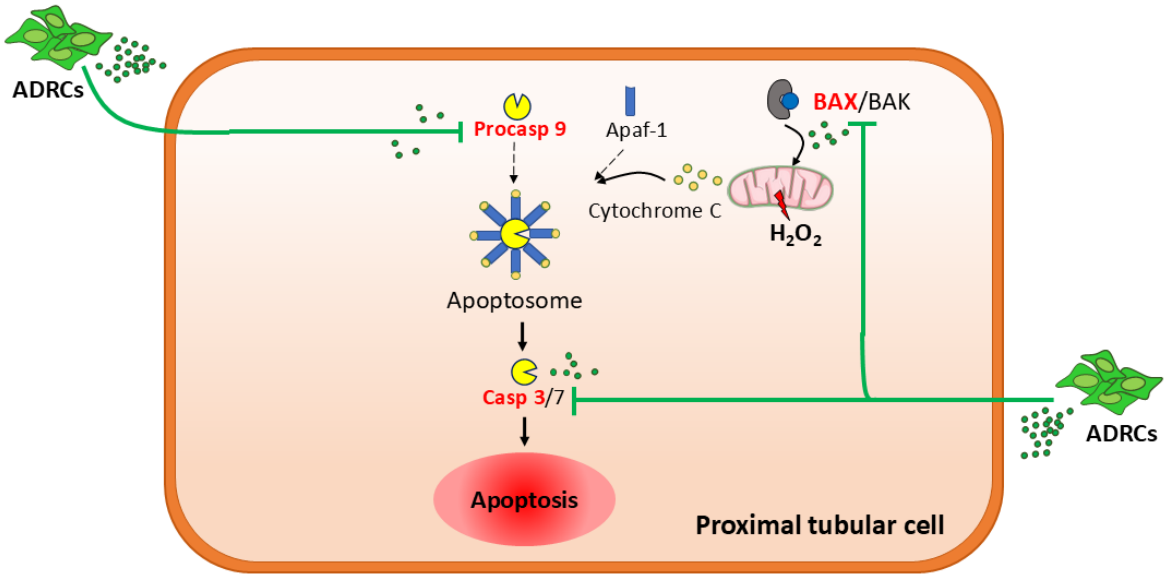

Figure 5-19 The expected effects of ADRCs on the intrinsic apoptotic pathway in proximal tubular cells in previous studies. ADRCs inhibit the expression of BAX, procaspase-9, and caspase-3 in the apoptotic pathway. The inhibition of these apoptotic markers results in decreased cellular signalling of apoptosis.

Caspase-independent apoptosis is a type of programmed cell death associated with mitochondrial proteins. Two key proteins involved in caspase-independent apoptosis are apoptosis-inducing factor (AIF) and endonuclease G (EndoG) (Daugas et al., 2000; Parrish et al., 2001). The translocation of AIF and EndoG to the nucleus leads to DNA fragmentation and cell death.

AIF is an oxidoreductase involved in apoptotic activation through its translocation from the mitochondria to the nucleus (Daugas et al., 2000). One study showed that hydrogen peroxide-exposed human B and T lymphoma cells initiated cell death without activation of the caspase pathway (Son et al., 2009). However, this study used glucose oxidase to induce hydrogen peroxide production with ATP depletion, and the cell types differ from those in my study; kidney cells might exhibit different responses regarding AIF release.

EndoG is a nuclease that induces internucleosomal DNA fragmentation. After translocation to the nucleus, EndoG cleaves DNA and induces internucleosomal DNA

fragmentation (Li et al., 2001). Another study showed that hydrogen peroxide can induce EndoG-related apoptosis in human squamous carcinoma cells (Hamada et al., 2014). Kidney cells might show different responses, and more studies are needed to assess the effect of AIF- and EndoG-related apoptosis in kidney cells.

Besides caspase-independent apoptosis, ferroptosis is an iron-dependent cell death characterized by the accumulation of lipid peroxides and the consumption of polyunsaturated fatty acids. This non-apoptotic cell death is induced by IRI through the inhibition of the conversion of ferrous ion (Fe^{2+}) to ferric ion (Fe^{3+}). An increase in ferrous ion and hydrogen peroxide triggers the Fenton-like reaction, which can oxidize membrane lipids to lipid oxides and subsequently lead to cell death (Hu et al., 2019). In my study, hydrogen peroxide was used as an inducer, which is a key substance in the Fenton-like reaction. Therefore, the increase in cell death markers without activation of caspase cascades might be due to ferroptosis, which would be an important pathway to assess in future work.

5.5.2 Anti-fibrotic progenitor properties of ADRCs

Previous studies have shown the potential of mesenchymal stem cells (MSCs) to exert anti-fibrotic effects in kidney injury. For example, Liang et al. (2023) demonstrated that kidney-derived MSCs could decrease the secretion of TNF-α, IL-1β, and IL-6 in cisplatin-induced kidney injury in male Sprague Dawley rats (Liang et al., 2023). In their study, kidney MSCs were harvested from 1-day-old male Sprague Dawley rats. The injured kidney group had a 50% mortality rate by day 6, whereas the MSC-treated injured group showed approximately 75% survival. This study also assessed both profibrotic markers and kidney function. However, its application to my research is limited due to the source of MSCs and the use of a cisplatin injury inducer instead of a surgical IRI rat model.

Another study in a pig model induced renal stenosis and metabolic syndrome by placing a local irritant coil in the main renal artery, followed by a single intra-renal injection of MSC-derived extracellular vesicles (EVs) from adipose tissue. The results showed that EVs could restore kidney function, decrease TNF-α, IL-1β, and IL-6, and increase IL-10 in the kidney (Eirin et al., 2017). The 16-week observation period was appropriate to investigate fibrotic progenitor levels in a chronic disease model, although this study lacked mechanistic investigation into pathways such as Akt or NF-κB (Korkmaz et al., 2021; Yuan et al., 2022). The use of adipose tissue-derived MSCs in this study is relevant to my research.

Leukaemia inhibitory factor (Lif), a member of the IL-6 family, is used as a fibrotic progenitor marker. Xu et al. (2022) demonstrated that Lif was upregulated and activated through the ERK and Stat3 pathways in a unilateral ureteral obstruction (UUO) mouse model (Xu et al., 2022), and using a Lif-neutralizing antibody reduced pro-inflammatory cytokines such as TNF, IL-11, and IL-1β. This study, with a 14-day observation period and the use of various Lif inhibitors, confirmed the relationship between Lif expression and renal fibrosis.

The expected outcomes for the anti-fibrotic progenitor properties of ADRCs in this study would be a decrease in Lif, TGF-β, and NF-κB gene expression, indicating reduced fibrotic progenitors. However, there was no difference in the gene expression of these markers between the injured group and the injured group treated with ADRCs in my study. Therefore, there was no evidence of anti-fibrotic properties of ADRCs in hydrogen peroxide-induced NRK-52E cell injury. This is in contrast to several preclinical studies that have demonstrated anti-fibrotic progenitor and anti-inflammatory effects of MSCs in various kidney injury models (Thompson et al., 2020; Yoshida et al., 2023; Yu et al., 2023; Chen et al., 2011b; Lin et al., 2016).

5.5.3 Tubular protective properties of ADRCs

This study described in this chapter showed that there were some protective properties of ADRCs on tubular injury, as observed using injured NRK-52E cells. The protective effect of ADRCs can be seen in the reduction of NGAL and KIM-1 expression.

KIM-1 and NGAL are commonly used as biomarkers for tubular injury in the kidney in both preclinical and clinical studies (Kim et al., 2021; Buonafine et al., 2018). In a preclinical study by Rached et al. (2008), male F344 rats exposed to 210 μg/kg of ochratoxin A had increased KIM-1 and NGAL mRNA expression after 14 days. This study also showed histopathological changes associated with kidney injury, including cellular degeneration, flattened apical membranes, and dedifferentiated cells. An increase in pathological scores of renal injuries-including EGTI score, Jablonski score, and pathohistological scores-correlated with increases in KIM-1 and NGAL mRNA levels in a unilateral 45-minute ischemic induction of an IRI rat model, suggesting that the correlation of KIM-1, NGAL, and kidney injury is valid and reliable (Khalid et al., 2016). In addition, KIM-1 has been used as a biomarker for early prediction of graft loss in the setting of kidney transplantation (Van Timmeren et al., 2007). Therefore, overall decreases in KIM-1 and NGAL expression relate

to a reduction in kidney injury. In my study, there was a significant difference in NGAL and KIM-1 mRNA expression between injured NRK-52E cells and ADRC-treated cells. Therefore, the reduction of tubular injury markers demonstrates the potential for ADRCs to impact tubular repair.

5.5.4 Statistical analysis for validation of KIM-1, NGAL, and PARP protein expression using western blot analysis in NRK-52E cells

The Mann-Whitney U test is a non-parametric statistical test used to compare two independent groups, while the Kruskal-Wallis H test is a non-parametric test used to compare more than two independent groups (Marino, 2014). Both tests are appropriate for data that are not normally distributed or are non-parametric in nature. For this reason, data with small sample sizes and non-normal distributions often utilize these tests for experimental comparison.

Although experimental groups may number more than two, several studies have used the Mann-Whitney U test or Student's t-test to compare each experimental group with its control (Byun et al., 2009; Skog et al., 2008; Li et al., 2023a). Therefore, the Mann-Whitney U test is a valid method to discriminate differences between the naïve group and groups at each exposure time point in the validation experiment of hydrogen peroxide in NRK-52E cells.

However, one-way analysis of variance (ANOVA) and the Kruskal-Wallis H test with post-hoc analysis are also commonly used for multiple group comparisons (Lee et al., 2012; Li et al., 2023b; Chen et al., 2017). These statistical methods can be applied to the validation experiment of hydrogen peroxide in NRK-52E cells. After applying the Kruskal-Wallis H test with post-hoc analysis, there was no difference in protein expression between the healthy group and the treatment group exposed to 500 μM hydrogen peroxide for 4 hours in NRK-52E cells (**Figure 5-20**). This result indicates a potential error in using the Mann-Whitney U test in that study. Therefore, future studies with a similar design should use the Kruskal-Wallis H test to select the suitable exposure time and concentration of hydrogen peroxide as an injury inducer in NRK-52E cell studies.

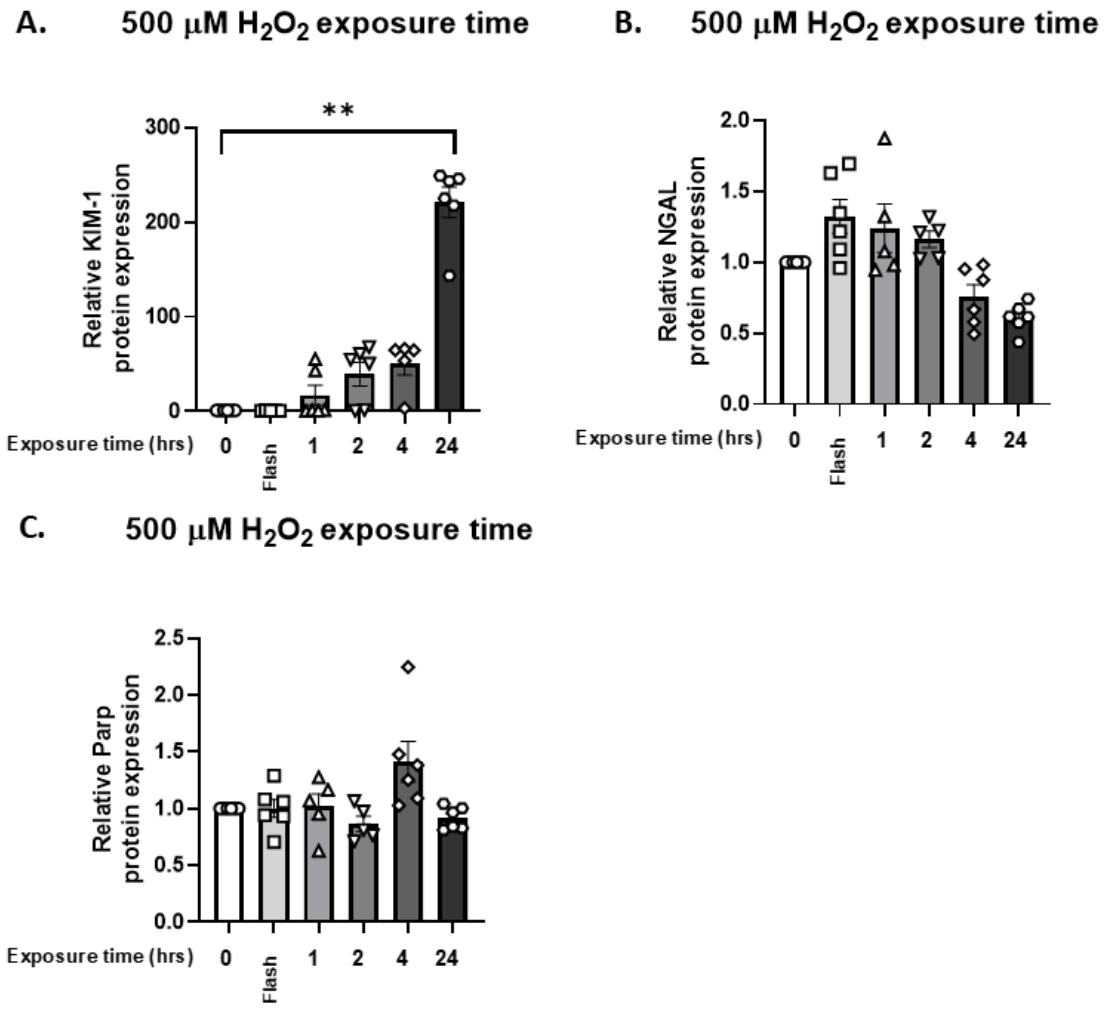

Figure 5-20 Protein profiling of KIM-1 expression (A), NGAL expression (B), and PARP expression (C) after treatment of NRK-52E cells with hydrogen peroxide using western blot analysis. Data are presented as means ± SEM (n = 6). Comparisons to control were analysed using the Kruskal-Wallis H test with Dunn's multiple comparisons test. ***p < 0.01*.

5.6 Strengths, limitations and future directions

There are some limitations to the studies described in this chapter:

1. In western blot analysis, there was no change or only a slight decrease in PARP protein expression. This might be due to low protein loading in the western blot, a weak antibody for the target protein, or human error.
2. In qPCR analysis, there was a short time window to detect mRNA levels, which might have affected the mRNA expression of biomarkers.

3. This was a bench-time-dependent study. In studies of apoptosis or cell death, longer laboratory times can affect the number of dead cells and cell survival. In flow cytometry analysis, there was a 6-hour bench time for lab processing before measurement, and the long laboratory time could diminish cell viability.
4. Sample sizes in some experiments were possibly too low to yield statistically significant results.
5. There is always the possibility of human error impacting the detection of results. In particular, I have concerns about the impact on apoptotic biomarkers. Ideally, I would rerun these assays, but unfortunately, I ran out of bench time, making repeated experiments impossible.

Although I did not demonstrate anti-apoptotic properties of ADRCs in my study, other therapeutic properties of ADRCs were observed. Further study of the therapeutic effects of ADRCs is needed. The following are suggestions for further study:

1. In western blotting, increasing protein load and trying different antibodies might improve protein expression detection.
2. Increasing sample size may yield more statistically robust results.
3. Studying the anti-apoptotic properties in an animal model may be an alternative approach to demonstrate or refute the anti-apoptotic properties of ADRCs.
4. Anti-tubular injury and anti-fibrotic properties of ADRCs have been observed in this study. These therapeutic effects should be further studied in a human tubular cell model or an animal model prior to moving towards clinical translation.

5.7 Conclusion

In an oxidatively injured continuous proximal tubular cell model, the findings suggested anti-tubular injury effects and a trend toward decreased dead cell markers alongside increased living cell markers in ADRCs. However, no anti-apoptotic or anti-fibrotic progenitor effects of ADRCs were observed in this study.

Chapter 6: Summary and general discussion

In my studies, cellular therapy with ADRCs and MSCs shows potential as a useful treatment in kidney transplantation models. ADRCs, the main focus of this thesis, have anti-fibrotic and anti-oxidative effects and, as a consequence, can be seen as protective against tubular injury. This cellular therapy may also be applicable to other kidney disease treatments. Future studies in animal models and clinical settings are required.

6.1 Therapeutic effects of ADRCs from a systematic review and in vitro study in the present study

This project demonstrated the therapeutic effects of ADRCs and/or MSCs using three different approaches: a systematic review of the therapeutic effects of MSCs on injured solid organ models, a laboratory investigation of the effects of ADRCs on injured kidney organoids, and a laboratory investigation of ADRCs on injured proximal tubular cells. The results reveal the potential of ADRCs as candidates for additional therapy in kidney transplantation. However, this thesis showed contrasting results regarding the anti-apoptotic properties of ADRCs in the systematic review and in injured NRK-52E cells and continuous rat proximal tubular cells. A summary of each chapter is provided below.

In the systematic review, I investigated the effectiveness of MSCs on injured solid organs. My initial plan was to investigate the effect of ADRCs on kidney transplantation models. However, a lack of high-quality literature limited this plan, so we expanded the scope of investigation to include other solid organs and MSCs instead of focusing solely on ADRCs. The results showed that: 1) MSCs have anti-apoptotic effects, with mechanisms associated with extracellular vesicles; 2) MSCs modulate inflammatory processes by regulating proinflammatory cytokines IL-1β, IL-6, and IL-8, as well as the anti-inflammatory cytokine IL-10; 3) MSCs improve tissue fibrosis through altered HGF and TGF-β1; and 4) MSCs reduce oxidative stress, as assessed by ROS and MDA production. These findings from previous literature suggest that MSCs have potential for therapy in solid organ transplantation.

In injured kidney organoids, I began by creating a kidney organoid model using E13.5–14.5 embryonic metanephros. The presence of adult kidney proteins-synaptopodin, megalin, and Wilms' tumour 1-was confirmed using immunofluorescence techniques. After confirming adult kidney structures, hydrogen peroxide was selected as an injury inducer due to its accessibility, with 10 μM hydrogen peroxide for 60 minutes chosen as the concentration and exposure time in this model. The size of the kidney organoids was observed, and the concentration of extracellular vesicles was measured to assess the effect of ADRCs. Initial findings showed that ADRCs could preserve the size of kidney organoids after hydrogen peroxide-induced injury. This effect might be due to either the anti-apoptotic properties or modulation of proliferation by ADRCs. However, other downstream assays were cancelled due to social isolation, limited time, and restricted laboratory access caused by the COVID-19 pandemic. Despite these limitations, a potential therapeutic effect of ADRCs was demonstrated. The mitigation plan for investigating ADRCs as therapy was to use an injured NRK-52E cell model.

In an injured continuous proximal tubular cell model, NRK-52E cells were exposed to 500 μM hydrogen peroxide for 4 hours. I investigated three different properties of ADRC therapy: pro-survival, anti-fibrotic, and anti-injury. First, the study of pro-survival properties was based on my previous systematic review and preliminary data from the kidney organoid model. The findings suggested pro-survival effects, showing a trend toward decreased dead cell markers, which surprisingly was not associated with the caspase pathway. Additionally, total NRK-52E cell numbers did not change after ADRC therapy. The reduction in dead cell markers in this study should form the basis for further research into mechanisms such as ferroptosis. Second, my anti-fibrotic investigations showed that fibrotic progenitor markers did not change after ADRC treatment. Lastly, mRNA expression of the tubular injury marker NGAL was reduced after ADRC treatment. These results demonstrate anti-tubular injury properties of ADRCs in hydrogen peroxide-induced NRK-52E cells, but anti-apoptotic and anti-fibrotic properties were not confirmed in my studies.

6.2 Strengths of the present study

The strength of this investigation into the effect of ADRCs lies in the use of different models. I have attempted to use a 3D kidney organoid model and successfully generated kidney organoids to mimic the complex structures of the kidney, rather than relying solely on single cell cultures or co-cultures. Different methods were used to confirm the results, especially

for apoptosis-related assays. I employed total cell counts, qPCR, ELISA, and flow cytometry to assess whether ADRCs possess anti-apoptotic properties. The measurement of extracellular vesicle concentration was conducted at several time points. While I have expressed the desire to increase sample sizes in many experiments, most studies used sample sizes of around 5–6 per group, with as many as 12 in the mRNA expression studies, in an attempt to achieve consistency. I hope this has improved the accuracy of the results in my study.

6.3 Limitations and weaknesses of the present study

My studies were mainly affected by the COVID-19 pandemic and associated regulations. There was no access to the laboratory for a period of time, and there was limited ability to maintain the rat colony. This changed my initial plan of investigating the effect of ADRCs on injured kidney organoids and a surgical rat model to a systematic review and a continuous proximal tubular cell model. The surgical rat model was cancelled due to the longer time required for training and authorizations during the pandemic.

Regarding potential weaknesses of the cell culture studies, different incubation times of hydrogen peroxide in NRK-52E cells should be considered. In addition, other laboratories and alternative methods should be used to confirm the results of my studies. Different concentrations and exposure times of hydrogen peroxide should be investigated. Different models should be considered, with 3D kidney organoids derived from iPSCs being an attractive potential model for further investigation. Moreover, since this thesis study was conducted using in vitro models and a systematic review, functional tests of kidney function and immune responses could not be observed.

6.4 Future direction of kidney organoids, ADRCs and MSCs therapy

6.4.1 Three-dimensional kidney organoids from iPSCs as a future experimental model

Three-dimensional kidney organoids are a new platform for preclinical studies. Current applications of organoids include disease modelling, drug screening, personalized medicine, and regenerative medicine (Khoshdel-Rad et al., 2022). Although they lack vascularization and immune response (Li and Izpisua Belmonte, 2019), in my opinion, the use of kidney

organoid models derived from iPSCs will serve as a surrogate for future human in vitro kidney models by avoiding ethical issues associated with much human research. This kidney organoid model can address the lack of human kidney models due to the complexity of kidney structure and contribute to the advancement of precision medicine.

6.4.2 ADRC or MSC treatment in kidney diseases

ADRC or MSC treatment may not be restricted to use in IRI kidney models; it can also be applied to other kidney diseases. The NEPHSTROM clinical study phase 1b/2b of MSC therapy in type 2 diabetes patients found that there was an improvement in eGFR with MSC treatment in the MSC-treated group compared to the placebo group (Perico et al., 2023). This study also showed that a single dose of intravenous MSCs at 80 $\times 10^6$ cells was safe to use in these diabetic patients. This finding indicates that the utility of MSCs is not limited to IRI kidney models but can be applied to other kidney diseases.

6.4.3 Other sources of cell therapy have showed potential usefulness in kidney transplantation

Adipose-derived regenerative cells (which contain a high proportion of MSCs) and bone marrow-derived MSCs are not the only sources for cellular therapy; researchers have also used other sources for cellular therapy in kidney transplantation. The ONE Study, a clinical kidney transplantation trial, demonstrated the potential of cellular therapy in a multicentre clinical study (Sawitzki et al., 2020). In this study, patients received one of six cell-based therapies containing regulatory T cells, dendritic cells, or macrophages. All cell products were delivered once intravenously between day –7 and day +10 relative to the day of kidney transplantation. The results showed that patients were successfully weaned from standard-of-care immunosuppression to monotherapy within one year and experienced fewer episodes of infections compared to those who did not receive cellular therapy. This indicates the importance of cellular therapy, which is not necessarily limited to mesenchymal stem cells.

6.5 Suggestions for future ADRC studies

I would suggest that future studies of ADRCs in kidney transplantation models address four strategies. Firstly, IRI should be studied in mouse or rat models by performing nephrectomy on one kidney and clamping the other kidney for a specified time to observe the effects in the IRI model. This approach allows evaluation of the functional therapeutic effects of ADRCs. Valid functional tests of the kidney include estimated glomerular filtration rate

(eGFR), the gold standard GFR measurement (Hinojosa-Laborde et al., 2015), renal blood flow (RBF) (Shimada and Cowley, 2022), serum creatinine, and blood urea nitrogen (Zou et al., 2016). Macrophage infiltration can also be observed histopathologically in this model (Shih et al., 2013). Additionally, long-term observation exceeding two weeks can be used to investigate renal fibrosis (Zou et al., 2016). Secondly, in vitro studies of the IRI model should be conducted using hypoxic cell culture conditions to mimic renal ischemia. Long-term culture of human iPSC-derived kidney organoids should be used to identify anti-fibrotic properties (Suhito et al., 2022). Thirdly, while this thesis used whole cells for treatment, recent studies suggest that therapeutic benefits may be derived from extracellular vesicles. Therefore, extracellular vesicle extraction and application should be tested in future studies (Kuang et al., 2020). Lastly, given that several studies have demonstrated the safety of using ADRCs and MSCs in clinical trials, pilot clinical studies of ADRCs in kidney IRI and transplantation should be conducted in the future after obtaining appropriate ethical approval.

6.6 Conclusion

The above findings from my studies-a systematic review, an injured kidney organoid model, and an injured continuous rat proximal tubular cell model-suggest that ADRCs have evidence of efficacy for anti-fibrosis and reduction of tubular injury; however, the pro-survival protection provided by ADRC therapy is still questionable. Further studies are required to address this proposed effect on cellular survival. The use of ADRCs for oxidative tissue injury in kidney transplantation still needs more investigation.

List of references

Agrelo, I.S., Schira-Heinen, J., Beyer, F., et al. (2020) Secretome analysis of mesenchymal stem cell factors fostering oligodendroglial differentiation of neural stem cells in vivo. *International Journal of Molecular Sciences*, 21 (12): 1–25. doi:10.3390/IJMS21124350,.

Alshaikh, E.A., Astor, B.C., Muth, B., et al. (2023) Delayed Graft Function Among Kidney Transplant Recipients Is Associated With an Increased Risk of Urinary Tract Infection and BK Viremia. *Transplantation Direct*, 9 (9): E1526. doi:10.1097/TXD.0000000000001526.

Alvarez, S., Suazo, C., Boltansky, A., et al. (2013) Urinary exosomes as a source of kidney dysfunction biomarker in renal transplantation. *Transplantation Proceedings*, 45 (10): 3719–3723. doi:10.1016/j.transproceed.2013.08.079.

Ammar, H.I., Sequiera, G.L., Nashed, M.B., et al. (2015) Comparison of adipose tissue- and bone marrow- derived mesenchymal stem cells for alleviating doxorubicin-induced cardiac dysfunction in diabetic rats. *Stem Cell Research & Therapy*, 6 (1): 148. doi:10.1186/S13287-015-0142-X.

An, S., Zang, X., Yuan, W., et al. (2013) Neutrophil Gelatinase-Associated Lipocalin (NGAL) May Play a Protective Role Against Rats Ischemia/Reperfusion Renal Injury via Inhibiting Tubular Epithelial Cell Apoptosis. *Renal Failure*, 35 (1): 143–149. doi:10.3109/0886022X.2012.741877.

Antar, S.A., Ashour, N.A., Marawan, M.E., et al. (2023) Fibrosis: Types, Effects, Markers, Mechanisms for Disease Progression, and Its Relation with Oxidative Stress, Immunity, and Inflammation. *International journal of molecular sciences*, 24 (4). doi:10.3390/ijms24044004.

Atta, H., El-Rehany, M., Hammam, O., et al. (2014) Mutant MMP-9 and HGF gene transfer enhance resolution of CCL4-induced liver fibrosis in rats: Role of ASH1 and EZH2 methyltransferases repression. *PLoS ONE*, 9 (11). doi:10.1371/journal.pone.0112384.

Aviña, A.E., De Paz, D., Huang, S.C., et al. (2023) IL-10 modified mRNA monotherapy prolongs survival after composite facial allografting through the induction of mixed chimerism. *Molecular Therapy - Nucleic Acids*, 31 (March): 610–627. doi:10.1016/j.omtn.2023.02.016.

Awdishu, L. and Mehta, R.L. (2017) The 6R's of drug induced nephrotoxicity. *BMC Nephrology*. 18 (1). doi:10.1186/s12882-017-0536-3.

Barba, J., Zudaire, J.J., Robles, J.E., et al. (2011) Is there a safe cold ischemia time interval for the renal graft? *Actas Urológicas Españolas (English Edition)*, 35 (8): 475–480. doi:https://doi.org/10.1016/j.acuroe.2011.03.007.

Bar-Ephraim, Y.E., Kretzschmar, K. and Clevers, H. (2020) Organoids in immunological research. *Nature Reviews Immunology*, 20 (5): 279–293. doi:10.1038/s41577-019-0248-y.

Barin-Le Guellec, C., Largeau, B., Bon, D., et al. (2018) Ischemia/reperfusion-associated tubular cells injury in renal transplantation: Can metabolomics inform about mechanisms and help identify new therapeutic targets? *Pharmacological Research*. 129 pp. 34–43. doi:10.1016/j.phrs.2017.12.032.

Barrett, C.W., Reddy, V.K., Short, S.P., et al. (2015) Selenoprotein P influences colitis-induced tumorigenesis by mediating stemness and oxidative damage. *Journal of Clinical Investigation*, 125 (7): 2646–2660. doi:10.1172/JCI76099.

Basile, D.P., Anderson, M.D. and Sutton, T.A. (2012) Pathophysiology of Acute Kidney Injury. *Comprehensive Physiology*, 2 (2): 1303. doi:10.1002/CPHY.C110041.

Bejoy, J., Farry, J.M., Qian, E.S., et al. (2023) Ascorbate protects human kidney organoids from damage induced by cell-free hemoglobin. *Disease Models & Mechanisms*, 16 (12): dmm050342. doi:10.1242/DMM.050342.

Bertheloot, D., Latz, E. and Franklin, B.S. (2021) Necroptosis, pyroptosis and apoptosis: an intricate game of cell death. *Cellular & Molecular Immunology 2021 18:5*, 18 (5): 1106–1121. doi:10.1038/s41423-020-00630-3.

Black, R.A., Rauch, C.T., Kozlosky, C.J., et al. (1997) A metalloproteinase disintegrin that releases tumour-necrosis factor-ø from cells. *Nature*, 385 (6618): 729–733. doi:10.1038/385729A0;KWRD=SCIENCE.

Bouchard, M., Souabni, A., Mandler, M., et al. (2002) Nephric lineage specification by Pax2 and Pax8. *Genes & Development*, 16 (22): 2958. doi:10.1101/GAD.240102.

Brasile, L., Henry, N., Orlando, G., et al. (2019) Potentiating Renal Regeneration Using Mesenchymal Stem Cells. *Transplantation*, 103 (2): 307–313. doi:10.1097/TP.0000000000002455.

Brennan, M.A. and Cookson, B.T. (2000) Salmonella induces macrophage death by caspase-1-dependent necrosis. *Molecular microbiology*, 38 (1): 31–40. doi:10.1046/J.1365-2958.2000.02103.X.

Brentnall, M., Rodriguez-Menocal, L., De Guevara, R.L., et al. (2013) Caspase-9, caspase-3 and caspase-7 have distinct roles during intrinsic apoptosis. *BMC Cell Biology*, 14 (1): 32. doi:10.1186/1471-2121-14-32.

Buendia, B., Santa-Maria, A. and Courvalin, J.C. (1999) Caspase-dependent proteolysis of integral and peripheral proteins of nuclear membranes and nuclear pore complex proteins during apoptosis. *Journal of cell science*, 112 (Pt 11) (11): 1743–1753. doi:10.1242/JCS.112.11.1743.

Buonafine, M., Martinez-Martinez, E., Fr´, F., et al. (2018) More than a simple biomarker: the role of NGAL in cardiovascular and renal diseases. *Clinical Science*, pp. 132–909. doi:10.1042/CS20171592.

Burgos-Silva, M., Semedo-Kuriki, P., Donizetti-Oliveira, C., et al. (2015) Adipose Tissue-Derived Stem Cells Reduce Acute and Chronic Kidney Damage in Mice. *PloS one*, 10 (11). doi:10.1371/JOURNAL.PONE.0142183.

Byun, Y.J., Kim, S.K., Kim, Y.M., et al. (2009) Hydrogen peroxide induces autophagic cell death in C6 glioma cells via BNIP3-mediated suppression of the mTOR pathway. *Neuroscience Letters*, 461 (2): 131–135. doi:10.1016/j.neulet.2009.06.011.

Cai, F.-H., Wu, W.-Y., Zhou, X.-J., et al. (2020) Diagnostic roles of urinary kidney microvesicles in diabetic nephropathy. *Annals of Translational Medicine*, 8 (21): 1431–1431. doi:10.21037/atm-20-441.

Chakraborty, S., Chopra, P., Hak, A., et al. (2013) Hepatocyte growth factor is an attractive target for the treatment of pulmonary fibrosis. *Expert Opinion on Investigational Drugs*. 22 (4) pp. 499–515. doi:10.1517/13543784.2013.778972.

Chan, F.K.M., Moriwaki, K. and De Rosa, M.J. (2013) Detection of necrosis by release of lactate dehydrogenase activity. *Methods in Molecular Biology*, 979: 65–70. doi:10.1007/978-1-62703-290-2_7.

Chen, J., Lu, H., Wang, X., et al. (2022a) VNN1 contributes to the acute kidney injury–chronic kidney disease transition by promoting cellular senescence via affecting RB1 expression. *FASEB Journal*, 36 (9): e22472. doi:10.1096/FJ.202200496RR;SUBPAGE:STRING:FULL.

Chen, W., Wang, L., Liang, P., et al. (2022b) Reducing ischemic kidney injury through application of a synchronization modulation electric field to maintain Na+/K+-ATPase functions. *Science Translational Medicine*, 14 (635). doi:10.1126/SCITRANSLMED.ABJ4906,.

Chen, X., Zhu, R., Zhong, J., et al. (2022c) Mosaic composition of RIP1–RIP3 signalling hub and its role in regulating cell death. *Nature Cell Biology 2022 24:4*, 24 (4): 471–482. doi:10.1038/s41556-022-00854-7.

Chen, Y.T., Sun, C.K., Lin, Y.C., et al. (2011a) Adipose-derived mesenchymal stem cell protects kidneys against ischemia-reperfusion injury through suppressing oxidative stress and inflammatory reaction. *J Transl Med*, 9: 51. doi:10.1186/1479-5876-9-51.

Chen, Y.T., Sun, C.K., Lin, Y.C., et al. (2011b) Adipose-derived mesenchymal stem cell protects kidneys against ischemia-reperfusion injury through suppressing oxidative stress and inflammatory reaction. *Journal of translational medicine*, 9. doi:10.1186/1479-5876-9-51.

Chen, Y.W., Huang, S.X., De Carvalho, A.L.R.T., et al. (2017) A three-dimensional model of human lung development and disease from pluripotent stem cells. *Nature Cell Biology*, 19 (5): 542–549. doi:10.1038/ncb3510.

Collino, F., Lopes, J.A., Tapparo, M., et al. (2020) Extracellular Vesicles Derived from Induced Pluripotent Stem Cells Promote Renoprotection in Acute Kidney Injury Model. *Cells*, 9 (2). doi:10.3390/CELLS9020453.

Cowland, J.B. and Borregaard, N. (1997) *Molecular Characterization and Pattern of Tissue Expression of the Gene for Neutrophil Gelatinase-Associated Lipocalin from Humans*.

Daugas, E., Nochy, D., Ravagnan, L., et al. (2000) Apoptosis-inducing factor (AIF): a ubiquitous mitochondrial oxidoreductase involved in apoptosis. *FEBS Letters*, 476 (3): 118–123. doi:10.1016/S0014-5793(00)01731-2.

Dewolf, S.E., Kasimsetty, S.G., Hawkes, A.A., et al. (2022) DAMPs Released from Injured Renal Tubular Epithelial Cells Activate Innate Immune Signals in Healthy Renal Tubular Epithelial Cells. *Transplantation*, 106 (8): 1589–1599. doi:10.1097/TP.0000000000004038,.

Dieterle, F., Sistare, F., Goodsaid, F., et al. (2010) Renal biomarker qualification submission: A dialog between the FDA-EMEA and Predictive Safety Testing Consortium. *Nature Biotechnology*. 28 (5) pp. 455–462. doi:10.1038/nbt.1625.

Dixon, S.J., Lemberg, K.M., Lamprecht, M.R., et al. (2012) *Ferroptosis: An Iron-Dependent Form of Non-Apoptotic Cell Death*. doi:10.1016/j.cell.2012.03.042.

Dominguez, J.M., Dominguez, J.H., Xie, D., et al. (2018) Human extracellular microvesicles from renal tubules reverse kidney ischemia-reperfusion injury in rats Camussi, G. (ed.). *PLOS ONE*, 13 (8): e0202550. doi:10.1371/journal.pone.0202550.

Dominici, M., Le Blanc, K., Mueller, I., et al. (2006) Minimal criteria for defining multipotent mesenchymal stromal cells. The International Society for Cellular Therapy position statement. *Cytotherapy*, 8 (4): 315–317. doi:10.1080/14653240600855905.

Dong, Y., Zhang, Q., Wen, J., et al. (2019) Ischemic duration and frequency determines AKI-to-CKD progression monitored by dynamic changes of tubular biomarkers in IRI mice. *Frontiers in Physiology*, 10 (FEB). doi:10.3389/fphys.2019.00153.

Donizetti-Oliveira, C., Semedo, P., Burgos-Silva, M., et al. (2012) Adipose tissue-derived stem cell treatment prevents renal disease progression. *Cell Transplant*, 21 (8): 1727–1741. doi:10.3727/096368911x623925.

Dye, B.R., Hill, D.R., Ferguson, M.A.H., et al. (2015) In vitro generation of human pluripotent stem cell derived lung organoids. *eLife*, 4. doi:10.7554/eLife.05098.

Eirin, A., Zhu, X.Y., Puranik, A.S., et al. (2017) Mesenchymal stem cell-derived extracellular vesicles attenuate kidney inflammation. *Kidney international*, 92 (1): 114–124. doi:10.1016/J.KINT.2016.12.023.

Elena-Real, C.A., Díaz-Quintana, A., González-Arzola, K., et al. (2018) Cytochrome c speeds up caspase cascade activation by blocking 14-3-3ε-dependent Apaf-1 inhibition article. *Cell Death and Disease*, 9 (3): 1–12. doi:10.1038/S41419-018-0408-1;TECHMETA=101,13,2,6;KWRD=LIFE+SCIENCES.

El-Habta, R., Andersson, G., Kingham, P.J., et al. (2021) Anti-apoptotic effect of adipose tissue-derived stromal vascular fraction in denervated rat muscle. *Stem Cell Research and Therapy*, 12 (1). doi:10.1186/s13287-021-02230-y.

Fajas-Coll, L., Lagarrigue, S., Hure, S., et al. (2014) “Cell Cycle and MetaboLic Changes During Tissue Regeneration and RemodeLing.” In *Pathobiology of Human Disease: A Dynamic Encyclopedia of Disease Mechanisms*. Elsevier Inc. pp. 542–549. doi:10.1016/B978-0-12-386456-7.02101-8.

Fatehullah, A., Tan, S.H. and Barker, N. (2016) Organoids as an in vitro model of human development and disease. *Nature cell biology*, 18 (3): 246–54. doi:10.1038/ncb3312.

Ferlini, C., Cesare, S. Di, Rainaldi, G., et al. (1996) Flow cytometric analysis of the early phases of apoptosis by cellular and nuclear techniques. *Cytometry*, 24 (2): 106–115. doi:10.1002/(SICI)1097-0320(19960601)24:2<106::AID-CYTO2>3.0.CO;2-H.

Fonseca, I., Reguengo, H., Almeida, M., et al. (2014) Oxidative stress in kidney transplantation: Malondialdehyde is an early predictive marker of graft dysfunction. *Transplantation*, 97 (10): 1058–1065. doi:10.1097/01.TP.0000438626.91095.50.

Freedman, B.S., Brooks, C.R., Lam, A.Q., et al. (2015) Modelling kidney disease with CRISPR-mutant kidney organoids derived from human pluripotent epiblast spheroids. *Nature Communications*, 6 (1): 1–13. doi:10.1038/ncomms9715.

Frieboes, H.B., Zheng, X., Sun, C.H., et al. (2006) An Integrated Computational/Experimental Model of Tumor Invasion. *Cancer Research*, 66 (3): 1597–1604. doi:10.1158/0008-5472.CAN-05-3166.

Fu, Y., Cao, J., Wei, X., et al. (2023) Klotho alleviates contrast-induced acute kidney injury by suppressing oxidative stress, inflammation, and NF-KappaB/NLRP3-mediated pyroptosis. *International Immunopharmacology*, 118. doi:10.1016/j.intimp.2023.110105.

Fu, Y., Sui, B., Xiang, L., et al. (2021) Emerging understanding of apoptosis in mediating mesenchymal stem cell therapy. *Cell Death & Disease 2021 12:6*, 12 (6): 1–12. doi:10.1038/s41419-021-03883-6.

Fuchs, Y. and Steller, H. (2015) Live to die another way: Modes of programmed cell death and the signals emanating from dying cells. *Nature Reviews Molecular Cell Biology*, 16 (6): 329–344. doi:10.1038/nrm3999.

Galluzzi, L., Vitale, I., Aaronson, S.A., et al. (2018) Molecular mechanisms of cell death: Recommendations of the Nomenclature Committee on Cell Death 2018. *Cell Death and Differentiation*, 25 (3): 486–541. doi:10.1038/s41418-017-0012-4.

Garmaa, G., Manzéger, A., Haghighi, S., et al. (2023) HK-2 cell response to TGF-β highly depends on cell culture medium formulations. *Histochemistry and Cell Biology*. doi:10.1007/s00418-023-02237-x.

Garreta, E., Prado, P., Tarantino, C., et al. (2019) Fine tuning the extracellular environment accelerates the derivation of kidney organoids from human pluripotent stem cells. *Nature Materials*, 18 (4): 397–405. doi:10.1038/s41563-019-0287-6.

Gavrieli, Y., Sherman, Y. and Ben-Sasson, S.A. (1992) Identification of programmed cell death in situ via specific labeling of nuclear DNA fragmentation. *Journal of Cell Biology*, 119 (3): 493–501. doi:10.1083/JCB.119.3.493,.

Gill, J., Dong, J., Rose, C., et al. (2016) The Risk of Allograft Failure and the Survival Benefit of Kidney Transplantation Are Complicated by Delayed Graft Function. *Kidney International*, 89 (6): 1331–1336. doi:10.1016/j.kint.2016.01.028.

Grassi, L., Alfonsi, R., Francescangeli, F., et al. (2019) Organoids as a new model for improving regenerative medicine and cancer personalized therapy in renal diseases. *Cell Death and Disease*, 10 (3). doi:10.1038/s41419-019-1453-0.

Gregorini, M., Corradetti, V., Pattonieri, E.F., et al. (2017) Perfusion of isolated rat kidney with Mesenchymal Stromal Cells/Extracellular Vesicles prevents ischaemic injury. *Journal of Cellular and Molecular Medicine*, 21 (12): 3381–3393. doi:10.1111/jcmm.13249.

Guo, Y., Tan, J., Miao, Y., et al. (2019) Effects of microvesicles on cell apoptosis under hypoxia. *Oxidative Medicine and Cellular Longevity*. 2019. doi:10.1155/2019/5972152.

Gupta, N., Matsumoto, T., Hiratsuka, K., et al. (2022) Modeling injury and repair in kidney organoids reveals that homologous recombination governs tubular intrinsic repair. *Science Translational Medicine*, 14 (634): 4772. doi:10.1126/scitranslmed.abj4772.

Hamada, M., Wakabayashi, K., Masui, A., et al. (2014) Involvement of Hydrogen Peroxide in Safingol-Induced Endonuclease G-Mediated Apoptosis of Squamous Cell Carcinoma Cells. *International Journal of Molecular Sciences*, 15 (2): 2660. doi:10.3390/IJMS15022660.

Havasi, A. and Borkan, S.C. (2011) Apoptosis and acute kidney injury. *Kidney International*. 80 (1) pp. 29–40. doi:10.1038/ki.2011.120.

Heldin, C.H. and Moustakas, A. (2012) Role of Smads in TGFβ signaling. *Cell and Tissue Research*, 347 (1): 21–36. doi:10.1007/s00441-011-1190-x.

Hendriks, K.D.W., Brüggenwirth, I.M.A., Maassen, H., et al. (2019) Renal temperature reduction progressively favors mitochondrial ROS production over respiration in hypothermic kidney preservation. *Journal of Translational Medicine*, 17 (1): 265. doi:10.1186/s12967-019-2013-1.

Higgins, S.P., Tang, Y., Higgins, C.E., et al. (2018) TGF-β1/p53 signaling in renal fibrogenesis. *Cellular Signalling*, 43: 1–10. doi:10.1016/J.CELLSIG.2017.11.005.

Hinojosa-Laborde, C., Jespersen, B. and Shade, R. (2015) Physiology Lab Demonstration: Glomerular Filtration Rate in a Rat. *Journal of Visualized Experiments : JoVE*, 2015 (101): 52425. doi:10.3791/52425.

Hu, Z., Zhang, H., Yang, S.K., et al. (2019) Emerging Role of Ferroptosis in Acute Kidney Injury. *Oxidative Medicine and Cellular Longevity*. 2019. doi:10.1155/2019/8010614.

Huang, R., Fu, P. and Ma, L. (2023) Kidney fibrosis: from mechanisms to therapeutic medicines. *Signal Transduction and Targeted Therapy*, 8 (1): 129. doi:10.1038/s41392-023-01379-7.

Huch, M., Dorrell, C., Boj, S.F., et al. (2013) In vitro expansion of single Lgr5 + liver stem cells induced by Wnt-driven regeneration. *Nature*, 494 (7436): 247–250. doi:10.1038/nature11826.

Jain, S., Plenter, R., Nydam, T., et al. (2020) Injury Pathways That Lead to AKI in a Mouse Kidney Transplant Model. *Transplantation*, 104 (9): 1832–1841. doi:10.1097/TP.0000000000003127.

Jayachandran, M., Miller, V.M., Heit, J.A., et al. (2012) Methodology for isolation, identification and characterization of microvesicles in peripheral blood. *Journal of Immunological Methods*, 375 (1–2): 207–214. doi:10.1016/j.jim.2011.10.012.

Ji, L., Chen, Y., Wang, H., et al. (2019) Overexpression of Sirt6 promotes M2 macrophage transformation, alleviating renal injury in diabetic nephropathy. *International Journal of Oncology*, 55 (1): 103–115. doi:10.3892/IJO.2019.4800,.

Jin, J., Shi, Y., Gong, J., et al. (2019) Exosome secreted from adipose-derived stem cells attenuates diabetic nephropathy by promoting autophagy flux and inhibiting apoptosis in podocyte. *Stem Cell Research and Therapy*, 10 (1). doi:10.1186/s13287-019-1177-1.

Jones, I.K.A., Orloff, S., Burg, J.M., et al. (2021) Blocking the IL-1 receptor reduces cardiac transplant ischemia and reperfusion injury and mitigates CMV-accelerated chronic rejection. *American Journal of Transplantation*, 21 (1): 44–59. doi:10.1111/ajt.16149.

Jun, D.Y., Kim, S.Y., Na, J.C., et al. (2018) Tubular organotypic culture model of human kidney. *PLoS ONE*, 13 (10). doi:10.1371/journal.pone.0206447.

Kang, H.M., Lim, J.H., Noh, K.H., et al. (2019) Effective reconstruction of functional organotypic kidney spheroid for in vitro nephrotoxicity studies. *Scientific Reports*, 9 (1): 17610. doi:10.1038/s41598-019-53855-2.

Kato, T. and Mizuno, S. (2017) Nephron, Wilms' tumor-1 (WT1), and synaptopodin expression in developing podocytes of mice. *Experimental Animals*, 66 (3): 183–189. doi:10.1538/expanim.16-0101.

Katz, L.H., Likhter, M., Jogunoori, W., et al. (2016) TGF-β signaling in liver and gastrointestinal cancers. *Cancer Letters*, 379 (2): 166–172. doi:10.1016/J.CANLET.2016.03.033.

Kawai, H., Chaudhry, F., Shekhar, A., et al. (2018) Molecular Imaging of Apoptosis in Ischemia Reperfusion Injury With Radiolabeled Duramycin Targeting Phosphatidylethanolamine: Effective Target Uptake and Reduced Nontarget Organ Radiation Burden. *JACC: Cardiovascular Imaging*, 11 (12): 1823–1833. doi:10.1016/j.jcmg.2017.11.037.

Kerr, J.F.R., Wyllie, A.H. and Curriet, A.R. (1972) APOPTOSIS: A BASIC BIOLOGICAL PHENOMENON WITH WIDE-RANGING IMPLICATIONS IN TISSUE KINETICS. *Br. J. Cancer*, 26: 239.

Khalid, U., Pino-Chavez, G., Nesargikar, P., et al. (2016) Kidney ischaemia reperfusion injury in the rat: the EGTI scoring system as a valid and reliable tool for histological assessment. *Journal of Histology and Histopathology*, 3 (1): 1. doi:10.7243/2055-091X-3-1.

Khoshdel-Rad, N., Ahmadi, A. and Moghadasali, R. (2022) Kidney organoids: current knowledge and future directions. *Cell and Tissue Research*, 387 (2): 207–224. doi:10.1007/s00441-021-03565-x.

Khundmiri, S.J., Chen, L., Lederer, E.D., et al. (2021) Transcriptomes of Major Proximal Tubule Cell Culture Models. *Journal of the American Society of Nephrology*, 32 (1): 86–97. doi:10.1681/ASN.2020010009.

Kim, H.R., Park, J.H., Lee, S.H., et al. (2022) Using intracellular metabolic profiling to identify novel biomarkers of cisplatin-induced acute kidney injury in NRK-52E cells. *Journal of toxicology and environmental health. Part A*, 85 (1): 29–42. doi:10.1080/15287394.2021.1969305.

Kim, K.S., Lee, J.S., Park, J.H., et al. (2021) Identification of novel biomarker for early detection of diabetic nephropathy. *Biomedicines*, 9 (5). doi:10.3390/biomedicines9050457.

Kishi, S., Brooks, C.R., Taguchi, K., et al. (2019) Proximal tubule ATR regulates DNA repair to prevent maladaptive renal injury responses. *Journal of Clinical Investigation*, 129 (11): 4797–4816. doi:10.1172/JCI122313.

Korkmaz, R., Yüksek, V. and Dede, S. (2021) The Effects of Sodium Fluoride (NaF) Treatment on the PI3K/Akt Signal Pathway in NRK-52E Cells. *Biological trace element research*. doi:10.1007/S12011-021-02927-4.

Kuang, Y., Zheng, X., Zhang, L., et al. (2020) Adipose-derived mesenchymal stem cells reduce autophagy in stroke mice by extracellular vesicle transfer of miR-25. *Journal of Extracellular Vesicles*, 10 (1). doi:10.1002/jev2.12024.

Kubota, T., Nishimura, K., Kanemaki, M.T., et al. (2013) The Elg1 Replication Factor C-like Complex Functions in PCNA Unloading during DNA Replication. *Molecular Cell*, 50 (2): 273–280. doi:10.1016/j.molcel.2013.02.012.

Kwiatkowska, E., Domański, L., Dziedziejko, V., et al. (2021) The mechanism of drug nephrotoxicity and the methods for preventing kidney damage. *International Journal of Molecular Sciences*. 22 (11). doi:10.3390/ijms22116109.

Kwiecinski, M., Noetel, A., Elfimova, N., et al. (2011) Hepatocyte growth factor (HGF) inhibits collagen I and IV synthesis in hepatic stellate cells by Mirna-29 induction. *PLoS ONE*, 6 (9). doi:10.1371/journal.pone.0024568.

Kwon, S.H. (2019) Extracellular vesicles in renal physiology and clinical applications for renal disease. *Korean Journal of Internal Medicine*, 34 (3): 470–479. doi:10.3904/kjim.2019.108.

Laing, R.W., Stubblefield, S., Wallace, L., et al. (2020) The Delivery of Multipotent Adult Progenitor Cells to Extended Criteria Human Donor Livers Using Normothermic Machine Perfusion. *Frontiers in Immunology*, 11. doi:10.3389/fimmu.2020.01226.

Lancaster, M.A., Renner, M., Martin, C.A., et al. (2013) Cerebral organoids model human brain development and microcephaly. *Nature*, 501 (7467): 373–379. doi:10.1038/nature12517.

Larios, J., Mercier, V., Roux, A., et al. (2020) ALIX- And ESCRT-III-dependent sorting of tetraspanins to exosomes. *Journal of Cell Biology*, 219 (3). doi:10.1083/jcb.201904113.

Lee, K.M. and Seong, S.Y. (2009) Partial role of TLR4 as a receptor responding to damage-associated molecular pattern. *Immunology Letters*, 125 (1): 31–39. doi:10.1016/J.IMLET.2009.05.006.

Lee, S.Y., Kim, S.I. and Choi, M.E. (2015) Therapeutic targets for treating fibrotic kidney diseases. *Translational research : the journal of laboratory and clinical medicine*, 165 (4): 512. doi:10.1016/J.TRSL.2014.07.010.

Lee, W.-C., Chau, Y.-Y., Ng, H.-Y., et al. (2019) Empagliflozin Protects HK-2 Cells from High Glucose-Mediated Injuries via a Mitochondrial Mechanism. *Cells*, 8 (9): 1085. doi:10.3390/cells8091085.

Lee, Y.M., Shin, J.W., Lee, E.H., et al. (2012) Protective effects of propofol against hydrogen peroxideinduced oxidative stress in human kidney proximal tubular cells. *Korean Journal of Anesthesiology*, 63 (5): 441–446. doi:10.4097/kjae.2012.63.5.441.

Li, B., Lee, C., Cadete, M., et al. (2019a) Neonatal intestinal organoids as an ex vivo approach to study early intestinal epithelial disorders. *Pediatric Surgery International*, 35 (1): 3–7. doi:10.1007/s00383-018-4369-3.

Li, C., Fleck, J.S., Martins-Costa, C., et al. (2023a) Single-cell brain organoid screening identifies developmental defects in autism. *Nature*, 621 (7978): 373–380. doi:10.1038/s41586-023-06473-y.

Li, C., Han, S., Zhu, J., et al. (2023b) MiR-132-3p activation aggravates renal ischemia-reperfusion injury by targeting Sirt1/PGC1alpha axis. *Cellular Signalling*, 110. doi:10.1016/j.cellsig.2023.110801.

Li, L., Fu, H. and Liu, Y. (2022a) The fibrogenic niche in kidney fibrosis: components and mechanisms. *Nature Reviews Nephrology 2022 18:9*, 18 (9): 545–557. doi:10.1038/s41581-022-00590-z.

Li, L., Wang, R., Jia, Y., et al. (2019b) Exosomes Derived From Mesenchymal Stem Cells Ameliorate Renal Ischemic-Reperfusion Injury Through Inhibiting Inflammation and Cell Apoptosis. *Frontiers in Medicine*, 6. doi:10.3389/fmed.2019.00269.

Li, L.Y., Luo, X. and Wang, X. (2001) Endonuclease G is an apoptotic DNase when released from mitochondria. *Nature 2001 412:6842*, 412 (6842): 95–99. doi:10.1038/35083620.

Li, M. and Izpisua Belmonte, J.C. (2019) Organoids — Preclinical Models of Human Disease. *New England Journal of Medicine*, 380 (6): 569–579. doi:10.1056/nejmra1806175.

Li, M., Zhang, B., Zeng, M., et al. (2022b) Four New Benzoylamide Derivatives Isolated from the Seeds of Lepidium apetalum Willd. and Ameliorated LPS-Induced NRK52e Cells via Nrf2/Keap1 Pathway. *Molecules*, 27 (3). doi:10.3390/molecules27030722.

Li, M.T., Ramakrishnan, A., Yu, M., et al. (2023c) Effects of Delayed Graft Function on Transplant Outcomes: A Meta-analysis. *Transplantation Direct*, 9 (2). doi:10.1097/TXD.0000000000001433.

Li, P., Nijhawan, D., Budihardjo, I., et al. (1997) Cytochrome c and dATP-Dependent Formation of Apaf-1/Caspase-9 Complex Initiates an Apoptotic Protease Cascade. *Cell*, 91 (4): 479–489. doi:10.1016/S0092-8674(00)80434-1.

Liang, H., Xu, F., Zhang, T., et al. (2018) Inhibition of IL-18 reduces renal fibrosis after ischemia-reperfusion. *Biomedicine & Pharmacotherapy*, 106: 879–889. doi:10.1016/J.BIOPHA.2018.07.031.

Liang, R. ning, Yan, D. qi, Zhang, X. ping, et al. (2023) Kidney Mesenchymal stem cells alleviate cisplatin-induced kidney injury and apoptosis in rats. *Tissue and Cell*, 80. doi:10.1016/j.tice.2022.101998.

Lim, S.W., Kim, K.W., Kim, B.M., et al. (2021) Alleviation of renal ischemia/reperfusion injury by exosomes from induced pluripotent stem cell-derived mesenchymal stem cells. *The Korean Journal of Internal Medicine*, 37 (2): 411. doi:10.3904/KJIM.2020.438.

Lin, K.C., Yip, H.K., Shao, P.L., et al. (2016) Combination of adipose-derived mesenchymal stem cells (ADMSC) and ADMSC-derived exosomes for protecting kidney from acute ischemia-reperfusion injury. *International journal of cardiology*, 216: 173–185. doi:10.1016/J.IJCARD.2016.04.061.

Lindroos, B., Suuronen, R. and Miettinen, S. (2011) The potential of adipose stem cells in regenerative medicine. *Stem Cell Rev*, 7 (2): 269–291. doi:10.1007/s12015-010-9193-7.

Little, M.H. and Quinlan, C. (2019) Advances in our understanding of genetic kidney disease using kidney organoids. *Pediatr Nephrol*. doi:10.1007/s00467-019-04259-x.

Lv, L.-L., Cao, Y.-H., Pan, M.-M., et al. (2014) CD2AP mRNA in urinary exosome as biomarker of kidney disease. *Clinica Chimica Acta*, 428: 26–31. doi:https://doi.org/10.1016/j.cca.2013.10.003.

Ma, J., Zou, C., Guo, L., et al. (2014) Novel Death Defying Domain in met entraps the active site of caspase-3 and blocks apoptosis in hepatocytes. *Hepatology*, 59 (5): 2010–2021. doi:10.1002/hep.26769.

Ma, N., Lu, H., Li, N., et al. (2024) CHOP-mediated Gasdermin E expression promotes pyroptosis, inflammation, and mitochondrial damage in renal ischemia-reperfusion injury. *Cell Death & Disease 2024 15:2*, 15 (2): 1–17. doi:10.1038/s41419-024-06525-9.

Mannon, R.B. (2018) Delayed Graft Function: The AKI of Kidney Transplantation. *Nephron*, 140 (2): 94–98. doi:10.1159/000491558.

Marino, M.J. (2014) The use and misuse of statistical methodologies in pharmacology research. *Biochemical Pharmacology*, 87 (1): 78–92. doi:10.1016/J.BCP.2013.05.017.

Matthiesen, S., Jahnke, R. and Knittler, M.R. (2021) A straightforward hypoxic cell culture method suitable for standard incubators. *Methods and Protocols*, 4 (2). doi:10.3390/mps4020025.

McIlroy, D., Sakahira, H., Talanian, R. V., et al. (1999) Involvement of caspase 3-activated DNase in internucleasomal DNA cleavage induced by diverse apoptotic stimuli. *Oncogene*, 18 (31): 4401–4408. doi:10.1038/SJ.ONC.1202868;KWRD=MEDICINE.

Meng, X.M., Nikolic-Paterson, D.J. and Lan, H.Y. (2016) TGF-Beta: The Master Regulator of Fibrosis. *Nat Rev Nephrol*, 12 (6): 325–338. doi:10.1038/nrneph.2016.48.

Micheau, O. and Tschopp, J. (2003) Induction of TNF receptor I-mediated apoptosis via two sequential signaling complexes. *Cell*, 114 (2): 181–190. doi:10.1016/S0092-8674(03)00521-X.

Miller, I., Min, M., Yang, C., et al. (2018) Ki67 is a Graded Rather than a Binary Marker of Proliferation versus Quiescence. *CellReports*, 24: 1105-1111.e6. doi:10.1016/j.celrep.2018.06.110.

Mizuno, S., Matsumoto, K., Li, M.-Y., et al. (2005) HGF reduces advancing lung fibrosis in mice: a potential role for MMP-dependent myofibroblast apoptosis. *FASEB journal : official publication*

of the Federation of American Societies for Experimental Biology, 19 (6): 1–18. doi:10.1096/FJ.04-1535FJE.

Mizushima, N., Noda, T., Yoshimori, T., et al. (1998) A protein conjugation system essential for autophagy. *Nature*, 395 (6700): 395–398. doi:10.1038/26506.

Mohammed, M.Z., Abdelrahman, S.A., El-Shal, A.S., et al. (2024) Efficacy of stem cells versus microvesicles in ameliorating chronic renal injury in rats (histological and biochemical study). *Scientific Reports*, 14 (1). doi:10.1038/s41598-024-66299-0.

Moon, J.O.K., Welch, T.P., Gonzalez, F.J., et al. (2009) Reduced liver fibrosis in hypoxia-inducible factor-1α-deficient mice. *American Journal of Physiology - Gastrointestinal and Liver Physiology*, 296 (3). doi:10.1152/ajpgi.90368.2008.

Morizane, R. and Bonventre, J. V. (2017) Kidney Organoids: A Translational Journey. *Trends in Molecular Medicine*, 23 (3): 246–263. doi:10.1016/j.molmed.2017.01.001.

Morizane, R., Lam, A.Q., Freedman, B.S., et al. (2015a) Nephron organoids derived from human pluripotent stem cells model kidney development and injury. *Nature Biotechnology*, 33 (11): 1193–1200. doi:10.1038/nbt.3392.

Morizane, R., Lam, A.Q., Freedman, B.S., et al. (2015b) Nephron organoids derived from human pluripotent stem cells model kidney development and injury. *Nature Biotechnology*, 33 (11): 1193–1200. doi:10.1038/nbt.3392.

Mu, Y., Gudey, S.K. and Landström, M. (2012) Non-Smad signaling pathways. *Cell and Tissue Research*, 347 (1): 11–20. doi:10.1007/s00441-011-1201-y.

Mundel, P., Heid, H.W., Mundel, T.M., et al. (1997) Synaptopodin: An Actin-associated Protein in Telencephalic Dendrites and Renal Podocytes. *The Journal of Cell Biology*, 139 (1): 193. doi:10.1083/JCB.139.1.193.

Nakamura, T. and Mizuno, S. (2010) The discovery of Hepatocyte Growth Factor (HGF) and its significance for cell biology, life sciences and clinical medicine. *Proceedings of the Japan Academy Series B: Physical and Biological Sciences*. 86 (6) pp. 588–610. doi:10.2183/pjab.86.588.

NHSBT (2022) *Annual Activity Report. Organ and Tissue Donation and Transplantation. 2021/22*. Available at: http://www.odt.nhs.uk.

Nielsen, R., Birn, H., Moestrup, S.K., et al. (1998) *Characterization of a Kidney Proximal Tubule Cell Line, LLC-PK1 , Expressing Endocytotic Active Megalin*.

Nunes, S.S., Maijub, J.G., Krishnan, L., et al. (2013) Generation of a functional liver tissue mimic using adipose stromal vascular fraction cell-derived vasculatures. *Scientific Reports 2013 3:1*, 3 (1): 1–7. doi:10.1038/srep02141.

Ogata, K., Shimamura, Y., Hamada, K., et al. (2012) Upregulation of HNF-1β during experimental acute kidney injury plays a crucial role in renal tubule regeneration. *American journal of physiology. Renal physiology*, 303 (5): F689-99. doi:10.1152/ajprenal.00086.2012.

Okami, N., Wakui, H., Azushima, K., et al. (2025) Leucine-rich alpha-2-glycoprotein 1 deficiency suppresses ischemia–reperfusion injury-induced renal fibrosis. *Scientific Reports*, 15 (1): 1–11. doi:10.1038/S41598-024-84798-Y;SUBJMETA=4022,443,631,692;KWRD=NEPHROLOGY,PHYSIOLOGY.

Palakkan, A.A., Tarnick, J., Waterfall, M., et al. (2022) Production of kidney organoids arranged around single ureteric bud trees, and containing endogenous blood vessels, solely from embryonic stem cells. *Scientific Reports 2022 12:1*, 12 (1): 1–16. doi:10.1038/s41598-022-16768-1.

Panizo, S., Martínez-Arias, L., Alonso-Montes, C., et al. (2021) Fibrosis in chronic kidney disease: Pathogenesis and consequences. *International Journal of Molecular Sciences*. 22 (1) pp. 1–19. doi:10.3390/ijms22010408.

Park, J.S., Choi, H.I., Bae, E.H., et al. (2017) Small heterodimer partner attenuates hydrogen peroxide-induced expression of cyclooxygenase-2 and inducible nitric oxide synthase by suppression of activator protein-1 and nuclear factor-κB in renal proximal tubule epithelial cells. *International Journal of Molecular Medicine*, 39 (3): 701–710. doi:10.3892/ijmm.2017.2883.

Parrish, J., Li, L., Klotz, K., et al. (2001) Mitochondrial endonuclease G is important for apoptosis in C. elegans. *Nature 2001 412:6842*, 412 (6842): 90–94. doi:10.1038/35083608.

Perico, N., Remuzzi, G., Griffin, M.D., et al. (2023) Safety and Preliminary Efficacy of Mesenchymal Stromal Cell (ORBCEL-M) Therapy in Diabetic Kidney Disease: A Randomized Clinical Trial (NEPHSTROM). *Journal of the American Society of Nephrology*, 34 (10): 1733–1751. doi:10.1681/ASN.0000000000000189.

Peterson, Q.P., Goode, D.R., West, D.C., et al. (2010) Preparation of the caspase-3/7 substrate Ac-DEVD-pNA by solution-phase peptide synthesis. *Nature Protocols 2010 5:2*, 5 (2): 294–302. doi:10.1038/nprot.2009.223.

Phipson, B., Er, P.X., Combes, A.N., et al. (2019) Evaluation of variability in human kidney organoids. *Nature Methods*, 16 (1): 79–87. doi:10.1038/s41592-018-0253-2.

Piret, S.E. and Mallipattu, S.K. (2020) Proximal Tubular Transcription Factors in Acute Kidney Injury: Recent Advances. *Nephron*. 144 (12) pp. 613–615. doi:10.1159/000508856.

Pliss, A., Kuzmin, A.N., Kachynski, A. V, et al. (2010) *Biophotonic probing of macromolecular transformations during apoptosis*. doi:10.1073/pnas.1006374107/-/DCSupplemental.

Pool, M., Eertman, T., Parraga, J.S., et al. (2019) Infusing mesenchymal stromal cells into porcine kidneys during normothermic machine perfusion: Intact MSCs can be traced and localised to Glomeruli. *International Journal of Molecular Sciences*, 20 (14). doi:10.3390/ijms20143607.

Pool, M.B.F., Vos, J., Eijken, M., et al. (2020) Treating Ischemically Damaged Porcine Kidneys with Human Bone Marrow- and Adipose Tissue-Derived Mesenchymal Stromal Cells during Ex Vivo Normothermic Machine Perfusion. *Stem Cells and Development*, 29 (20): 1320–1330. doi:10.1089/scd.2020.0024.

Quiroga, I., McShane, P., Koo, D.D.H., et al. (2006) Major effects of delayed graft function and cold ischaemia time on renal allograft survival. *Nephrology Dialysis Transplantation*, 21 (6): 1689–1696. doi:10.1093/NDT/GFL042.

Ren, L.L., Li, X.J., Duan, T.T., et al. (2023) Transforming growth factor-β signaling: From tissue fibrosis to therapeutic opportunities. *Chemico-Biological Interactions*. 369. doi:10.1016/j.cbi.2022.110289.

Rigo, F., De Stefano, N., Navarro-Tableros, V., et al. (2018) Extracellular Vesicles from Human Liver Stem Cells Reduce Injury in an Ex Vivo Normothermic Hypoxic Rat Liver Perfusion Model. *Transplantation*, 102 (5): e205–e210. doi:10.1097/TP.0000000000002123.

Roodnat, J.I., Mulder, P.G.H., Van Riemsdijk, I.C., et al. (2003) Ischemia times and donor serum creatinine in relation to renal graft failure. *Transplantation*, 75 (6): 799–804. doi:10.1097/01.TP.0000056632.00848.8D,.

Roth, K.J. and Copple, B.L. (2015) Role of Hypoxia-Inducible Factors in the Development of Liver Fibrosis. *CMGH*. 1 (6) pp. 589–597. doi:10.1016/j.jcmgh.2015.09.005.

Saad, A., Dietz, A.B., Herrmann, S.M.S., et al. (2017) Autologous mesenchymal stem cells increase cortical perfusion in renovascular disease. *Journal of the American Society of Nephrology*, 28 (9): 2777–2785. doi:10.1681/ASN.2017020151.

Sáenz-Morales, D., Escribese, M.M., Stamatakis, K., et al. (2006) Requirements for proximal tubule epithelial cell detachment in response to ischemia: role of oxidative stress. *Experimental cell research*, 312 (19): 3711–27. doi:10.1016/j.yexcr.2006.05.024.

Sakai, Y., Fukunishi, S., Takamura, M., et al. (2021) Clinical trial of autologous adipose tissue-derived regenerative (stem) cells therapy for exploration of its safety and efficacy. *Regenerative Therapy*, 18: 97–101. doi:10.1016/j.reth.2021.04.003.

Sander, V., Przepiorski, A., Crunk, A.E., et al. (2020) Protocol for Large-Scale Production of Kidney Organoids from Human Pluripotent Stem Cells. *STAR Protocols*, 1 (3): 100150. doi:10.1016/j.xpro.2020.100150.

Sander, V., Przepiorski, A., Hukriede, N.A., et al. (2023) *Large-Scale Production of Kidney Organoids from Human Pluripotent Stem Cells*. In pp. 69–83. doi:10.1007/978-1-0716-3179-9_6.

Sanz, A.B., Santamaría, B., Ruiz-Ortega, M., et al. (2008) Mechanisms of Renal Apoptosis in Health and Disease. *Journal of the American Society of Nephrology*, 19 (9): 1634–1642. doi:10.1681/ASN.2007121336.

Sato, T., Vries, R.G., Snippert, H.J., et al. (2009) Single Lgr5 stem cells build crypt-villus structures in vitro without a mesenchymal niche. *Nature*, 459 (7244): 262–265. doi:10.1038/nature07935.

Sauvant, C., Schneider, R., Holzinger, H., et al. (2009) Implementation of an in vitro model system for investigation of reperfusion damage after renal ischemia. *Cellular physiology and biochemistry : international journal of experimental cellular physiology, biochemistry, and pharmacology*, 24 (5–6): 567–76. doi:10.1159/000257513.

Sawai, H. and Domae, N. (2011) Discrimination between primary necrosis and apoptosis by necrostatin-1 in Annexin V-positive/propidium iodide-negative cells. *Biochemical and Biophysical Research Communications*, 411 (3): 569–573. doi:10.1016/j.bbrc.2011.06.186.

Sawitzki, B., Harden, P.N., Reinke, P., et al. (2020) Regulatory cell therapy in kidney transplantation (The ONE Study): a harmonised design and analysis of seven non-randomised, single-arm, phase 1/2A trials. *The Lancet*, 395 (10237): 1627–1639. doi:10.1016/S0140-6736(20)30167-7.

Schroppel, B., Legendre, C., Schrö, B., et al. (2014) Delayed Kidney Graft Function: From Mechanism to Translation. *Kidney Int*, 86 (2): 251–258. doi:10.1038/ki.2014.18.

Schweighofer, S. V., Jans, D.C., Keller-Findeisen, J., et al. (2024) Endogenous BAX and BAK form mosaic rings of variable size and composition on apoptotic mitochondria. *Cell Death & Differentiation 2024 31:4*, 31 (4): 469–478. doi:10.1038/s41418-024-01273-x.

Scotland, P.H. (2022) *Scottish Renal Registry Annual Report 2022*.

Serrano, O.K., Vock, D.M., Chinnakotla, S., et al. (2018) The Relationships Between Cold Ischemia Time, Kidney Transplant Length of Stay, and Transplant-Related Costs. *Transplantation*. doi:10.1097/tp.0000000000002309.

Shankar, A.S., Du, Z., Mora, H.T., et al. (2021) Human kidney organoids produce functional renin. *Kidney International*, 99 (1): 134–147. doi:10.1016/J.KINT.2020.08.008.

Sharfuddin, A.A. and Molitoris, B.A. (2011) Pathophysiology of ischemic acute kidney injury. *Nature Reviews Nephrology 2011 7:4*, 7 (4): 189–200. doi:10.1038/nrneph.2011.16.

Shi, Q., Shi, J., Luo, F., et al. (2018) Major Differences in Hypoxia Tolerance and P38 Regulation among Different Renal Cells. *Cellular Physiology and Biochemistry*, 46 (4): 1483–1492. doi:10.1159/000489188.

Shih, Y.-C., Lee, P.-Y., Cheng, H., et al. (2013) Adipose-Derived Stem Cells Exhibit Antioxidative and Antiapoptotic Properties to Rescue Ischemic Acute Kidney Injury in Rats. *Plastic and Reconstructive Surgery*, 132 (6): 940e–951e. doi:10.1097/PRS.0b013e3182a806ce.

Shimada, S. and Cowley, A.W. (2022) Long-Term Continuous Measurement of Renal Blood Flow in Conscious Rats. *Journal of Visualized Experiments*, 2022 (180). doi:10.3791/63560,.

Sierra Parraga, J.M., Rozenberg, K., Eijken, M., et al. (2019) Effects of Normothermic Machine Perfusion Conditions on Mesenchymal Stromal Cells. *Frontiers in Immunology*, 10: 765. doi:10.3389/fimmu.2019.00765.

Singh, N.P. (2000) A simple method for accurate estimation of apoptotic cells. *Experimental Cell Research*, 256 (1): 328–337. doi:10.1006/excr.2000.4810.

Skog, J., Würdinger, T., van Rijn, S., et al. (2008) Glioblastoma microvesicles transport RNA and proteins that promote tumour growth and provide diagnostic biomarkers. *Nature Cell Biology*, 10 (12): 1470–1476. doi:10.1038/ncb1800.

Son, Y.O., Jang, Y.S., Heo, J.S., et al. (2009) Apoptosis-inducing factor plays a critical role in caspase-independent, pyknotic cell death in hydrogen peroxide-exposed cells. *Apoptosis*, 14 (6): 796–808. doi:10.1007/s10495-009-0353-7.

Strzalka, W. and Ziemienowicz, A. (2011) Proliferating cell nuclear antigen (PCNA): A key factor in DNA replication and cell cycle regulation. *Annals of Botany*. 107 (7) pp. 1127–1140. doi:10.1093/aob/mcq243.

Su, X., Zenios, S.A., Chakkera, H., et al. (2004) Diminishing significance of HLA matching in kidney transplantation. *American Journal of Transplantation*, 4 (9): 1501–1508. doi:10.1111/j.1600-6143.2004.00535.x.

Sugiyama, S., Hanaki, Y., Ogawa, T., et al. (1988) The effects of sun 1165, a novel sodium channel blocker, on ischemia-induced mitochondrial dysfunction and leakage of lysosomal enzymes in canine hearts. *Biochemical and Biophysical Research Communications*, 157 (2): 433–439. doi:10.1016/S0006-291X(88)80267-5.

Suhito, I.R., Kim, J.W., Koo, K.M., et al. (2022) In Situ Detection of Kidney Organoid Generation From Stem Cells Using a Simple Electrochemical Method. *Advanced Science*, 9 (20): 2200074. doi:10.1002/ADVS.202200074.

Taguchi, A., Kaku, Y., Ohmori, T., et al. (2014) Redefining the in vivo origin of metanephric nephron progenitors enables generation of complex kidney structures from pluripotent stem cells. *Cell Stem Cell*, 14 (1): 53–67. doi:10.1016/j.stem.2013.11.010.

Takahashi, K. and Yamanaka, S. (2006) Induction of pluripotent stem cells from mouse embryonic and adult fibroblast cultures by defined factors. *Cell*, 126 (4): 663–76. doi:10.1016/j.cell.2006.07.024.

Takasato, M., Er, P.X., Chiu, H.S., et al. (2015) Kidney organoids from human iPS cells contain multiple lineages and model human nephrogenesis. *Nature*, 526 (7574): 564–568. doi:10.1038/nature15695.

Takasato, M. and Little, M.H. (2017) Making a Kidney Organoid Using the Directed Differentiation of Human Pluripotent Stem Cells. *Methods Mol Biol*, 1597: 195–206. doi:10.1007/978-1-4939-6949-4_14.

Tang, P.M.K., Zhang, Y.Y., Mak, T.S.K., et al. (2018) Transforming growth factor-β signalling in renal fibrosis: from Smads to non-coding RNAs. *Journal of Physiology*, 596 (16): 3493–3503. doi:10.1113/JP274492.

Tao, Y., Kim, J., Stanley, M., et al. (2005) Pathways of caspase-mediated apoptosis in autosomal-dominant polycystic kidney disease (ADPKD). *Kidney International*, 67 (3): 909–919. doi:10.1111/j.1523-1755.2005.00155.x.

Thompson, E.R., Bates, L., Ibrahim, I.K., et al. (2020) Novel delivery of cellular therapy to reduce ischemia reperfusion injury in kidney transplantation. *American Journal of Transplantation*, 00: 1–13. doi:10.1111/ajt.16100.

Van Timmeren, M.M., Vaidya, V.S., Van Ree, R.M., et al. (2007) *High Urinary Excretion of Kidney Injury Molecule-1 Is an Independent Predictor of Graft Loss in Renal Transplant Recipients*. doi:10.1097/01.tp.0000295982.78039.ef.

Tirunavalli, S.K., Kuncha, M., Sistla, R., et al. (2023) Targeting TGF-β/periostin signaling by sesamol ameliorates pulmonary fibrosis and improves lung function and survival. *The Journal of Nutritional Biochemistry*, 116: 109294. doi:10.1016/J.JNUTBIO.2023.109294.

Tonelli, M., Wiebe, N., Knoll, G., et al. (2011) Systematic review: Kidney transplantation compared with dialysis in clinically relevant outcomes. *American Journal of Transplantation*, 11 (10): 2093–2109. doi:10.1111/j.1600-6143.2011.03686.x.

Tonnus, W., Meyer, C., Steinebach, C., et al. (2021) Dysfunction of the key ferroptosis-surveilling systems hypersensitizes mice to tubular necrosis during acute kidney injury. *Nature Communications*, 12 (1): 1–14. doi:10.1038/S41467-021-24712-6.

Tsang, T.E., Shawlot, W., Kinder, S.J., et al. (2000) Lim1 activity is required for intermediate mesoderm differentiation in the mouse embryo. *Developmental biology*, 223 (1): 77–90. doi:10.1006/DBIO.2000.9733.

Tseng, W.C., Lee, P.Y., Tsai, M.T., et al. (2021) Hypoxic mesenchymal stem cells ameliorate acute kidney ischemia-reperfusion injury via enhancing renal tubular autophagy. *Stem Cell Research and Therapy*, 12 (1): 1–22. doi:10.1186/S13287-021-02374-X/TABLES/2.

Tsukada, M. and Ohsumi, Y. (1993) Isolation and characterization of autophagy-defective mutants of Saccharomyces cerevisiae. *FEBS Letters*, 333 (1–2): 169–174. doi:10.1016/0014-5793(93)80398-E.

Tsurusaki, S., Kanegae, K. and Tanaka, M. (2022) “In Vivo Analysis of Necrosis and Ferroptosis in Nonalcoholic Steatohepatitis (NASH).” In *Methods in Molecular Biology*. Humana Press Inc. pp. 267–278. doi:10.1007/978-1-0716-2128-8_21.

Vijay, J., Gauthier, M.F., Biswell, R.L., et al. (2020) Single-cell analysis of human adipose tissue identifies depot- and disease-specific cell types. *Nature Metabolism*, 2 (1): 97–109. doi:10.1038/s42255-019-0152-6.

Vitale, M., Zamai, L., Mazzotti, G., et al. (1993) *Histochemistry Differential kinetics of propidium iodide uptake in apoptotic and necrotic thymocytes*.

Vliet, A. van der and Janssen-Heininger, Y.M.W. (2014) Hydrogen peroxide as a damage signal in tissue injury and inflammation: Murderer, mediator, or messenger? *Journal of cellular biochemistry*, 115 (3): 427. doi:10.1002/JCB.24683.

Wang, S., Zeng, M., Li, B., et al. (2020) Raw and salt-processed Achyranthes bidentata attenuate LPS-induced acute kidney injury by inhibiting ROS and apoptosis via an estrogen-like pathway. *Biomedicine and Pharmacotherapy*, 129. doi:10.1016/j.biopha.2020.110403.

Weaver, A.N. and Yang, E.S. (2013) Beyond DNA repair: Additional functions of PARP-1 in cancer. *Frontiers in Oncology*, 3 NOV. doi:10.3389/fonc.2013.00290.

Wei, M.C., Zong, W.X., Cheng, E.H.Y., et al. (2001) Proapoptotic BAX and BAK: A Requisite Gateway to Mitochondrial Dysfunction and Death. *Science (New York, N.Y.)*, 292 (5517): 727. doi:10.1126/SCIENCE.1059108.

Whitfield, M.L., George, L.K., Grant, G.D., et al. (2006) Common markers of proliferation. *Nature Reviews Cancer*. 6 (2) pp. 99–106. doi:10.1038/nrc1802.

Wijeratne, S.S.K., Cuppett, S.L. and Schlegel, V. (2005) Hydrogen peroxide induced oxidative stress damage and antioxidant enzyme response in Caco-2 human colon cells. *Journal of Agricultural and Food Chemistry*, 53 (22): 8768–8774. doi:10.1021/jf0512003.

Wu, H., Chen, G., Wyburn, K.R., et al. (2007) TLR4 activation mediates kidney ischemia/reperfusion injury. *Journal of Clinical Investigation*, 117 (10): 2847–2859. doi:10.1172/JCI31008,.

Wu, W., Wang, X., Yu, X., et al. (2022) Smad3 Signatures in Renal Inflammation and Fibrosis. *International Journal of Biological Sciences*. 18 (7) pp. 2795–2806. doi:10.7150/ijbs.71595.

Wynn, T.A. (2008) Cellular and molecular mechanisms of fibrosis. *Journal of Pathology*. 214 (2) pp. 199–210. doi:10.1002/path.2277.

Xia, J.L., Dai, C., Michalopoulos, G.K., et al. (2006) Hepatocyte growth factor attenuates liver fibrosis induced by bile duct ligation. *American Journal of Pathology*, 168 (5): 1500–1512. doi:10.2353/ajpath.2006.050747.

Xinaris, C., Benedetti, V., Rizzo, P., et al. (2012) In vivo maturation of functional renal organoids formed from embryonic cell suspensions. *Journal of the American Society of Nephrology*, 23 (11): 1857–1868. doi:10.1681/ASN.2012050505.

Xu, S., Yang, X., Chen, Q., et al. (2022) Leukemia inhibitory factor is a therapeutic target for renal interstitial fibrosis. *eBioMedicine*, 86: 104312. doi:10.1016/J.EBIOM.2022.104312.

Yan, R., Ren, J., Wen, J., et al. (2022) Enzyme Therapeutic for Ischemia and Reperfusion Injury in Organ Transplantation. *Advanced Materials*, 34 (1): 1–10. doi:10.1002/adma.202105670.

Yang, L., Cao, H., Sun, D., et al. (2020a) Bone marrow mesenchymal stem cells combine with normothermic machine perfusion to improve rat donor liver quality—the important role of hepatic microcirculation in donation after circulatory death. *Cell and Tissue Research*, 381 (2): 239–254. doi:10.1007/s00441-020-03202-z.

Yang, L., Cao, H., Sun, D., et al. (2020b) Normothermic Machine Perfusion Combined with Bone Marrow Mesenchymal Stem Cells Improves the Oxidative Stress Response and Mitochondrial Function in Rat Donation after Circulatory Death Livers. *Stem Cells and Development*, 29 (13): 835–852. doi:10.1089/scd.2019.0301.

Yang, N., Ray, S.D. and Krafts, K. (2014) “Cell Proliferation.” In *Encyclopedia of Toxicology: Third Edition*. Elsevier. pp. 761–765. doi:10.1016/B978-0-12-386454-3.00274-8.

Yao, W., Hu, Q., Ma, Y., et al. (2015) Human adipose-derived mesenchymal stem cells repair cisplatin-induced acute kidney injury through antiapoptotic pathways. *Experimental and Therapeutic Medicine*, 10 (2): 468–476. doi:10.3892/etm.2015.2505.

Ye, Y., Wang, B., Jiang, X., et al. (2011) Proliferative capacity of stem/progenitor-like cells in the kidney may associate with the outcome of patients with acute tubular necrosis. *Human Pathology*, 42 (8): 1132–1141. doi:10.1016/j.humpath.2010.11.005.

Yoshida, M., Nakashima, A., Ishiuchi, N., et al. (2023) Comparison of the Therapeutic Effects of Adipose- and Bone Marrow-Derived Mesenchymal Stem Cells on Renal Fibrosis. *International Journal of Molecular Sciences*, 24 (23): 16920. doi:10.3390/IJMS242316920/S1.

Yu, Y., Chen, M., Guo, Q., et al. (2023) Human umbilical cord mesenchymal stem cell exosome-derived miR-874-3p targeting RIPK1/PGAM5 attenuates kidney tubular epithelial cell damage. *Cellular and Molecular Biology Letters*, 28 (1). doi:10.1186/s11658-023-00425-0.

Yuan, Q., Ren, Q., Li, L., et al. (2022) A Klotho-derived peptide protects against kidney fibrosis by targeting TGF-β signaling. *Nature Communications*, 13 (1). doi:10.1038/s41467-022-28096-z.

Yue, Y., Meng, K., Pu, Y., et al. (2017) Transforming growth factor beta (TGF-β) mediates cardiac fibrosis and induces diabetic cardiomyopathy. *Diabetes Research and Clinical Practice*, 133: 124–130. doi:10.1016/J.DIABRES.2017.08.018.

Zhang, J.-B.B., Wang, X.-Q.Q., Lu, G.-L.L., et al. (2017) Adipose-derived mesenchymal stem cells therapy for acute kidney injury induced by ischemia-reperfusion in a rat model. *Clin Exp Pharmacol Physiol*, 44 (12): 1232–1240. doi:10.1111/1440-1681.12811.

Zhao, M., Wang, L., Wang, M., et al. (2022) Targeting fibrosis, mechanisms and cilinical trials. *Signal Transduction and Targeted Therapy*. 7 (1). doi:10.1038/s41392-022-01070-3.

Zhao, M., Wang, Y., Li, L., et al. (2021) Mitochondrial ROS promote mitochondrial dysfunction and inflammation in ischemic acute kidney injury by disrupting TFAM-mediated mtDNA maintenance. *Theranostics*, 11 (4): 1845–1863. doi:10.7150/THNO.50905,.

Zhao, M., Zhou, Y., Liu, S., et al. (2018) Control release of mitochondria-targeted antioxidant by injectable self-assembling peptide hydrogel ameliorated persistent mitochondrial dysfunction and inflammation after acute kidney injury. *Drug Delivery*, 25 (1): 546–554. doi:10.1080/10717544.2018.1440445.

Zhong, Y., Jin, C., Han, J., et al. (2021) Inhibition of ER stress attenuates kidney injury and apoptosis induced by 3-MCPD via regulating mitochondrial fission/fusion and Ca2+ homeostasis. *Cell Biology and Toxicology*, 37 (5): 795–809. doi:10.1007/s10565-021-09589-x.

Zhou, H., Hasni, S.A., Perez, P., et al. (2013) MiR-150 promotes renal fibrosis in lupus nephritis by downregulating SOCS1. *Journal of the American Society of Nephrology*, 24 (7): 1073–1087. doi:10.1681/ASN.2012080849,.

Zhu, X., Li, W. and Li, H. (2018) miR-214 ameliorates acute kidney injury via targeting DKK3 and activating of Wnt/ β-catenin signaling pathway. *Biological Research*, 51 (1). doi:10.1186/s40659-018-0179-2.

Zimmerlin, L., Donnenberg, V.S., Rubin, J.P., et al. (2013) Mesenchymal markers on human adipose stem/progenitor cells. *Cytometry. Part A : the journal of the International Society for Analytical Cytology*, 83 (1): 134. doi:10.1002/CYTO.A.22227.

Zou, C., Zhou, Z., Tu, Y., et al. (2020) Pioglitazone attenuates reoxygenation injury in renal tubular NRK-52E cells exposed to high glucose via inhibiting oxidative stress and endoplasmic reticulum stress. *Frontiers in Pharmacology*, 10: 1607. doi:10.3389/FPHAR.2019.01607/BIBTEX.

Zou, H., Li, Y., Liu, X., et al. (1999) An APAF-1·Cytochrome c Multimeric Complex Is a Functional Apoptosome That Activates Procaspase-9. *Journal of Biological Chemistry*, 274 (17): 11549–11556. doi:10.1074/JBC.274.17.11549.

Zou, X., Gu, D., Xing, X., et al. (2016) Human mesenchymal stromal cell-derived extracellular vesicles alleviate renal ischemic reperfusion injury and enhance angiogenesis in rats. *Am J Transl Res*, 8 (10): 4289–4299. Available at: www.ajtr.org.

Zuk, P.A., Zhu, M., Mizuno, H., et al. (2001) Multilineage cells from human adipose tissue: implications for cell-based therapies. *Tissue engineering*, 7 (2): 211–228. doi:10.1089/107632701300062859.